Analysis of a novel function of P-selectin glycoprotein ligand-1 (PSGL-1)

（P-selectin glycoprotein ligand-1（PSGL-1）の新規機能の解析）

The United Graduate School of Veterinary Science

Yamaguchi University

Saori Umeki

March 2013

TABLE OF CONTENTS

GENERAL INTRODUCTION

Canine lymphoma is a common malignant tumor in dogs, accounting for approximately 7–24% and 83% of all canine and hematopoietic tumors, respectively [Vail *et al.*, 2007]. Although B-cell lymphomas generally respond well to chemotherapy upon commencement, they can become resistant to chemotherapy after subsequent treatments [Dobson *et al.*, 2001; Moore *et al.*, 1995]. In contrast, T-cell lymphomas do not respond well to chemotherapy under any circumstances [Dobson *et al.*, 2001]. It is necessary to develop new therapeutic approaches for improving the treatment outcome of canine lymphoma. To develop targeted therapy in small animals, further investigation of canine lymphoma pathophysiology, such as incidence and dissemination mechanisms, is necessary. Patient samples and cell lines from dogs with lymphoma have been used in previous studies; however, these samples are limited and consist of a heterogeneous population. Therefore, the establishment of additional canine lymphoma cell lines would be useful for elucidating the pathophysiology of canine lymphoma.

In chapter 1, the establishment of a new canine lymphoma cell line has been described. The *in vitro* properties of these cell lines has been investigated through a comparison of cell morphology and growth, and gene expression. *In vivo*, the extent and sites of tumor infiltration were investigated.

There are many antibodies (Abs) available against cell surface antigens of human or mouse cells; however, relatively few of these Abs exist against canine or feline cell surface antigens. A small number of human Abs cross-react with canine orthologs, or most of them nonspecifically bind to unrelated molecules. In human medicine, Abs against cell surface antigens are widely used to

confirm clinical diagnoses, and for therapy [Keating *et al.*, 2011; Ismael *et al.*, 2012]. The establishment of monoclonal antibodies (mAbs) against canine cell surface antigens would be important for advancing veterinary medicine.

In chapter 2, the production of antibodies that recognize cell surface antigens of a canine lymphoma cell line is reported. Thirteen different mAbs were found to recognize canine P-selectin glycoprotein ligand-1 (cPSGL-1) using a panning expression cloning method [Shimojima *et al.*, 2003]. Subsequently, the Abs were classified according to their recognition sites.

The PSGL-1 molecule is a dimeric 120 kDa glycoprotein expressed on the surface of leukocytes such as neutrophils, lymphocytes, monocytes, and endothelial cells [Laszik *et al.*, 1996; da Costa Martins *et al.*, 2007]. It is a ligand for several adhesion receptors, such as P-, E- and L-selectin, and participates in selectin-mediated leukocyte adhesion (tethering) [Tauxe *et al.*, 2008].

It was observed that adherent cells overexpressing cPSGL-1 detached from culture dishes. This "anti-adhesive" property of PSGL-1 conflicts with results reported to date. Only Matsumoto *et al.* reported a similar anti-adhesive property of PSGL-1 in lymphocytes [Matsumoto *et al.*, 2009]. In that study, T-cells lacking mouse PSGL-1 (mPSGL-1) showed increased homotypic aggregation. A reintroduction of mPSGL-1 expression in T-cells reversed the increased adhesion phenotype. However, Matsumoto *et al.* failed to elucidate the mechanisms of this anti-adhesive phenomenon induced by PSGL-1. Furthermore, in their report these researchers did not describe anti-adhesive properties in adherent cells. In chapter 3, an explanation of the possible mechanisms behind this

anti-adhesive property of PSGL-1 when it is overexpressed or knocked-down has been presented.

Chapter 1

Establishment of five canine lymphoma cell lines and tumor formation in a xenotransplantation model

SUMMARY

Five novel, canine lymphoma cell lines (Ema, CLC, CLK, Nody-1 and UL-1) were established from dogs suffering from lymphoma and characterized *in vitro* and *in vivo*. All cell lines, except CLC, were characterized with T-cell phenotypes, by flow cytometric analysis and polymerase chain reaction for antigen receptor rearrangement. Cell proliferation rates and transcriptional levels of *MYC*, *PTEN*, *KIT*, and *FLT3* varied between each cell line. Intraperitoneal xenotransplantation of Ema, CLC, Nody-1 and UL-1 lymphoma cell lines into NOD/SCID mice induced ascites, intraperitoneal tumors and severe infiltration of lymphoma cells into the pancreas and mesentery. Establishment of novel canine lymphoma cell lines with different characteristics is critical for elucidating the pathophysiology of canine lymphoma and improving current therapies.

INTRODUCTION

Canine lymphoma is a common malignant tumor in dogs and has been recently recognized as an informative animal model to study human lymphoma [Marconato *et al.*, 2012]. Although canine lymphoma is typically treated by chemotherapy, B-cell lymphomas become resistant to chemotherapy after subsequent treatments, and T-cell lymphomas often do not respond well to chemotherapy from the onset of treatment [Marconato *et al.*, 2012]. Many studies have been performed to decipher the pathophysiology of canine lymphoma in order to improve curative treatments. Prognosis depends on many factors such as histological type and lymphoma stage. Currently, there are several canine lymphoma cell lines available [Momoi *et al.*, 1997; Nakaichi *et al.*, 1996; Zwingenberger *et al.*, 2012]. However, the establishment of additional canine lymphoma cell lines is important to further enhance our understanding of canine lymphoma pathophysiology.

Few studies have reported the xenotransplantation of canine lymphoma cells into immunodeficient mice [Ito *et al.*, 2011; Kisseberth *et al.*, 2007; Nadella *et al.*, 2008]. Xenotransplantation of tumor cells is a method to elucidate the mechanisms of tumor formation and invasion. Additionally, the effects of newly developed therapies can be evaluated *in vivo* using established tumor cell lines in xenotransplantation models.

In the present study, I established five canine lymphoma cell lines and investigated the *in vitro* and *in vivo* properties of these cell lines.

MATERIALS AND METHODS

Case presentation: Case 1

Case 1: a six-year-old female English Springer Spaniel Dog was referred to Yamaguchi University Animal Medical Center (YUAMEC), presenting with multiple abdominal lymphadenopathy, pleural effusion and ascites.

Case presentation: Case 2

Case 2: an eight-year-old female French Bulldog was referred to YUAMEC with multiple abdominal lymphadenopathy, splenomegaly, pleural effusion and ascites.

Case presentation: Case 3

Case 3: an eight-year-old female Great Pyrenees Dog was referred to YUAMEC presenting with multiple abdominal lymphadenopathy and ascites.

Case presentation: Case 4

Case 4: an eight-year-old male Shiba with abdominal mass and ascites, was referred to Iwate University Veterinary Teaching Hospital. All dogs were diagnosed with gastrointestinal lymphoma with cytology of the abdominal lymph node.

Case presentation: Case 5

Case 5: a six-year-old male Labrador Retriever mix with renal mass, was referred to the University of Tokyo Veterinary Medical Center, and ascites was observed after treatment with chemotherapy. The dog was diagnosed with renal lymphoma with cytological sample of the kidney.

Cell culture of the primary materials

Primary lymphoma cells were obtained from clinical specimens, pleural or ascitic fluid and were cultured within 3 hr post collection. Clinical specimens were also analyzed by flow cytometry and polymerase chain reaction for antigen receptor rearrangement (PARR). In case 3, specimens were separated using the Lymphoprep™ kit (Axis-Shield PoC AS, Oslo, Norway) to avoid the contamination of inflammatory cells. Lymphoma cells were cultured in R10 complete medium [RPMI1640 supplemented with 10% fetal bovine serum (FBS), 100 U/ml penicillin, 100 μg/ml streptomycin and 55 μM 2-mercaptoethanol], except in case 1, in which recombinant human interleukin-2 (IL-2) (100 IU/ml; PeproTech, Rocky Hill, NJ, U.S.A.) was added to the R10 complete medium for the first 21 days. All cells were grown at 37°C in a humidified 5% CO_2 incubator. Cells were cultured in fresh R10 complete medium every 2-3 days, at a ratio of 1:3 (Nody-1), 1:4 (Ema, CLK and UL-1) or 1:9 (CLC). Limiting dilution cloning was performed for the UL-1 cell line only. Each cell line grew stably without the addition of growth factors for more than 100 passages.

Flow cytometry

Primary lymphoma cells or established cell lines were collected and resuspended in FACS buffer (PBS containing 2% FBS and 0.1% NaN3). 2×10^5 cells were stained with primary antibody for 30 min on ice. After incubation, cells were washed and incubated with secondary antibody for 30 min on ice. After washing, cells were fixed in 1% paraformaldehyde and stored until analysis. Primary

and secondary antibodies are shown in Table I-1. For every specific antibody, a corresponding isotype control of the same IgG was used. The samples were analyzed using CyFlow® Space (Partec GmbH, Münster, Germany), and results were analyzed using FlowJo software (Tree Star, Inc., San Carlos, CA, U.S.A.).

Polymerase chain reaction for antigen receptor rearrangement (PARR)

DNA was extracted from each cell line using the QIAamp DNA Mini Kit (QIAGEN, Valencia, CA, U.S.A.) according to the manufacturer's instructions. PARR was performed as described previously [Bernett *et al.*, 2003; Kaneko *et al.*, 2009]. Briefly, each sample was amplified by two sets of primers (major and minor) for *IgH* and one set of primers for *TCRγ*. As a positive control for the DNA extraction process, the constant region of IgM (Cμ) was amplified for each sample. As positive and negative controls for the PCR amplification, genomic DNA previously shown to have *IgH* or *TCRγ* rearrangements by sequence analysis (or not), respectively, were used [Kaneko *et al.*, 2009]. PCR products were electrophoresed on 12% polyacrylamide gels, stained with ethidium bromide and visualized with a UV illuminator.

Cell proliferation assay

All cell lines described above were suspended in cell culture medium and seeded in 12-well plates. CLC (1×10^4 cells) or other cell lines (3×10^4 cells) were cultured in triplicates. Cells were

collected after 24, 48 and 72 hr of incubation and counted by trypan blue dye exclusion using a hemocytometer.

Gene expression analysis by real-time PCR

Lymph nodes were obtained and frozen from two healthy Beagle dogs, which were housed indoors and maintained according to the Yamaguchi University Animal Care and Use Committee regulations. For real-time PCR analysis, total RNA was isolated from cell pellets or frozen tissues with ISOGEN II reagent (Nippon Gene, Tokyo, Japan) according to the manufacturer's instructions. Total RNA (1 μg) was treated using the Turbo DNA-free kit (Ambion/Applied Biosystems, Tokyo, Japan), and cDNA was transcribed using the Superscript III kit (Invitrogen Life Technologies, Carlsbad, CA, U.S.A.) according to the manufacturer's instructions. Oligo dT primers were used to prime the first-strand synthesis for each reaction. cDNA was subject to real-time PCR amplification using the QuantiTect SYBR Green PCR kit (QIAGEN) according to the manufacturer's protocol. The primers used for assaying canine *KIT*, *PTEN*, *MYC*, *FLT3* and *RPL32* were as follows: forward 239 5′-CGAAGATGTGTGAAGCAGGA-3′, and reverse 240, 5′-GTGTCCGCTACCCTGGAATA-3′; forward 235 5′- ACCAGGACCAGAGGAAACCT-3′, and reverse 236, 5′-CTGGCGTCACAGAAGTTGAA-3′; forward 233, 5′-CGCTGGTCCTTAAGAGATGC-3′, and reverse 234, 5′-CGCCTCTTGTCATTCTCCTC-3′; forward 1003, 5′-CAGAGGCAGTGTATGGAGCA-3′, and reverse 1004, 5′-GGCAATTCAGGGAACTGTGT-3′; forward 370, 5′-TGGTTACAGGAGCAACAAGAAA-3′,

and reverse 371, 5′-GCACATCAGCAGCACTTCA-3′, respectively. Each assay was performed in duplicate. PCR cycling conditions were as follows: 95°C for 15 min, followed by 45 cycles of 94°C for 15 sec, 60°C for 30 sec and 72°C for 30 sec. PCR and fluorescence intensity detection were performed with the StepOne PCR system (PerkinElmer, Inc., Waltham, MA, U.S.A.). The data were analyzed using StepOne software v.2.2.2. Briefly, the PCR cycle number at the threshold was represented as C_T, and the difference between C_T for the target and internal control (ΔC_T) was calculated. The value of $2^{-\Delta CT}$ was considered to represent the amount of target mRNA relative to the amount of internal control.

Engraftment of canine lymphoma cell lines into NOD/SCID mice

All experiments involving NOD/SCID mice were approved by the Yamaguchi University Animal Care and Use Committee (approval number 164). Immune-deficient NOD/SCID mice at 6–8 weeks of age were obtained from Kyudo Co., Ltd. (Saga, Japan). All mice were kept in accordance with institutional guidelines and maintained in autoclaved isolator cages in a specific pathogen-free area.

Viability of each cell line was assessed by trypan blue dye exclusion (viability exceeded 98% in all experiments), and cells were resuspended at 20×10^6 cells/ml in RPMI1640 medium alone. For each cell line, 10×10^6 cells were injected intraperitoneally into recipient mice (four mice per group). After inoculation, mice were observed daily for any abnormal clinical signs such as weakness, ascites accumulation or dyspnea. At 21 days post-inoculation, mice were sacrificed using diethyl ether anesthesia. Ascites was collected from each mouse, and liver, spleen, kidney, pancreas,

stomach, small intestine, large intestine, heart, lung, brain, spinal cord and lymph nodes were removed. Tissues were fixed in 10% neutral-buffered formalin for 24 hr, transferred to 70% ethanol and embedded in paraffin. Glass slides with 3-μm sections were prepared and stained with hematoxylin and eosin.

RESULTS

Characteristics of the primary lymphoma cells

Pleural fluid was collected from cases 1 and 2, and ascites were collected from cases 3, 4 and 5. All fluid samples contained malignant lymphoblastoid cells. PARR analysis of clinical samples showed a monoclonal *TCRy* gene rearrangement in case 1, 3 and 5, but not in case 2. Only case 5 displayed a biallelic rearrangement of *IgH* (Table I-2). Flow cytometric analysis of lymphoblastoid cells from cases 2, revealed positive expression of CD3 and CD45RA,while cells were negative for CD4, CD8α, CD11b, CD21, MHCII, IgM and IgG (Table I-2). Lymphoblastoid cells from case 3 were positive for CD8α, MHCII and CD90, and negative for CD4, CD21, IgM and IgG, while certain populations were positive for CD3 (Table I-2). Lymphoblastoid cells from case 5 were positive for CD8α and CD45RA and negative for CD3, CD4, CD90, TCRαβ, TCRγδ, CD21, MHCII, IgM and IgG (Table I-2). Owing to limited sample availability, immunophenotyping was not performed for case 1, and PARR and immunophenotyping were not performed for case 4.

Cases 1 and 3, from which the Ema and CLK cell lines were later derived, were diagnosed as T-cell lymphoma using PARR. Case 2, from which the CLC cell line was derived, was diagnosed as T-cell lymphoma by flow cytometric analysis of CD3 expression. The cellular phenotype of cases 4 and 5, from which the Nody-1 and UL-1 cell lines were derived, could not be identified, since immunophenotyping and PARR analysis were not carried out in case 4, and PARR analysis revealed rearrangement of both *TCRy* and *IgH* gene in case 5.

Characteristic analysis of established cell lines

Ema, CLC, CLK, Nody-1 and UL-1 cell lines were established from cases 1, 2, 3, 4 and 5, respectively. Ema and Nody-1 cell lines were characterized by growth in small clusters of cells, whereas CLC, CLK and UL-1 cell lines grew as single cells (Fig. I-1A). Ema, CLC, Nody-1 and UL-1 cells showed mostly round morphology, and CLK cells exhibited a characteristic spindle-like shape. Analysis of intracellular morphology by Giemsa staining, revealed that all cell lines appeared to be immature, large lymphocytes (Fig. I-1A). The cytoplasm of all cell lines was moderately basophilic, and the cytoplasm of CLC, Nody-1 and UL-1 had minute vacuoles. Ema, CLK, Nody-1 and UL-1 cell lines had slightly unclear nucleoli, whereas the nucleus of CLC cells contained apparent nucleoli.

Immunophenotypic analysis of established cell lines

Flow cytometric analysis of surface antigens revealed characteristic expression patterns for each cell line (Table I-3). All cell lines expressed CD45 and CD45RA, indicating these cells were derived from lymphocytes. All cell lines were negative for CD4, CD11b, CD14, CD21, CD34, TCRαβ, IgM and IgG. In addition, the Ema cell line expressed CD3, CD90 and TCRγδ, and was negative for CD8α, CD11a, CD11c, CD18 and MHCII expression. The CLC cell line expressed CD18 and MHCII, and was negative for CD3, CD8α, CD11a, CD11c, CD90 and TCRγδ expression. The CLK cell line expressed CD8α, CD11a, CD11c, CD18 and CD90, and was negative for CD3, TCRγδ and

MHCII expression. The Nody-1 cell line expressed CD3, CD18 and MHCII, and was negative for CD8α, CD11a, CD11c, CD90 and TCRγδ. The UL-1 cell line expressed CD8α and CD18, and was negative for CD3, CD11a, CD11c, CD90, TCRγδ and MHCII expression. Ema, CLK, Nody-1 and UL-1 cells were considered to represent T-cell phenotypes, since they expressed at least one T-cell marker (CD3 or CD8α) and were negative for all B-cell markers (CD21, IgM and IgG).

Antigen receptor rearrangement of the established cell lines

No cell lines contained immunoglobulin rearrangements by PARR analysis using B major and B minor primer pairs (Fig. I-1B). All cell lines, except CLC, showed single or multiple TCRγ γrearrangements (Fig. I-1B). Taken together, all cell lines, except CLC, displayed T-cell phenotypes, however, in the case of CLC, immunophenotype could not be inferred from flow cytometric and PARR analyses.

In vitro cell growth analysis

Analysis of cell growth revealed a doubling time of 14.5, 20.9, 21.5, 26.6 and 36.2 hr, for CLC, UL-1, Nody-1, Ema and CLK cells, respectively (Fig. I-2). The CLC cell line displayed the fastest cell growth rate. In contrast, CLK showed the slowest cell growth rate. UL-1 and Nody-1 cells grew at comparable rates, which were faster than that of the Ema cell line.

Gene expression analysis of cell lines

Real-time PCR was used to investigate the expression of *MYC*, *PTEN*, *KIT*, and *FLT3* transcripts. *MYC* expression was clearly upregulated in all cell lines compared with normal lymph nodes, except for Ema, in which a similar expression level was identified (Fig. I-3A). I identified a significant upregulation of *KIT* in Nody-1 cells (Fig. I-3C). All cell lines displayed upregulation of *PTEN* (Fig. I-3B) and downregulation of *FLT3* (Fig. I-3D) compared with normal lymph nodes.

Examination of inoculated NOD/SCID mice post mortem

The *in vivo* characteristics of these five canine lymphoma cell lines were investigated by xenotransplantation into NOD/SCID mice. 75% (3/4 mice) injected with the CLC cell line died 12-13 days post-transplantation, while 25% (1/4 mice) injected with the Nody-1 cell line died 19 days post-transplantation (Table I-4). Mice transplanted with other cell lines were dissected 21 days post-transplantation. Ascites were observed in all xenotransplanted mice, except for CLK-transplanted mice (Table I-4, Fig. I-4A). Large amounts of ascitic fluid were present in CLC-transplanted mice compared to mice transplanted with the other three cell lines. Lymphoma cells were observed by Diff-Quick staining of smears of ascitic fluid obtained from all mice (data not shown).

Mice transplanted with the CLK cell line did not form tumors in any organs, except for one mouse that exhibited an enlarged mediastinal lymph node. All canine lymphoma cell lines, except CLK, formed tumors in some peritoneal organs in at least three out of four xenotransplanted mice (Table I-4). It was difficult to accurately measure the size of each tumor, because they strongly

adhered to the gastrointestinal tract serosal surface and poorly marginated. The extent of each tumor varied among each group of mice.

Microscopic infiltration of lymphoma cells to the cellular structures of abdominal organs and lymph nodes is described in Table I-4. No microscopic infiltration of tumor cells was observed in any organs from CLK-injected mice, consistent with the macroscopic observation. In most cases, tumor cells infiltrated from the serosal surface of the abdominal organs. All cell lines, except CLK, displayed severe pancreatic infiltration where the pancreases was almost entirely replaced by tumor cells (Fig. I-4B). Infiltration of lymphoma cells to the kidney and spleen were only detected in Nody-1-transplanted mice (Fig. I-4C). Although no infiltration of tumor cells was observed in the kidneys of mice transplanted with Ema and CLC, infiltration was observed in the fatty tissue around the kidneys. Infiltration of lymphoma cells to the liver was observed in CLC-, Nody-1-, and UL-1-transplanted mice (Fig. I-4D,E). In particular, the degree of infiltration of Nody-1 cells into the liver was the most severe-as infiltration occurred around the hepatic triad, unlike in other cell lines.

DISCUSSION

In the present study, I established five canine lymphoma cell lines and compared their *in vitro* and *in vivo* properties. Of these, Ema, CLK, Nody-1 and UL-1, were identified as T-cell lymphoma cell lines by PARR analysis, however, the immunophenotype of CLC was not identified in this study. Although the original patient sample from which CLC line was derived was positive for CD3 expression by flow cytometry, a cellular phenotype could not be identified by PARR or flow cytometry analyses. In some cases, the cell surface markers on established cell lines are lost during long-term culture compared to the primary isolated tumor cells [Zwingenberger et al., 2012]. Flow cytometric analysis of the CLC and CLK cell lines revealed that the expression of many antigens was lost compared to the original patient samples (Table I-3).

Previous studies have shown that the expression levels of various genes associated with tumorigenesis (*MYC*, *KIT*, *FLT3*, and *PTEN*) are altered in canine lymphoma cell lines owing to genomic amplification or deletion, as elucidated by CGH analysis [Kisseberth et al., 2007]. The expression of *MYC* is often upregulated in canine lymphoma cell lines, partly due to a gain in copy numbers of dog chromosome 13 (CFA13) [Seiser et al., 2011]. Consistent with this study, I observed upregulation of *MYC* in four of five cell lines. While *KIT* was also reported to be upregulated in several canine lymphoma cell lines, I observed overexpression of *KIT* in only one of five cell lines (Nody-1). Mutation of *FLT3* also contributes to tumorigenesis in certain canine acute lymphoblastic leukemia cases [Suter et al., 2011]. In this study, however, I observed significant downregulation of

FLT3 expression compared to normal lymph nodes in all five cell lines. This suggests that *FLT3* may not be relevant to tumorigenesis in the cell lines used in this study, although I did not examine the expression of *FLT3* in primary samples. Unexpectedly, *PTEN* was overexpressed in all five cell lines derived in this study. Previous studies demonstrated decreased *PTEN* expression due to homozygous deletion on CFA26 in 2 out of 5 cell lines [Seiser et al., 2011], and thus the significance of *PTEN* overexpression in my cell lines remains to be explored.

Xenotransplantation of cell lines in this study revealed several differences in the sites and degree of tumor infiltration among the five canine lymphoma cell lines. The majority of mice injected with Ema, CLC, Nody-1 and UL-1 cells formed tumors, whereas CLK-transplanted mice did not. In keeping with this observation, the growth rate of CLK cells was significantly lower compared with the other cell lines, which may have led to early elimination of tumor cells affecting tumor formation.

In these xenotransplantation studies, four mice died before being euthanized on day 21 (one CLC, day 12; two CLC, day 13; one Nody-1, day 19; Table I-4). Microscopic analysis of organs in these mice, revealed tumor cell infiltration in many organs in CLC- and Nody-1-injected mice, compared to mice injected with the other cell lines. Since mice with greater volumes of ascitic fluid tend to die earlier, the cause of death may have been because of high pressure on the pleural cavity and abdominal organs due to the ascitic fluid.

In xenotransplanted mice, the pancreas and mesentery were the most tumor-infiltrated organs for all cell lines, except CLK. These results are consistent with a previous study where canine T-cell

lymphoma cell lines were transplanted intraperitoneally into NOD/SCID mice [Nadella et al., 2008]. Since tumor cells were injected intraperitoneally, it is reasonable that the mesentery was often affected, however, why the pancreas was also a primary target in most mice remains unclear. Tumor infiltration of the kidney and spleen was detected only in Nody-1-transplanted mice. Tumor infiltration of other organs, including the liver and gastrointestinal tract was also severe in Nody-1-transplanted mice, compared with the other cell lines. Infiltration by lymphoma cells was detected in the visceral surfaces of most organs (Table I-4 and Fig. I-4). However, lymphoma cells infiltrated around the hepatic triad of the liver in Nody-1-transplanted mice, suggesting hematogenous dissemination. No infiltration was observed in the gastrointestinal tracts of mice transplanted with UL-1 cells or in the livers of mice transplanted with Ema cells. These results demonstrate clear differences in the sites of tumor infiltration between the five canine lymphoma cell lines. Thus, in addition to differences in growth rates, each cell line may preferentially disseminate to different organs, and these characteristics may be related to lymphoma pathogenesis.

In this study, lymphoma cell lines were injected intraperitoneally into mice, since most cell lines were established from ascitic samples. However, this method of delivery may not necessarily reflect the behavior of the original tumor samples. Future studies employing other routes of injection, such as intravenous or subcutaneous xenotransplantation, are also required to completely characterize these lymphomas.

In the present study, I established and characterized five canine lymphoma cell lines, Ema, CLC, CLK, Nody-1 and UL-1, using both *in vitro* and *in vivo* methods. To date, our knowledge of the

mechanisms of pathophysiology underlying canine lymphoma, is limited by an insufficient number of canine lymphoma cell lines. The development of several cell lines with different characteristics will significantly enhance our understanding of canine lymphoma pathophysiology and the development of new therapies. Recently, five canine B-cell lymphoma cell lines were described [Zwingenberger et al., 2012]. Comparison of the cell lines established in this study with these published cell lines will aid our understanding of canine lymphoma and the differences in prognosis or resistance to chemotherapy between T-cell and B-cell lymphoma in dogs.

Chapter 2

Characterization of monoclonal antibodies against canine P-selectin glycoprotein ligand-1 (PSGL-1)

SUMMARY

Thirteen different monoclonal antibodies against canine P-selectin glycoprotein ligand-1 (cPSGL-1) were obtained by immunization of rats with cells of a canine lymphoma cell line (Ema). *O*-sialoglycoprotein endopeptidase treatment of Ema cells showed that all of these antibodies recognized *O*-glycosylated peptides of canine PSGL-1. Experiments using deletion or point mutants of cPSGL-1 indicated that these antibodies could be categorized into several groups based on their cPSGL-1 recognition characteristics. These anti-cPSGL-1 monoclonal antibodies will be useful for analysis of the canine P-selectin and PSGL-1 system.

INTRODUCTION

Antibodies against cell surface antigens are important tools for identification of cell phenotypes. Discrimination of cell types often leads to a definitive or a differential diagnosis in clinical cases. Furthermore, the recent development of Ab-based immunotherapy has facilitated elimination of specific types of cells from the body in cases of cancer or autoimmune diseases [Bussel *et al.*, 2007].

In veterinary medicine, especially in small animal medicine, there are only a few Abs available that were specifically developed against molecules of a particular species. Some Abs that were raised against molecules of species other than dogs or cats can be used for the detection of their orthologs in dogs or cats [Sinkora *et al.*, 2007; Mizuno *et al.*, 2009]. However, the lack of Abs that are specific to molecules of dogs or cats discourages clarification of disease pathogenesis, as well as attempts to diagnose diseases and subdivide them into smaller categories.

In the present study, I immunized rats with cells of a canine lymphoma cell line and obtained a hybridoma library that produced several different Abs. Using a panning method for screening of Ab ligands [Shimojima *et al.*, 2003], some of these Abs were found to bind to canine P-selectin glycoprotein ligand-1 (cPSGL-1).

PSGL-1 is a highly *O*-glycosylated protein that was isolated as a ligand for P-selectin [Sako *et al.*, 1993]. PSGL-1 is expressed mainly in hematopoietic cells [Laszik *et al.*, 1996] and has an important role in trafficking and rolling of neutrophils on endothelial cells during inflammation [Yang *et al.*, 1999]. Intestinal inflammation in a murine model of Crohn's disease was reportedly

reduced by injection of an anti-PSGL-1 Ab, which bound to PSGL-1 expressed by endothelial cells [Rivera-Nieves *et al.*, 2006]. Understanding of the contribution of PSGL-1 to inflammation is important for development of new therapies as well as for elucidation of the mechanism of leukocyte rolling. For this reason, the anti-cPSGL-1 Abs obtained in the present study were characterized.

MATERIALS AND METHODS

Cell culture

A canine T cell lymphoma cell line, Ema, which was established in chapter 1, the mouse myeloma cell line P3U1, and the canine mammary gland cell line CHMm (kindly provided by Dr. Nobuo Sasaki, University of Tokyo, Japan) were maintained in R10 complete medium (RPMI1640 supplemented with 10% FBS, 100 units/ml penicillin and 100 μg/ml streptomycin, and 55 μM 2-mercaptoethanol). The retroviral packaging cell line PLAT-E was kindly provided by Dr. Toshio Kitamura (University of Tokyo, Japan) and grown in D10 complete medium (DMEM supplemented with the same reagents as R10). The HL-60 and Chinese hamster ovary (CHO) cell lines were obtained from the Cell Resource Center for Biomedical Research (Institute of Development, Aging and Cancer, Tohoku University, Sendai, Japan) and were maintained in R10 or DMEM/Ham's F12 culture medium (Wako Pure Chemical Industries, Ltd., Osaka, Japan) containing 10% FBS and 100 units/ml penicillin and 100 μg/ml streptomycin, respectively. These cell lines were cultured at 37 °C in a humidified incubator with 5% CO_2 in air.

Production of a rat monoclonal Ab library

To obtain a panel of Abs against antigens expressed on canine lymphoma cells, Ema cells (1×10^7 in 500 μl) emulsified with an equal amount of Titer Max Gold (CytRx, Los Angeles, CA,

USA) were injected intracutaneously into the hind footpads of 7-week old Sprague-Dawley rats (Kyudo, Kumamoto, Japan). Two weeks after injection, popliteal lymph nodes cells were isolated and fused with P3U1 cells. After colonies were obtained, Ema cell-positive hybridomas were identified using flow cytometry and the resulting hybridomas were cloned by limiting dilution.

Ab purification

After cloning of each hybridoma, the culture media was switched from GIT (Wako Pure Chemical Industries, Ltd.) containing 10% FBS to GIT without FBS, except for two hybridoma clones producing mAb 64-1 and 90-1, which were continuously maintained in GIT containing 10% FBS and 5% of BM Condimed H1 (Roche Diagnostics K.K., Tokyo, Japan). Supernatants were collected from each hybridoma culture and Abs were purified using the mAb Trap kit (GE Healthcare Japan, Tokyo, Japan). Subsequently, the Ab solution was desalted using PD10 Desalting columns (GE Healthcare Japan) or dialysis. Antibody isotyping was performed using a rat monoclonal Ab isotyping kit (AbD serotec, Kindlington, UK).

Retroviral cDNA expression libraries

Total RNA was isolated from Ema cells using the TRI reagent (Molecular Research Center, Inc., Cincinnati, OH, USA). Double-stranded cDNA was synthesized by isolating poly (A) RNA from the

total RNA using a Small Scale mRNA Purification kit (MicroPoly(A) Purist™, Applied Biosystems, Tokyo, Japan). Double-stranded cDNA was synthesized using 5 μg mRNA and a CloneMiner cDNA Library Construction kit (Life Technologies Japan Ltd., Tokyo, Japan). After synthesis of the double-stranded cDNA library, the adaptors attB1 and attB2 were added to both ends of the cDNA fragments, which were cloned into the pDONR222 vector using the BP reaction. The cDNA library in pDONR222 was subcloned into the pMxs-IG-Gateway vector, which is a bicistronic vector expressing the inserted gene and the EGFP (enhanced green fluorescent protein) reporter, using the Gateway LR reaction.

Retroviral transduction

Retroviral transduction was done as described previously [Mizuno *et al.*, 2009]. In the case of P3U1 cells transduced with the pMxs-IP-based vector, cells were cultured in the presence of 2 μg/ml of puromycin (Sigma–Aldrich) to obtain P3U1 cells stably expressing cPSGL-1 constructs.

Panning for expression cloning

To identify the antigens recognized by hybridoma Abs, panning for expression cloning was performed as described [Shimojima *et al.*, 2003]. A Petri dish (Bio-Bik, Osaka, Japan) was coated with 5 ml of 20 μg/ml anti-rat IgG (SIGMA-ALDRICH) in PBS at 4 °C overnight. After removal of the supernatant, the dish was washed once with 3 ml of wash buffer (2% FBS in PBS), and 7 ml of

the hybridoma culture supernatant containing rat polyclonal antibodies was added, and incubated at 37 °C for 30 min. After incubation, the dish was washed as above. P3U1 cells (1×10^7 cells) expressing cDNA libraries made from Ema cells were then suspended in 4 ml of culture medium, seeded on the dish and incubated at 4 °C for 90 min. The dish was washed, 4 ml of culture medium was gently added, and the culture was started. On days 3 and 6, the dish was washed 4 times with 4 ml of culture medium and colony-forming cells were transferred to a 24-well plate.

PCR amplification of the inserted cDNA in candidate clones

PCR amplifications were performed in a final volume of 25 μl containing a pair of primers (0.4 μM each), 200 ng genome, 1×Colorless GoTaq Reaction Buffer (Promega, Tokyo, Japan), and 0.2 μM dNTPs. After incubation at 95 °C for 10 min, 0.625 units of Go Taq (Promega) was added, and PCR was carried out under the following conditions: denaturation at 95 °C for 30 s, annealing at 58 °C for 30 s, and polymerization at 72 °C for 4 min. After 30 cycles, the polymerization step was extended at 72 °C for 10 min.

Nucleotide sequencing of the inserted cDNA in candidate clones

Genomic DNA was extracted from EGFP-expressing colony-forming cells using the QIAamp DNA mini kit (QIAGEN, Tokyo, Japan). The inserted cDNAs were amplified using the primers YTM178 and YTM206 (Table II-1), which bind to sites upstream and downstream, respectively of

the multicloning site of pMxs-IG. The amplified PCR products were gel-purified and subjected to a sequencing reaction using the Big Dye Terminator v3.1 Cycle Sequencing kit (PerkinElmer Japan Co., Ltd., Kanagawa, Japan), followed by sequence analysis using the ABI PRISM3100-Avant sequencer (Applied Biosystems). The sequence data was searched on the BLAST canine database of NCBI. To validate the crossreactivity of Abs produced by the hybridoma library, each gene was retrovirally expressed in P3U1 cells and analyzed by flow cytometry.

PCR amplification for constructing expression vector

PCR amplifications were performed in a final volume of 25 μl containing a pair of primers (0.3 μM each), 1 μl cDNA, 1× PCR buffer for KOD Plus, 0.2 μM dNTP, 1 mM $MgSO_4$ and 1.0 unit of KOD Plus (TOYOBO, Osaka, Japan). After incubation at 94 °C for 2 min, PCR was carried out under the following conditions: denaturation at 98 °C for 10 s, annealing at 56 °C for 30 s, and polymerization at 72 °C for 1.5 min. After 40 cycles, the polymerization step was extended at 72 °C for 10 min.

Construction of a canine PSGL-1 expression vector

To construct a vector that expressed cPSGL-1, cPSGL-1 was amplified as described above using the Ema cDNA library as a template and the primers YTM263 and YTM264 (Table II-1). The amplified PCR products were subcloned into the SmaI site of the pBluescript SK(−) vector (pBS-cPSGL-1).

For addition of 2 FLAG tag sequences at the C-terminus of the cPSGL-1 sequence, the C-terminus of the cPSGL-1 sequence was PCR amplified using a 5′ specific primer (YTM263) and a 3′ specific primer (YTM310) that contained one FLAG tag sequence. A second PCR was subsequently performed using YTM263 and a specific 3′ primer (YTM311) containing a second FLAG tag sequence, which was annealed with the first FLAG tag sequence. The PCR product was cloned into pBluescript SK (−) using the SmaI restriction site. The sequence of the amplified fragment was confirmed by nucleotide sequence analysis. The XhoI/NotI fragment of pBS-cCRT-2xFLAG was inserted into a retroviral expression vector, pMxs-IG or pMxs-IP (kindly provided by Dr. T. Kitamura), using enzyme technology (pMx-IG-cPSGL-flag#1 or pMx-IP-cPSGL-1 flag#1).

To construct expression vectors encoding cPSGL-1 deletion mutants, sequential PCR amplification was performed as follows: The first PCR was performed using pMx-IG-cPSGL-1-flag#1 as a template with a 5′ primer (YTM178) and one of a number of 3′ primers (either YTM516, YTM 518, YTM 520, or YTM 522) to amplify the cPSGL-1 region upstream of the deleted domain. The second PCR was performed using pMx-IG-cPSGL-1-flag#1 as a template with one of a number of 5′ primers (YTM515, YTM517, YTM519, or YTM521) and a 3′ primer (YTM179) to amplify the region downstream of the deleted domain. For the third PCR amplification, the appropriate overlapping PCR products were used as templates and were amplified using 2 cycles of denaturation at 94 °C for 15 s, annealing at 50 °C for 30 s, and polymerization at 68 °C for 1.5 min, after which the primers YTM178 and YTM179 were added and PCR was

continued for an additional 25 cycles to generate cPSGL-1 deletion constructs. These PCR products were cleaved with XhoI and NotI and subcloned into the pMxs-IG vector to generate pMx-IG-cPSGL-DM1, pMx-IG-cPSGL-DM2, pMx-IG-cPSGL-DM3, and pMx-IG-cPSGL-DM4, which had truncations of 69 bp (23 amino acids), 309 bp (103 amino acids), 390 bp (130 amino acids) and 213 bp (71 amino acids) respectively in pMx-IG-cPSGL-1-flag#1 (Figure II-1A).

Point mutated cPSGL-1 constructs were constructed using a similar methodology to that described above. The first PCR was performed using pMx-IG-cPSGL-1-flag#1 as a template with a 5′ primer (YTM178) and one of a number of 3′ primers (either YTM574, YTM 576 or YTM 578) to amplify the region upstream of the mutation. The second PCR was performed using pMx-IG-cPSGL-1-flag#1 as a template with one of a number of 5′ primers (YTM573, YTM575 or YTM577) and a 3′ primer (YTM179) to amplify the region downstream of the mutation. For the third PCR amplification, the appropriate overlapping PCR products were used as templates and were amplified using 2 cycles of denaturation at 94 °C for 15 s, annealing at 50 °C for 30 s, and polymerization at 68 °C for 1.5 min, after which the primers YTM178 and YTM179 were added and PCR was continued for an additional 25 cycles to generate point mutated cPSGL-1 constructs. These products were cleaved with EcoRI and subcloned into the pMxs-IG vector to generate pMx-IG-cPSGL-Y52F-FLAG, pMx-IG-cPSGL-Y54F-FLAG, and pMx-IG-cPSGL-Y52,54F-FLAG (Figure II-1C). All of the clones were sequenced using the Big Dye Terminator v3.1 Cycle Sequencing kit (PerkinElmer), followed by sequencing using the ABI PRISM3100-Avant sequencer (Applied Biosystems) to confirm the nucleotide sequences.

Flow cytometry

Cell staining for flow cytometry was done as described previously [Mizuno *et al.*, 2009]. Primary Abs used here were as follows: hybridoma culture supernatant (1:4 dilution), purified hybridoma Ab, anti-human CD15s (BD Biosciences, San Diego, CA, USA) (1:100 dilution), or anti-FLAG Ab (Rockland Immunochemicals Inc., Gilbertsville, PA, USA) (1:500 dilution). Secondary Abs were as follows: anti-rat IgG-FITC (Jackson ImmunoResearch Laboratories, Inc., West Grove, PA, USA) (1:1000 dilution), anti-rat IgG-RPE (Southern Biotech, Birmingham, AL, USA) (1:250 dilution), anti-mouse IgM-PE (Southern Biotech) (1:1000 dilution), or anti-rabbit IgG-PE (Santa Cruz Biotechnology, Inc., Santa Cruz, CA, USA) (1:400 dilution). After staining, the samples were analyzed using EPICS XL (Beckman Coulter, Inc., Tokyo, Japan) or CyFlow space (Partec, Munster, Germany), and the results obtained were analyzed using FlowJo software (Treestar, Inc., San Carlos, CA, USA).

Western blotting

Cells (1×10^7) were lysed at 4 °C for 30 min in ice-cold CHAPS buffer (3% CHAPS (3-[(3-Cholamidopropyl)dimethylammonio]-1-propanesulfonate hybrate) (Nakarai tesque, Kyoto, Japan), 30 mM Tris HCl (pH 7.5), 150 mM NaCl) supplemented with Complete, Mini EDTA-free protease inhibitor mixture (Roche Diagnostics K.K.). Cell lysates were clarified by centrifugation at 12,000 × *g* for 10 min at 4 °C and were stored at −80 °C until SDS-PAGE analysis. SDS-PAGE and

Western blotting were done as described previously [Okawa *et al.*, 2011]. Hybridoma supernatant, anti-FLAG Ab (Sigma–Aldrich) (1:500 dilution) or anti-actin Ab (Santa Cruz Biotechnology, Inc.) were used as primary Abs, and horseradish peroxidase (HRP)-conjugated secondary Abs; anti-rat Ab (Zymed Laboratories, San Francisco, CA, USA), anti-rabbit IgG Ab (Zymed Laboratories) or anti-goat IgG Ab (Bethyl Laboratories, Inc., Montgomery, TX, USA) were used as secondary Abs. The membrane was visualized by immersion in Western Lightning Chemiluminescence reagent (PerkinElmer). Immunoreactive bands were visualized using the Luminescent Image Analyzer LAS 3000 mini (FUJIFILM, Tokyo, Japan), and analyzed using Science lab 2005 (FUJIFILM).

Immunoprecipitation

Cells (1×10^7) were lysed at 4 °C for 30 min in ice-cold CHAPS buffer supplemented with Complete, Mini EDTA-free protease inhibitor mixture. Cell lysates were clarified by centrifugation at 12,000 × *g* for 5 min at 4 °C and the supernatant was precleared with 10 μl of protein A/G agarose (Santa Cruz Biotechnology, Inc.) for 1 h at 4 °C with rotation. The resultant supernatants were mixed at 4 °C overnight with 1 μg of each mAb, which was premixed with 10 μl of protein A/G agarose for 1 h at 4 °C. The immunoprecipitate was washed three times with PBS and used for Western blotting as described above.

Enzyme treatment

For enzyme treatment, Ema cells suspended in culture medium (5×10^6/ml) were incubated with 60 μg/ml *O*-Sialoglycoprotein endopeptidase (OSGE, Cedarlane Laboratories Ltd., Burlington, NC, USA) or 0.2 U/ml Neuraminidase (Roche Diagnostics K.K.) for 1 h at 37 °C. After incubation, the cells were washed once with medium, and stained with the appropriate Abs described in the text, followed by flow cytometric analysis.

Fusion of mononuclear cells and P3U1 cells to produce a rat monoclonal antibody library

Lymph node mononuclear cells (1×10^8) were mixed with P3U1 cells (2×10^7) and washed twice with serum-free RPMI1640. After removal of the supernatant, the cells were incubated at 37 °C for 2 min, then 0.5 ml of Polyethylene Glycol 1500 (Roche Diagnostics K.K., Tokyo, Japan) at 37 °C was added, followed by addition of 9 ml of serum-free RPMI1640 at 37 °C, and centrifugation at 900 rpm for 5 min at RT. After removal of the supernatant, the cells were suspended in 36 ml of GIT medium (Wako) containing 10% FBS and hypoxanthine-aminopterin-thymidine (HAT, Life Technologies Japan Ltd., Tokyo, Japan), and were cultured for 1 h at 37 °C in a humidified incubator with 5% CO_2 in air. BM-Condimed H1 medium (4 ml, Roche Diagnostics K.K.) was added, and the cells were seeded in four 96-well tissue-culture plates (100 μl/well), and cultured.

Construction of a retroviral expression vector with a Gateway cassette

Conversion of the retroviral expression vector pMxs-IG (kindly provided by Dr. T. Kitamura), which includes an IRES and GFP downstream of the multiple cloning site (MCS), to a

Gateway-compatible destination vector was carried out using the Gateway Vector Conversion System (Life Technologies Japan Ltd.) according to the manufacturer's instructions. pBluescript SK (-) was digested with SmaI, and then ligated with the Gateway reading–frame cassette A fragment. This vector was digested with SpeI, blunted with the Klenow fragment, and digested with XhoI, followed by ligation to the XhoI and SnaBI sites of the pMxs-IG vector. The resulting vector was designated as pMxs-IG-Gateway.

RESULTS AND DISCUSSION

By immunizing the rats with Ema cells, 179 different hybridomas that secreted Ab into the culture supernatant were obtained. Of these 179 supernatants, 69 were confirmed to react with Ema cells by flow cytometric analysis. Ultimately the mAb 6-1 was selected for identification of its cognate antigen that was expressed on canine lymphoid cell lines. By screening with panning methodology, some of EGFP-expressing colonies were isolated and were positively stained with mAb 6-1 (Fig. II-2A,B). PCR amplification of integrated cDNAs and nucleotide sequence analysis showed that the amplified product was highly homologous to canine P-selectin glycoprotein ligand-1 (cPSGL-1). The nucleotide sequence of cPSGL-1 cDNA and its deduced amino acid sequence are shown in Fig. II-3A (The DNA Data Bank of Japan (DDBJ)/European Molecular Biology Laboratory (EMBL)/GenBank ID: AB614446). This product has a 1323-bp coding region that contains the entire open reading frame of cPSGL-1, 5 bp of the 5' noncoding region, and more than 1.0 kbp of the 3' flanking region. Alignment of the predicted amino acid sequence of the cPSGL-1 cDNA clone with those of the human and mouse PSGL-1 cDNA is shown in Fig. II-3B. The sequences of the transmembrane and cytoplasmic domains were highly conserved between species, though the sequences of the extracellular domains were less conserved. Downstream of the PACE (paired basic-amino acid-converting enzymes) consensus motif in the extracellular domains, the region containing amino acids 42–144 showed low homology between species, except for two tyrosine residues near the threonine residue at amino acid 59 that are consistently found in other

species. In human PSGL-1, there are three tyrosines near this threonine residue and these tyrosines were shown to be essential for P-selectin binding. EGFP-expressing population in cPSGL-1-transduced P3U1 cells reacted with mAb 6-1 as well as anti-FLAG Ab (Fig. II-1B). This result indicated that the mAb 6-1 recognizes cPSGL-1. Among other mAbs produced by the hybridoma library, in addition to mAb 6-1, 12 other mAbs (30-2, 53-1, 64-1, 85-1, 88-1, 90-1, 97-1, 150-5, 151-7, 167-1, 176-15, and 177-1) reacted with cPSGL-1 (data not shown). The reactivity of each mAb, which was assessed by calculation of the mean fluorescent intensity (MFI), roughly classified these mAbs into two groups based on whether they showed weakly positive (ex. 6-1 in Fig. II-1B) or strongly positive (ex. 30-2 and 88-1 in Fig. II-1B) reactivity (Table II-2). Determination of the subclass of these Abs indicated that 53-1 and 176-15 were IgG1, κ and IgG2b, κ, respectively, and that the remaining Abs were IgG2a, κ (Table II-2).

Most of the Abs reacted with cPSGL-1 overexpressed in P3U1 by Western blotting, showing bands of 120 kDa (Fig. II-4A). However, some of the Abs (6-1, 64-1, 150-5 or 177-1) could only very weakly detect it (data not shown). Immunoprecipitation of overexpressed cPSGL-1 with each of the mAbs, 6-1, 64-1, 150-5, 177-1, as well as by anti-FLAG, and blotting with the anti-FLAG Ab, showed that all of the mAbs 6-1, 64-1, 150-5 and 177-1 immunoprecipitated a dimeric form of cPSGL-1 with a molecular weight of > 240 kDa, as well as a monomeric 120-kDa form (Fig. II-4B). The results showed that cPSGL-1 had much higher molecular weight than that calculated based on its amino acid sequence, indicating that cPSGL-1 is a highly glycosylated protein as has been shown for other species.

To clarify the domain of cPSGL-1 that was bound by each mAb, seven cPSGL-1 mutants with different deletions (Fig. II-1A) or different point mutations (Fig. II-1C) in the extracellular domain were constructed and expressed in P3U1 cells. All deleted mutant proteins expressed as the expected sizes on Western blotting (Fig. II-5). All mutants were expressed at a similar level by flow cytometric analysis using anti-FLAG Ab (Fig. II-1B,D). Deletion of the residues 145–274 (cPSGL-1-DM3) or residues 275–345 (cPSGL-1-DM4) did not alter the efficacy of binding of any Ab compared with wild-type cPSGL-1 binding (Fig. II-1B, Table II-2). In contrast, none of the mAbs reacted with cPSGL-1-DM2. Deletion of residues 19–41 (cPSGL-1-DM1) decreased the reactivities of mAbs 30-2, 53-1, and 85-1.

Tyrosine mutated constructs were expressed in P3U1 (Fig. II-1C). Most of the mAbs reacted with all three forms of mutated PSGL-1 in a similar manner to wild-type cPSGL-1. However, mAbs 88-1, 90-1, and 97-1 bound poorly to cPSGL-1/Y52F and cPSGL-1/Y52FY54F. The mAbs 151-7 and 167-1 only reacted with cPSGL-1 wild-type but not with any of the mutants (Fig. II-1D).

To determine if the mAbs recognized *O*-glycans or sialylated peptides of cPSGL-1, I wished to examine Ab reactivity following treatment of Ema cells with OSGE or neuraminidase. OSGE treatment abrogated PL-1 Ab reactivity to hPSGL-1 on HL-60 cells, but none of the mAbs bound to Ema cells after OSGE treatment (Fig. II-6A). Following neuraminidase treatment, the binding of mAb 6-1 to Ema cells was lower than that to the no treatment control, and mAb 177-1 showed no binding to Ema cells, but most of the mAbs with Ema cells were not altered (Fig. II-6B).

A total of 13 different mAbs against cPSGL-1 were characterized in this study and were categorized into at least 5 groups (Table II-2). The Abs in group A appeared to react with the cPSGL-1 protein domain involving the region spanning around amino acids 41 and 42. Within this domain, the Abs in groups B and C were shown to react with the region containing tyrosine at position 52, or with the two tyrosines at positions 52 and 54, respectively. In humans, sulfation of one of the three tyrosine residues was shown to be very important for binding to P-selectin [Pouyani *et al.*, 1995; Sako *et al.*, 1995; Wilkins *et al.*, 1995]. I have not determined whether the Abs that recognize the tyrosine residue(s) could block the binding of canine P-selectin to cPSGL-1, because a canine P-selectin protein is not available. However, group B and C Abs may possibly be useful for inhibition of canine P-selectin binding to cPSGL-1. It was indicated that mAbs 6-1 and 177-1 (group E) recognize sialylated polypeptides in the cPSGL-1 domain that spans amino acids 42–144. It has been reported that sialidase treatment of neutrophils abolishes PSGL-1 binding to P-selectin [Norgard *et al.*, 1993], indicating that sialylation of PSGL-1 is quite important for P-selectin binding in humans. Thus, these Abs could also be useful for blocking P-selectin binding to cPSGL-1.

In this study, I did not examine Ab reactivities to primary canine cells or tissues. I obtained the Abs of this study through immunization of rats with canine lymphoma cell line, which is consistent with the fact that PSGL-1 is expressed in leukocytes in other species. However, the types of cells that express cPSGL-1 need to be determined using these Abs. I also need to examine the difference in reactivities of these Abs with canine lymphoma cells and lymphocytes.

In conclusion, thirteen Abs that reacted to cPSGL-1 were obtained in this study and these Abs were classified into at least 5 groups. To date, no Abs have been available to detect cPSGL-1. These Abs appear to recognize different epitopes of cPSGL-1, indicating their potential usefulness in future studies of cPSGL-1.

Chapter 3

Anti-adhesive property of P-selectin glycoprotein ligand-1 (PSGL-1) due to steric hindrance effect

SUMMARY

P-selectin glycoprotein ligand-1 (PSGL-1) is an adhesive molecule that is known to be a ligand for P-selectin. An anti-adhesive property of PSGL-1 has not been previously reported. In this study, I show that PSGL-1 expression is anti-adhesive for adherent cells and I have elucidated the underlying mechanism. Overexpression of PSGL-1 induced cell rounding and floating in HEK293T cells. Similar phenomena were demonstrated in other adherent cell lines with overexpression of PSGL-1. PSGL-1 overexpression inhibits access of antibodies to cell surface molecules such as integrins, HLA and CD25. Cells transfected with PSGL-1 deletion mutants that lack a large part of the extracellular domain and chimeric construct expressing extracellular CD86 and intracellular PSGL-1 only showed rounded morphology, but there are no floating cells. These results indicated that PSGL-1 causes steric hindrance due to the extended structure of its extracellular domain that is highly *O*-glycosylated, but intracellular domain also has some effect on cell rounding. This study implies that PSGL-1 has Janus-faced functions, being both adhesive and anti-adhesive.

INTRODUCTION

P-selectin glycoprotein ligand-1 (PSGL-1) is a ligand for several adherent molecules, such as P-selectin, E-selectin, and L-selectin. PSGL-1 is expressed mainly by hematopoietic cells, including myeloid, lymphoid, and, in some circumstances, endothelial cells [Laszik *et al.*, 1996; da Costa Martins *et al.*, 2007]. PSGL-1 expressed on leukocytes functions as an adhesive molecule by binding to P-selectin or other adhesive molecules on endothelial cells during inflammation, and participates in tethering [Cummings, 1999]. In PSGL-1^{null} mice, leukocyte infiltration in the chemical peritonitis model was delayed, and leukocyte rolling *in vivo* was markedly decreased, after trauma [Yang *et al.*, 1999]. On the other hand, it was recently reported that PSGL-1-deficient T cells from PSGL-$1^{-/-}$ mice showed increased homotypic adhesion compared with wild-type cells [Matsumoto *et al.*, 2009]. This result indicates that PSGL-1 might function as an anti-adhesive molecule, in addition to its known function as an adhesive molecule.

One other molecule, CD43, has been previously reported to have a Janus-faced function, being both adhesive and anti-adhesive [Ostberg *et al.*, 1998]. Thus, whereas CD43 binds to its receptor on a neighboring cell, peripheral B cells from CD43-B cell transgenic mice showed a decreased ability to homotypically aggregate [Ostberg *et al.*, 1996], indicating that CD43 has two opposite effects; an adhesive and an anti-adhesive effect. Matsumoto *et al.* also showed that the loss of CD43, in addition to loss of PSGL-1, leads to a further increase in T cell adhesion [Matsumoto *et al.*, 2009].

Cell detachment caused by anti-adhesive activity is an important step in the process by which

cancer cells start to leave the primary tumor site for metastasis. In addition to CD43 as described above, many other molecules have been reported to have an anti-adhesive function, and most of them induce cell rounding and cell detachment from culture dishes after transfection into adherent cells. MUC1 and MUC21/Epiglycanin overexpression inhibits integrin-mediated cell adhesion to extracellular matrix components [Wesseling *et al.*, 1995; Yi *et al.*, 2010]. Sialomucin complex (SMC)/MUC4 overexpression disrupts cell-cell or cell-ECM interactions [Komatsu *et al.*, 1997]. Of these proteins, MUC1 is aberrantly overexpressed in human breast carcinomas and may relate to malignancy and poor prognosis in prostate, lung, and thyroid cancers [Lapointe *et al.*, 2004; Wreesmann *et al.*, 2004; Khodarev *et al.*, 2009]. MUC4 expression is upregulated in carcinomas of the pancreas, gall bladder, ovary, breast and lung, and was shown to be associated with the development of metastases [Komatsu *et al.*, 2000].

In this study, I analyzed the anti-adhesive properties of PSGL-1 and elucidated their mechanism.

MATERIALS AND METHODS

Cell culture

The B16F10 (mouse melanoma) and P3U1 (mouse myeloma) cell lines were maintained in R10 complete medium (RPMI1640 supplemented with 10% Fetal Bovine Serum (FBS), 100 units/ml penicillin, 100 μg/ml streptomycin and 55 μM 2-mercaptoethanol). The retroviral packaging cell line PLAT-E and PLAT-gp [Morita *et al.*, 2000], HEK293T [DuBridge *et al.*, 1987], HeLa, Mandin-Darby canine kidney (MDCK) and HEK 293 Tet-On® Advanced cell lines were grown in D10 complete medium (DMEM supplemented with the same reagents as R10). The Chinese hamster ovary (CHO) cell line was maintained in DMEM/Ham's F-12 culture medium (Wako Pure Chemical Industries, Ltd., Osaka, Japan) containing 10% FBS, 100 units/ml penicillin and 100 μg/ml streptomycin. These cell lines were cultured at 37 °C in a humidified incubator with 5% CO_2 in air. The CHO, HeLa and B16F10 cell lines were obtained from the Cell Resource Center for Biomedical Research (Institute of Development, Aging and Cancer, Tohoku University, Sendai, Japan). The PLAT-E cell line was kindly provided by Dr. Toshio Kitamura (University of Tokyo, Japan). The HEK 293 Tet-On® Advanced cell line was purchased from Clontech Laboratories, Inc. (Mountain View, CA, USA).

Construction of PSGL-1 expression vectors

To construct a vector that expresses human PSGL-1 (hPSGL-1), hPSGL-1 was amplified by PCR

using HL60 cDNA as a template and the primers YTM407 and YTM408 (Table III-1). PCR amplifications were performed in a final volume of 25 μl containing a pair of primers (0.3 μM each), 1 μl cDNA, 1× PCR buffer for KOD Plus, 0.2 mM dNTP, 2.5 mM $MgSO_4$ and 1.0 unit of KOD Plus (TOYOBO, Osaka, Japan). After incubation at 94 °C for 2 min, PCR was carried out under the following conditions: denaturation at 98 °C for 10 s, annealing at 56 °C for 30 s, and polymerization at 68 °C for 1.5 min. After 35 cycles, the polymerization step was extended at 68 °C for 10 min. The amplified PCR products were subcloned into the SmaI site of the pBluescript SK(-) vector, and the insert was cut with XhoI and NotI for insertion into the retroviral expression vectors pMXs-IG or pMXs-IP (kindly provided by Dr. T. Kitamura), generating pMx-IG-hPSGL-1#1 or pMx-IP-hPSGL-1.

To construct a vector that express mouse PSGL-1 (mPSGL-1), mPSGL-1 was excised from pEF-mPsgl-1 [Nishimura *et al.*, 2009] using BamHI and NotI and was cloned into the same sites of pMXs-IG or pMXs-IP (pMx-IG-mPSGL-1 or pMx-IP-mPSGL-1, respectively).

To construct expression vectors encoding hPSGL-1 deletion mutants, sequential PCR amplification was performed as follows: The first PCR was performed using pMx-IG-hPSGL-1#1 as a template with a 5′ primer (YTM178) and one of a number of 3′ primers (either YTM469, YTM473, YTM477, YTM535, YTM537, or YTM539) to amplify the hPSGL-1 region upstream of the deleted domain. The second PCR was performed using pMx-IG-hPSGL-1#1 as a template with one of a number of 5′ primers (YTM468, YTM472, YTM476, YTM534, YTM536, or YTM538) and a 3′ primer (YTM179) to amplify the region downstream of the deleted domain. For the third PCR

amplification, the appropriate overlapping PCR products were used as templates and were amplified using two cycles of denaturation at 94 °C for 15 s, annealing at 50 °C for 30 s, and polymerization at 68 °C for 1.5 min, after which the primers YTM178 and YTM179 were added and PCR was continued for an additional 25 cycles to generate hPSGL-1 deletion constructs. These PCR products were cleaved with XhoI and NotI and subcloned into the pMXs-IG vector to generate pMx-IG-hPSGL-DM1, pMx-IG-hPSGL-DM3, pMx-IG-hPSGL-DM5, pMx-IG-hPSGL-DM8, pMx-IG-hPSGL-DM9, and pMx-IG-hPSGL-DM10, which had truncations of 69 bp (23 amino acids), 450 bp (150 amino acids), 129 bp (43 amino acids), 54 bp (18 amino acids), 525 bp (175 amino acids), 210 bp (70 amino acids) and 81 bp (27 amino acids) respectively in pMx-IG-hPSGL-1#1 (Fig. III-12A).

To construct CD86 expression plasmids, mouse CD86 was amplified using mouse spleen cDNA as a template and the primers YTM618 and YTM619 (Table III-1). PCR amplifications were performed as described above. The amplified PCR products were subcloned into the SmaI site of the pBluescript SK (-) vector. Mouse CD86 was amplified using the primers YTM620 and YTM627 to add MluI and HpaI sites. The 5′ part of hPSGL-1 was amplified using the primers YTM178 and YTM622 to add a MluI site to the 3′ end. The 3′ part of hPSGL-1 was amplified using the primers YTM628 and YTM179. To construct a hPSGL-1 and mCD86 chimera (Fig. III-14A), mouse CD86, the 5′ part of hPSGL-1 and the 3′ part of hPSGL-1 were cut with MluI and HpaI, XhoI and MluI, and NotI, respectively, and these fragments were ligated into the XhoI and NotI sites of pMXs-IG (pMx-IG-hPSGL-mCD86#1).

To construct the canine CD25 expression plasmid that simultaneously expresses EGFP under the control of IRES, canine CD25 was excised from pMx-IP-cCD25 [Mizuno *et al.*, 2009] and cloned into the EcoRI and NotI sites of pMXs-IG, generating pMx-IG-cCD25#1.

To construct an expression plasmid containing a fusion of EGFP and canine CD25, canine CD25 was excised from pMx-IP-cCD25 and cloned into the EcoRI and XhoI sites of pcDNA3.1+ vector, and the insert was cut with NheI and XhoI for insertion into the expression vectors pEGFP-N1, generating pEGFP-N1-cCD25.

To construct a Tet-on inducible vector, pMx-IG-hPSGL-1#1 was cleaved with BamHI and NotI and subcloned into the pTRE-2pur vector to generate pTRE-2pur-hPSGL-1.

To construct the CD29 expression plasmids, pCMV-SPORT6 inserted with CD29 cDNA (HDG1180) (Health Science Research Resources Bank (HSRRB), Osaka, Japan) was digested with NcoI, blunted with the Klenow fragment, and digested with SalI, followed by ligation to the XhoI and SnaBI sites of the pMxs-IB vector, generating pMx-IB-ITGB1.

To construct the CD49e expression plasmids, CD49e cDNA was amplified by PCR using pOTB7 inserted with CD49e (HDG1353) (HSRRB) as a template and the primers YTM910 and YTM911 (Table III-1). The PCR product was incubated with Taq polymerase (Invitrogen Life Technologies, Carlsbad, CA, USA), and ligated into pCR2.1-TOPO vector (Invitrogen Life Technologies), generating pCR-ITGA5#2. This plasmid was cut with BamHI and XhoI, XhoI and NotI, and these fragments were ligated into the BamHI and NotI sites of pMXs-IP (pMx-IP-ITGA5#4).

The nucleotide sequences of all of the clones were confirmed by sequencing using the BigDye

Terminator v3.1 Cycle Sequencing kit (PerkinElmer, Inc., Waltham, MA, USA), followed by sequencing using the ABI PRISM3100-Avant sequencer (Applied Biosystems, Foster City, CA, USA).

Transfection

HEK293T cells (2.5×10^5) or other adherent cell lines (1.0×10^5) were seeded in a 6-well dish 1 or 2 days before transfection. Transfection of these cells was performed using TransIT-LT1 (Mirus Bio LLC, Madison, WI, USA) or Lipofectamine 2000 (Invitrogen) according to the manufacturer's instructions. The transfected cells were incubated for the indicated times and then used for further analysis.

Retroviral transduction

Retroviral transduction using PLAT-E cells was done as described previously [Umeki *et al.*, 2011]. When PLAT-gp cells was used as a packaging cells, pCMV-VSVG was cotransfeted with the retroviral vector. The viral supernatant were concentrated 10-fold with PEG-*it* Virus Precipitation Solution (System Biosciences, Mountain View, CA, USA) only when P3U1 cells were transduced with pSIREN-RetroQ retroviral vectors (QIAGEN, Valencia, CA, USA). After transfection, P3U1 or MDCK cells were cultured in the presence of 4 μg/ml of puromycin (Sigma Aldrich Japan K.K., Tokyo, Japan) to obtain stably transduced cells.

Tet-On inducible system

The Tet-dependent inducible PSGL-1 expression plasmid, pTRE-2pur-hPSGL-1, was transfected into HEK 293 Tet-On® Advanced cell lines using TransIT-LT1. Twenty-four hours after transfection, transfected cells were cultured in the presence of 2 μg/ml of puromycin (Sigma-Aldrich Japan K.K.) to select colonies which stably expressed Tet-responsive hPSGL-1. Once the colonies were obtained, I cloned each colony by applying the limiting dilution method and further analyzed these clones to confirm the expression of hPSGL-1. The resulting clone that was used for further experiments was termed HEK293/Tet-ON/hPSGL-1.

PSGL-1 knockdown

Two siRNAs against mouse PSGL-1 sequences and the negative control siRNA were designed by QIAGEN. Based on these siRNA sequences, oligonucleotides for each siRNA were designed, annealed and cloned into the BamHI and EcoRI sites of the pSIREN-RetroQ Retroviral vector (Clontech Laboratories, Inc.). pSIREN-NC#2 (NC#2) was used as a negative control while pSIREN-mSleplg-2#1 (2#1) and pSIREN-mSleplg-3#3 (3#3) were used as vector of siRNA of mouse PSGL-1.

Flow cytometry

Flow cytometric analysis was done as previously described [Umeki *et al.*, 2011]. Primary antibodies were follows: anti-human PSGL-1 (PL-1; Santa Cruz Biotechnology, Inc., Santa Cruz,

CA, USA); anti-mouse PSGL-1, anti-mouse CD86-FITC (all from BD Biosciences, San Diego, CA, USA); anti-CD49a, anti-CD49b, anti-CD49d (all from Millipore, Bedford, MA, USA); anti-CD49c, anti-CD29, anti-CD49e, anti-CD49f, anti-CD51 (all from Biolegend, San Diego, CA, USA); anti-HLA-ABC Biotin and anti-mouse MHCI biotin (eBioscience, San Diego, CA, USA) and anti-CD25-PE (Dako, Carpinteria, CA, USA). The appropriate secondary antibodies were follows; anti-rat IgG-RPE (Southern Biotech, Birmingham, AL, USA), anti-mouse IgG-PE (Santa Cruz Biotechnology, Inc.), anti-mouse IgM-PE (Southern Biotech) or Streptavidin-PE (eBioscience). For intracellular staining, the cells were fixed and permeabilized using the Fixation and Permeabilization Solution (BD Biosciences) according to the manufacturer's instructions, and were stained with anti-PSGL-1 antibody (C-19) (Santa Cruz Biotechnology, Inc.) followed by staining with anti-goat IgG-PE (Abcam, Cambridge, UK).

The samples were analyzed using CyFlow space (Partec, Munster, Germany), and the results obtained were analyzed using FlowJo software (Treestar, Inc., San Carlos, CA, USA).

Confocal microscopy

HEK293/Tet-ON/hPSGL-1 cells were transfected with pEGFP-N1-cCD25. Twenty-four hours after transfection, 1 μg/ml of doxycycline was added to the culture to induce the expression of PSGL-1. A further 24 h incubation after addition of doxycycline, the cells were stained with anti-PSGL-1 antibody (PL-1) as primary antibody for 30 min at 4°C. After two washes at 4°C, the cells were incubated with an Alexa Fluor 633-conjugated goat anti-mouse antibody (Invitrogen Life

Technologies) for 30 min at 4°C. The samples were analyzed by confocal microscopy, a LSM 510 META (Carl Zeiss, Jena, Germany).

Western blotting

Cells were lysed at 4 °C for 30 min in ice-cold CHAPS buffer (3% CHAPS, 30 mM Tris HCl (pH 7.5), 150 mM NaCl) or NP40 buffer (1% NP40, 10 mM Tris HCl (pH 7.5), 150 mM NaCl, 1mM EDTA) supplemented with complete, Mini EDTA-free protease inhibitor mixture (Roche Diagnostics K.K., Tokyo, Japan). SDS-PAGE and Western blotting were done as described previously [Umeki *et al.*, 2011]. Primary antibodies were follows: anti-hPSGL-1 (PL-1) and anti-actin (all from Santa Cruz Biotechnology, Inc.); anti-mouse PSGL-1 (BD Biosciences); anti-CD29, anti-CD49d, anti-CD49e, anti-CD51, anti-Akt antibody, anti-cyclin D1 antibody, anti-cyclin D2 antibody, and anti-cyclin D3 antibody (all from Cell Signaling Technology, Inc., Danvers, MA, USA); anti-CD49f (GeneTex Inc.); anti-HLA-ABC Biotin (eBioscience); anti-Bcl-2 antibody (Biolegend). For detection, horseradish peroxidase (HRP)-conjugated Streptavidin (Sigma-Aldrich Japan K.K.) or with the appropriate HRP-conjugated secondary antibody, anti-rabbit IgG antibody, anti-mouse IgG antibody, anti-rat IgG antibody (all from Zymed Laboratories), or anti-goat IgG antibody (Bethyl Laboratories, Inc., Montgomery, TX, USA) were used.

Cell counting of detached and attached cells

For examination of PSGL-1-induced anti-adhesive properties, the number of detached or

attached cells was counted after induction of PSGL-1. Suspended cells were collected and counted at the indicated time point. Subsequently, adherent cells were trypsinized and counted. For cell counting using a transient transfection system, suspended cells were collected for counting at the indicated time point after transfection, and were used for flow cytometric analysis of the percentage of EGFP-positive cells. EGFP-positive adherent cells were counted under a fluorescent microscope to analyze the numbers of adherent cells showing non-rounded or rounded-shapes. For counting P3U1 cells stably overexpressing mPSGL-1, the cells were seeded in 6-well plate at 2.0 x 10^5 per well. Twenty-four hours after seeding, floating and adherent cells in P3U1 were counted.

Counting of ECM-attached cells

Ten μg/ml of collagen type I-C (Cellmatrix, Nitta Gelatin, Osaka, Japan), fibronectin (Roche Diagnostics K.K.) or laminin (Roche Diagnostics K.K) were seeded in a 24-well plate and incubated overnight at 4 °C. Ten μg/ml of Poly-L-lysine (Sigma-Aldrich Japan K.K.) was incubated in a 24-well plate for 5 min at RT and then dried for 2 h at RT. Subsequently, these wells were blocked with 3% BSA in PBS for 3 h at RT. Twenty-four hours after treatment with doxycycline, either floating or the remaining attached HEK293/Tet-ON/hPSGL-1 cells were collected, and seeded at 8.0 × 10^4 per well. P3U1 cells were seeded at 1.3 x 10^5 per well. After incubation for 1 h at 37 °C, the supernatant was removed. The remaining attached cells were counted using a hemocytometer after trypsin treatment.

Anoikis assay

Polyhydroxyethylmethacrylate (poly-HEMA; Sigma-Aldrich Japan K.K.) was dissolved at 120 mg/ml in 95% ethanol and diluted 1:10 with 95% ethanol [Folkman and Moscona, 1978]. Then, 96-well plate was coated three times with poly-HEMA and washed twice with PBS before use. MDCK cells stably expressing hPSGL-1 (MDCK/pMx-IP-hPSGL-1) or empty vector (MDCK/pMxs-IP) were established. Trypsinized MDCK/pMxs-IP and floating fraction of MDCK/pMx-IP-hPSGL-1 cells were seeded in poly-HEMA coated 96-well plates at a density of 1.0 $\times$ 10^5 cells/ml. The cells were stained with 40 μg/ml propidium iodide (Nacalai Tesque, Kyoto, Japan) or 2 μg/ml Hoechst 33342 (Sigma-Aldrich Japan K.K.) at indicated time points and counted under a fluorescent microscope to analyze the number of dead cells.

RESULTS

Overexpresion of PSGL-1 induced cell detachment in several adherent cell lines

During analysis of canine PSGL-1 function in previous report [Umeki *et al.*, 2011], I observed that PLAT-E cells overexpressing flag-tagged canine PSGL-1 had a round morphology and detached from the culture dish. This result prompted me to analyze the potential anti-adhesive properties of PSGL-1 in adherent cells. I next expanded my investigation of PSGL-1-induced cell detachment to human and mouse PSGL-1 in HEK293T cells. Transient transfection of the EGFP-expressing empty vector or unrelated single-spanning transmembrane protein, canine CD25 (cCD25) [Mizuno *et al.*, 2009], -expressing vector did not induce any morphological change in the EGFP-positive HEK293T cells (Fig. III-1A). However, when hPSGL-1- or mPSGL-1-expressing plasmids were transfected, the EGFP-positive HEK293T cells started to round up and float at 18 h after transfection and most of them were floated at 48 h after transfection, whereas cells weakly expressing EGFP tended to remain attached (Fig. III-1A,B,C). This result indicated that PSGL-1 exerted anti-adhesive activity irrespective of the species origin of PSGL-1. Based on this result, I decided to further investigate the anti-adhesive properties of hPSGL-1.

I therefore further tested the anti-adhesive effect of PSGL-1 following transfection into other adherent cell lines, HeLa, B16F10 or CHO cells, which did not show any endogenous PSGL-1 expression (data not shown). Cell lines transfected with the empty EGFP-expressing vector or cCD25-expressing vector did not show any morphological change, but overexpression of hPSGL-1

in the same vector induced rounding and floating of the EGFP-expressing cells (Fig. III-2). These results indicated that adherent cell lines displayed altered morphology and decreased attachment after overexpression of PSGL-1, independent of the type of cell line used.

Inducible expression of PSGL-1 resulted in cell detachment

To analyze the time dependent kinetics of PSGL-1-induced morphological changes, a tetracycline-inducible system was established, in which hPSGL-1 expression was reversibly regulated by addition or removal of doxycycline.

Addition of doxycycline at concentrations ranging from 0.001 μg/ml to 0.1 μg/ml induced a dose-dependent expression of hPSGL-1 by flow cytometry (Fig. III-3A) and Western blotting (Fig. III-4A). In the absence of doxycycline, no rounded or floating cells were observed under this condition (Fig. III-3B). Following 0.1 μg/ml treatment, only 10% of the cells were attached to the dish without any noticeable morphological change. The remaining cells were rounded, and most of these cells were floating (Fig. III-3B). Ten μg/ml of doxycycline did not induce any morphological change in parental HEK293/Tet-ON cells (Fig. III-4B,C).

Time-course experiments showed that PSGL-1 was already strongly expressed, and could be easily detected 9 h after the addition of doxycycline (Fig. III-5A,B). PSGL-1 expression was further enhanced at 18 h and subsequently did not change dramatically up to 72 h. At 18 h after induction, more than half of the cells had detached from the dishes and were floating (Fig. III-5C). The number of floating cells gradually increased over time up to 72 h, at which time most of the cells were

floating.

Floating cells could survive in long-term culture and re-attach to dishes upon PSGL-1 downregulation

After addition of doxycycline, cell death was not observed in detached and floating cells and these floating cells were shown to survival by trypan blue dye exclusion. Furthermore, in the presence of doxycycline, detached, suspended cells grew well until day 19 when I stopped the culture (Fig. III-3C). To clarify whether cell cycle progression factors such as cyclin D1, D2, D3, and survival factor Bcl-2 are induced by PSGL-1 in floating cells, Western blotting was performed. In HEK293/Tet-ON/hPSGL-1 treated with doxycycline, the levels of cyclin D1, D2, D3 and Bcl-2 were continuously detected and were not different as compared with those in control cells, except Bcl-2 was transiently increased in PSGL-1-induced floating cells 48 h after induction (Fig. III-6). Moreover, I examined whether anoikis was inhibited in PSGL-1-induced floating cells. MDCK cell line, sensitive to anoikis, expressing empty vector showed time dependent increment of dead cells, but floating MDCK cell line which was induced by hPSGL-1 overexpression showed less amount of cell death at 24 and 48 h after culture (Fig. III-7).

I next determined if the floating cells could reversibly attach to the dish after floating in culture for several days. Following culture for seven days in the presence of doxycycline, doxycycline was then removed. Approximately half of the cells showed a rounded morphology and remained floating, but the other half of the cells started to attach to the dish over the next 24 h, showing a fibroblast-like

morphology (Fig. III-3D). At 48 h after the removal of doxycycline, during which time the cells were continuously cultured in the absence of doxycycline, most of the cells were attached to the dish (Fig. III-3D). PSGL-1 expression was detected in the floating cells at day 8 after Dox treatment, but, after further 4 days culture without Dox, most of cells were reattached, in which PSGL-1 expression was lost (Fig. III-3E).

PSGL-1 overexpression inhibited cell adhesion to the ECM and antibody access to the integrins

Adherent cells attach to the dish via interaction between adherent molecules such as integrins on the cells and the extracellular matrix (ECM). The type of ECM molecule that was responsible for binding of HEK293T cells to the dishes and that is affected by PSGL-1 induction, was examined. Approximately half of the HEK293/Tet-ON/hPSGL-1 cells were attached to collagen, fibronectin, or laminin after 1 h incubation without doxycycline (Fig. III-8A). However, doxycycline-induced PSGL-1 overexpression significantly reduced the number of attached cells. This result indicated that PSGL-1 expression inhibited the interaction between cell surface molecules and the ECM on the dish.

Adherent cells attach to cell dishes through an interaction between the ECM and cell surface integrins. HEK293/Tet-ON/hPSGL-1 cells expressed several integrins; CD29, CD49a, CD49b, CD49d, CD49e, CD49f and CD51 but minimal CD49c on the cell surface (Fig. III-8B). Whereas doxycycline treatment of HEK293/Tet-ON/hPSGL-1 induced the expression of PSGL-1, it reduced the reactivity of each antibody with its cognate integrin (Fig. III-8B). I next determined the protein

expression level of each integrin using Western blotting. The expression levels of CD29 and CD49e were reduced by doxycycline treatment, but the expression level of CD49f and CD51 was similar before and after doxycycline treatment and CD49d integrin expression was increased after treatment (Fig. III-8C). These results indicated that the level of cell surface integrins that was detected was lower than that before induction of PSGL-1 expression. For some, but not all, integrins this decreased detection was due to reduced protein expression.

Furthermore, I determined the expression levels of integrins in adherent and foating cells in HEK293T transiently transfected with pMxs-IG (mock), pMx-IG-cCD25 (cCD25), pMx-IG-hPSGL-1#1 (hPSGL-1) or pMx-IG-mPSGL-1 (mPSGL-1) (Fig. III-1D,E). The reactivity of integrin antibodies against CD29, CD49e and CD49f in floating cells were completely lost after induction of human or mouse PSGL-1 (Fig. III-1D). On the other hand, Western blotting showed that the protein expression levels of CD29 and CD49e in floating cells were lower than that in adherent cells (Fig. III-1E), but the expression level of CD49f was not altered in adherent and floating cells. These results are consistent with the results of doxycycline treatment of HEK293/Tet-ON/hPSGL-1 (Fig. III-8B,C).

To prove that the reduced expression of CD29 and CD49e shown by Western blotting not contributed to the cell detachment of hPSGL-1-induced cells, HEK293T cells were tritransfected with pMx-IB-ITGB1 (CD29), pMx-IP-ITGA5#4 (CD49e), and either of pMxs-IG (mock), pMx-IG-cCD25 (cCD25) or pMx-IG-hPSGL-1#1 (hPSGL-1) (Fig. III-9A,B). Even if CD29 and CD49e were overexpressed together with PSGL-1, cell floating and rounding were induced (Fig.

III-9B). This result suggested that downregulated integrin proteins were not major concerns of cell detachment induced by PSGL-1.

Increment of PSGL-1 expression inhibited the accessibility of other molecules

Since PSGL-1 has been reported to be a rod-shaped extended protein [Li *et al.*, 1996], which possibly sterically hinders the access of antibody to cell surface molecules, the effect of PSGL-1 expression on the reactivity of an antibody to another cell surface molecule was determined. Cell surface expression of HLA-ABC was detected by flow cytometry before induction of PSGL-1 in HEK293/Tet-ON/hPSGL-1 cells, but a dose-dependent reduction in detectable HLA-ABC expression was observed after induction of PSGL-1 (Fig. III-10A). However, the total level of HLA-ABC protein expression, as determined by Western blotting, was not different in cells expressing different levels of PSGL-1 (Fig. III-10B).

I next examined whether overexpressed PSGL-1 sterically hinders antibody detection of an exogenously expressed molecule. Canine CD25 was transfected into HEK293/Tet-ON/hPSGL-1 cells and PSGL-1 expression was induced by doxycycline (Fig. III-10C). The EGFP gate in flow cytometric analysis indicated that, in CD25-transfected cells, the detection of cell surface expression of CD25 was clearly reduced in PSGL-1-expressing cells (Fig. III-10C). I performed the confocal microscopy to examine CD25 distribution before or after PSGL-1 overexpression. CD25 and PSGL-1 were equally and similarly distributed in the floating cells as well as adherent cells (after trypsinized), even after both molecules were overexpressed (Fig. III-11).

These data indicated that overexpressed PSGL-1 sterically inhibited antibody access to cell surface molecules, and that the phenomenon of floating may occur as a result of inhibition of the interaction between integrins and ECM molecules.

The extracellular domain of PSGL-1 is important for cell detachment

To determine the region of PSGL-1 that is responsible for cell detachment, several deletion mutants that lack specific regions of the extracellular domain were constructed (Fig. III-12A). All deletion mutants were expressed at a similar level in HEK293T cells as judged by intracellular flow cytometry (Fig. III-13) and Western blotting (data not shown). Floating cells accounted for approximately 30% of the total number of cells in HEK293T cells transfected with hPSGL-1 WT, and almost all of these cells were EGFP positive (Fig. III-12B). Of the adherent cells that expressed EGFP, half of the cells were rounded and the other half showed the original morphology. The EGFP signal of the rounded adherent cells was brighter than that of the non-round adherent cells. The proportion of EGFP-positive cells that were floating, rounded adherent or non-round adherent cells was similar for most of the deletion mutants; pMx-IG-hPSGL-DM1, -DM5, -DM9, and -DM10. In contrast, cells transfected with either pMx-IG-hPSGL-DM3 or -DM8 did not show any floating cells and EGFP-positive cells were composed only of rounded and non-round adherent cells (Fig. III-12B). The percentage of rounded adherent cells was fairly similar to that in the other mutants.

Since DM3 and DM8 lack a large part of the extracellular domain of PSGL-1, which has many *O*-glycosylation sites, I investigated the contribution of *O*-glycosylation to PSGL-1-mediated effects.

I therefore constructed a plasmid that encodes a chimeric protein in which 202 amino acids in the extracellular domain of hPSGL-1 were replaced with 205 amino acids of the extracellular domain of mouse CD86 (Fig. III-14A). This region of mouse CD86 has a similar number of amino acids as the region of the PSGL-1 extracellular domain it replaces, but has a lower number of *O*-glycosylation sites. Flow cytometric analysis of HEK293T cells overexpressing this chimeric protein showed that the fluorescent intensity of PL-1 bound to hPSGL-1 and hPSGL-mCD86 expressed in HEK293T cells was similar (Fig. III-15A). Interestingly, when hPSGL-mCD86 was transfected into HEK293T cells, EGFP-positive cells showed a rounded morphology that was similar to that of hPSGL-1-transfected HEK293T cells, but none of the cells were floating (Fig. III-14B). This result may suggest that the region of PSGL-1 that was replaced with the region of mCD86 contributes to the anti-adhesive property of PSGL-1, but is not related to events that resulted in a rounded morphology.

Increment of PSGL-1 expression inhibited the accessibility of cell surface molecules and increased the floating cells in P3U1 cells

To extend my observation that PSGL-1 has steric hindrance effect in adherent cells, I tested if PSGL-1 has similar effect in non-adherent, but semi-adherent rounded cell line, mouse myeloma P3U1 cell line, which constitutively expressed PSGL-1 on the cell surface. I explored the alteration of PSGL-1 expression on cell surface could change the accessibility of other molecules. Mouse PSGL-1 was retrovirally transduced into P3U1 cell line, resulting in P3U1/mPSGL-1.

P3U1/mPSGL-1 expressed more PSGL-1 on their cell surface than parental P3U1 cell line (Fig. III-16A). Cell surface expression of CD49f was detected by flow cytometry in P3U1 cell line, but was decreased in the P3U1/mPSGL-1 cell line (Fig. III-16A). Furthermore, in P3U1/mPSGL-1 cell line, MHCI expression was decreased as compared to empty vector-transduced P3U1 cells (Fig. III-16B). Although P3U1 cells were semi-adhesive cells expressing endogenous PSGL-1, additional overexpression of PSGL-1 induced cell detachment in more than half of the cells (Fig. III-16C). This result indicated that steric hindrance effect by PSGL-1 expression on cell surface is not limited to the adherent cell line, but is observed even in the cells, which already expressed PSGL-1 to some extent.

Finally, I examined the loss of function of PSGL-1 in P3U1 cells on cell adherence and accessibility of other molecules. PSGL-1 expression was reduced in P3U1 transduced with 2#1 or 3#3, but not in NC#2 (Fig. III-17A) by flow cytometry. Reactivities of MHCI and CD49f antibodies were not altered in PSGL-1-knockdowned P3U1 cells (Fig. III-17A). PSGL-1-knockdowned P3U1 cells did not show any increment of binding to ECM proteins, collagen, fibrinogen and laminin, as compared to mock or NC#2 transduced P3U1 cells (Fig. III-17B).

DISCUSSION

In this study, I found that expression of exogenous PSGL-1 induced morphological changes, such as cell rounding, in adherent cells in which there is no endogenous expression of PSGL-1. This cell morphological change led to cell floating in some cases. PSGL-1 has been considered as an adherent molecule and as a ligand for P-selectin, but my observations indicate that PSGL-1 also has the opposite property of anti-adhesion when it is ectopically expressed in adherent cells, such as HEK293T, HeLa, B16F10 or CHO cells. PSGL-1 is expressed mainly in hematopoietic cells [Laszik *et al.*, 1996] and not in other kinds of tissues. Therefore, it is unclear if PSGL-1 is ectopically expressed under any condition in cell types other than hematopoietic cells. A previous study reported that PSGL-1 was expressed in the prostate cancer cell line, MDA PCa 2b, and that metastatic bone tissues of prostate cancer, but normal prostate tissue or benign prostate tumor, expressed PSGL-1 [Dimitroff *et al.*, 2005]. These results suggested that PSGL-1 expression in metastatic prostate cancer cells is important as a ligand for E-selectin in bone tropism of prostate tumor cells, but that the anti-adhesive property of PSGL-1 may also be an important characteristic of cancer cells in these metastatic processes. Most of experiments in this study have been done using HEK293 cell line, because this cell line was easy to be transfected and expresses high level of protein. Furthermore, HEK293T cell was used in many previous studies, in which function of the other anti-adhesive molecules were examined [Van Brocklyn *et al.*, 1999; Kinoshita *et al.*, 2001; Lawrenson *et al.*, 2002; Yi *et al.*, 2010]. But, the increased expression of PSGL-1 even in the cells expressing

endogenous PSGL-1, such as leukocytes, may contribute to adhesive function of cells to ECM, as shown in P3U1 cell line (Fig. III-16). On the other hands, I did not elucidate a functional role of PSGL-1 in physiological condition in this study, because overexpression of PSGL-1 in the cell lines was an artificial system. Further investigations were required to prove the physiological importance of PSGL-1-induced cell detachment.

One mechanism by which cells detach from culture dishes is considered to be a decreased interaction between ECMs on the dish surface and cell surface integrins. PSGL-1-overexpressing HEK293T cells showed lower binding to each of the ECM proteins collagen, fibrinogen and laminin that I tested, whereas PSGL-1-expressing and non-expressing HEK293T cells bound similarly to a Poly-L-lysine-coated dish (Fig. III-8A). This result is consistent with the fact that integrin expression was reduced after PSGL-1 induction, as detected by flow cytometry. However, unexpectedly, some of the integrins (CD29 and CD49e) were downregulated at the protein level whereas others were not (Fig. III-8C). I did not determine the mechanism by which the protein levels of these integrins were decreased during PSGL-1 induction. In contrast, the protein level of CD49d was actually increased following PSGL-1 induction despite the fact that no CD49d was detected by flow cytometry. Furthermore, exogenous transduction of CD29 and CD49e to compensate the reduced expressions of both proteins still induced the PSGL-1-induced cell floating phenomenon (Fig. III-9). These results indicated that, although some integrins might be downregulated at the protein level during PSGL-1 induction, this decrease was not the main reason for the lower expression of all of the integrins tested in this study that was detected by flow cytometry in PSGL-1-overexpressing cells compared with

PSGL-1-non-expressing cells (Fig. III-8B). Similar results were observed for HLA-ABC or CD25 molecules. The reduced detection of HLA-ABC by flow cytometry, but an unaltered level of protein expression as shown by Western blotting. PSGL-1 also inhibits the access of antibody to the exogenously transduced CD25. These results indicated the possibility that PSGL-1 overexpression might inhibit the access of antibodies to cell surface molecules. These results further encouraged my speculation that antibody detection of cell surface molecules was inhibited by PSGL-1 overexpression due to steric hindrance effect.

PSGL-1 is a highly *O*-glycosylated protein, which forms a rod-like structure that extends over 50 nm from the cell surface [Li *et al.*, 1996]. This highly *O*-glycosylated sites expanded in the extracellular domain of PSGL-1, containing various number of tandem repeats. Because human and mouse PSGL-1 have many tandem repeats similarly in the extracellular domain despite that the numbers of repeats were variable [Yang *et al.*, 1996], transduction of human and mouse PSGL-1 caused cell detachment similarly (Fig. III-1A,C). The length of most cell surface molecules does not exceed 35 nm [Ostberg *et al.*, 1998]. This long structure seen in PSGL-1-overexpressing cells may inhibit the access of other molecules such as antibodies to cell surface molecules, resulting in poor detection of the surface molecule by antibody. This phenomenon is known for other molecules and steric hindrance has been reported to be a feature of other cell surface molecules such as MUC1 [Gendler, 2001], Sialomucin complex (SMC)/MUC4 [Komatsu *et al.*, 1997] and Mucin21/Epiglycanin [Yi *et al.*, 2010]. I did not evaluate whether the degycosylated form of PSGL-1 alters cell detachment properties, because treatment with *O*-sialoglycoprotein endopeptidase

during cell culture induced cell death of HEK293T cells. Transfection of deletion mutants of PSGL-1 in HEK293T cells showed that the propeptide (PP) domain, the domain between PP and the decameric repeat (DR) domain, and the domain between the DR and the transmembrane (TM) domain was not essential for the anti-adhesive property of PSGL-1. However, the deletion mutants, DM3 and DM8, which lacked large part of the extracellular domain, had fewer floating cells, although a similar number of rounded attached cells was still observed. DM3 and DM8 had a much smaller molecular weight than the other deletion mutants (data not shown), indicating that both deletion mutants lacked a large amount of glycosylation, which occurs in the deleted region. This result indicates that an extended structure that is heavily *O*-glycosylated may contribute to the anti-adhesive property of PSGL-1.

Cells overexpressing a hPSGL-mCD86 chimeric protein showed fewer floating cells, but a similar number of rounded cells as cells overexpressing WT hPSGL-1 (Fig. III-14B). The cell surface expression of this hPSGL-mCD86 protein was similar to that of hPSGL-1 when overexpressed in HEK293T cells, as shown by flow cytometry. The region of PSGL-1 that was replaced with mCD86 had a similar number of amino acids as the substituted mCD86 region, but had more potential *O*-glycosylation (53 vs. 28 serine/threonine residues), and fewer potential *N*-glycosylation (2 vs. 7) sites. The hPSGL-mCD86 protein migrated as a 140 kDa dimer in a non-reducing gel analyzed by Western blotting, whereas the hPSGL WT dimer has a molecular weight of 250 kDa. These data indicate that hPSGL-mCD86 did have less *O*-glycosylation than hPSGL-1 WT, as was expected based on the amino acid sequence of the substituted mCD86 region.

Transfection of DM3, DM8, hPSGL-mCD86 into HEK293T cells induced fewer floating cells. However, most of the cells showed a round shape, although they still attached to the culture dishes. I did not determine how cell rounding occurred without induction of cell floating in these hPSGL-1 mutant-transfected cells. It is indicated that transmembrane and cytoplasic domains of PSGL-1 might be sufficient to induce cell rounding property in adherent cells.

Floating cells induced by PSGL-1 overexpression survived for more than 2 weeks in the presence of doxycycline (Fig. III-3C). This was an unexpected result. It was previously reported that sphingosine 1-phosphate (S1P) induced cell floating, similar to PSGL-1, but these floating cells died by apoptosis [Van Brocklyn *et al.*, 1999]. Usually adherent cells receive growth signal from adherent molecules such as integrins. Once cells start to float, this means that there is no growth signal from adherent molecules, which results in cell death. However, the number of PSGL-1-induced floating cells actually increased over time, and cell death was not observed in this study. This observation means that PSGL-1-expressing cells could survive for a while after detachment, which is a very important phenomenon. Thus, if PSGL-1 was ectopically expressed in adherent cells in some pathological situation, detached PSGL-1-expressing cells could circulate and survive for long enough to find a new place to reside in. Furthermore, PSGL-1 overexpression in MDCK cell line, which was shown to be anoikis-sensitive [Emoto, 2008], inhibited the cell death as compared to control at 24 and 48 h after culture (Fig. III-7). Cell survival and resistance of anoikis observed in PSGL-1-indced cell lines may be important mechanism for cancer cell survival. But I could not identify the proteins participating in these mechanisms in this study (Fig. III-6). Therefore further

investigation may need to clarify this in detail. There has been no report of cancer cells that express PSGL-1, except for human metastatic prostate tumor cells in bone marrow [Dimitroff *et al.*, 2005]. In that study, normal, benign and malignant prostatic tissues were shown to be largely negative for PSGL-1 expression, but PSGL-1 expression was higher in prostate tumor cells in bone metastasis. A survey of the expression of PSGL-1 in cancer tissues therefore needs to be carried out, especially in metastatic tissues.

I also observed effect of PSGL-1 in P3U1 cells, which are semi-adherent and express PSGL-1 constitutively. PSGL-1 overexpression in P3U1 cells decreased antibody accessibility to HLA or CD49f and attached cell (Fig. III-16). Against my expectations, PSGL-1 knockdown in P3U1 cells did not increase antibody accessibility to HLA or CD49f and the binding to the ECM (Fig. III-17). These results indicate that overexpression of PSGL-1 induced steric hindrance effect in the rounded cells such as P3U1 as well as adherent cells, but knockdown of PSGL-1 did not show the inhibition of steric hindrance effect. As shown by flow cytometry (Fig. III-17), the reduction efficiency of PSGL-1 expression by knockdown may not be sufficient to increase the antibody accessibility to HLA or CD49f. Or, the floating cells in origin, such as leukocytes, express not only PSGL-1 but other surface molecules such as CD43, which have long structure as similar as PSGL-1 [Ardman *et al.*, 1992] and may contribute to the remaining function of steric hindrance effect.

In addition to the property of decreased attachment, a second possible important effect of steric hindrance is escape from immunosurveillance during metastasis, since it has been previously shown that MUC1 and MUC4 inhibited tumor killing by LAK cells [van de Wiel-van Kemenade *et al.*,

1993; Komatsu *et al.*, 1999]. Although P3U1 constitutively and highly expressed PSGL-1 on their cell surface, increment of PSGL-1 in P3U1 showed less binding property of anti-CD49f antibody and anti-MHCI antibody of cell surface molecule and increase of the floating cells (Fig. III-16). This means that alteration of PSGL-1 expression on cells, which constitutively expressed PSGL-1, such as lymphocytes, change accessibility by other cell surface molecules on the neighbor cells. This may be one of the mechanisms of increased homotypic aggregation in PSGL-1-deficient T cells from PSGL-$1^{-/-}$ mice in previous report [Matsumoto *et al.*, 2009]. My findings in this study thus indicate that PSGL-1 might be new key factor for cancer biology.

In this study, I found important cell biological phenomenon caused by PSGL-1. Cell detachment of adherent cells, reduction of antibody accessibility, enhanced survival and resistance of anoikis, which were observed in PSGL-1-transduced cell lines, were new findings. Since PSGL-1 was exogenously overexpressed into several cell lines but not primary cells, physiological importance of these phenomenon were not elucidated. But further investigation may lead to the demonstration of importance of PSGL-1-induced steric hindrance effect in physiological status.

GENERAL DISCUSSION

In chapter 1, the five canine lymphoma cell lines (Ema, CLC, CLK, Nody-1 and UL-1) that were established in this work, and a comparison of their *in vitro* and *in vivo* properties were presented.

The establishment of canine lymphoma cell lines from many types of clinical samples including lymph node, body fluid, or lymphoma masses from dogs was attempted. Unfortunately, this was not possible except from bodily fluids. This confirms that it is easier to establish canine lymphoma cell lines from bodily fluids rather than tissues, as previously reported by other researchers [Kisseberth *et al.*, 2007; Momoi *et al.*, 1997; Nakaichi *et al.*, 1996]. There are few B-cell lymphoma cell lines available for researchers to utilize [Zwingenberger *et al.*, 2012]. The establishment of cell lines from dogs with B-cell lymphoma is more difficult, as lymphoma samples are generally obtained from peripheral lymph nodes rather than bodily fluids.

At present, there are few studies on xenotransplantation of canine lymphoma cell lines in NOD/SCID mice [Kisseberth *et al.*, 2007; Nadella *et al.*, 2008]. This thesis provides useful information to researchers who wish to perform xenotransplantation of canine lymphoma cells in NOD/SCID mice. In this study, lymphoma cell lines were intraperitoneally transplanted into NOD/SCID mice and this might not reflect the pathogenesis of original tumors. Therefore, transplantation of lymphoma cells by intravenous or subcutaneous injection is superior in elucidating the reproducibility of various conditions. The NOD/SCID mice that were used in this study have natural killer (NK) cell activity, but lack T- or B-cells. On the other hand, NOD/Scid/Jak3null (NOJ) or NOD/Shi-scid IL2rγ null (NOG) mice are severely immunodeficient mice, lacking NK cells along with T- and B-cells; these mice also have high engraftment rates for xenotransplanted cells [Okada *et*

al., 2008; Ito *et al.*, 2002]. Therefore, xenotransplanation into NOJ or NOG mice, instead of NOD/SCID mice, might display a more profound phenotype, or one that is similar to the original tumor.

The results presented in chapter 1 will help to elucidate the pathophysiology of canine lymphoma, and assist in evaluating the effects of antitumor agents or a new therapy.

As outlined in chapter 2, 13 mAbs against cPSGL-1 were obtained by immunizing rats with the Ema cell line that was established (Chapter 1). These mAbs were categorized into five groups based on the recognition pattern of cPSGL-1.

It has been known that antibodies against certain glycans are useful for the treatment and detection of tumor cells because glycosylation pattern of cell membrane protein on some tumor cells is different from that on non-tumor cells [Sawada *et al.*, 2011; Engelstaedter *et al.*, 2012]. Therefore, I examined whether mAbs against cPSGL-1 could detect differences between canine lymphoma (T- or B-cell) samples and peripheral blood mononuclear cells (PBMCs) derived from healthy dogs because all antibodies recognized *O*-glycans or sialylated peptides of cPSGL-1. Consequently, no clear differences were observed between the reactivity of these antibodies to canine lymphoma cells and PBMCs (data not shown). This possibly means that these antibodies are unable to distinguish normal and tumor cells, although lymphoma cell line, Ema, was used for immunization. Besides, it remains unknown if there is any difference between glycans of cPSGL-1 on lymphoma cells and those on PBMCs.

This is the first report of the establishment of anti-cPSGL-1 antibodies. As the expression level and function of cPSGL-1 has not yet been studied in depth, these mAbs will be very useful in future research.

The cPSGL-1 protein was recognized by the 13 mAbs as described in chapter 2, even though a total of 56 Abs were generated in this study. As their recognition molecules have not been identified yet, it may be worthwhile to identify these molecules. Furthermore, if the reactivity of an Ab to the lymphocytes of a healthy dog is lower than that to lymphoma cells, it might be possible to use that antibody in future therapies.

The mechanisms relating to the detachment of adherent cultured cells when PSGL-1 was overexpressed were presented in chapter 3. The detachment of cells occurred as a result of inhibition of interactions between cell surface integrins and the extracellular matrix (ECM). This was due to steric hindrance of the extracellular domain of PSGL-1. The floating phenomenon, induced by overexpression of PSGL-1, was observed in various tumor cell lines that were adherent and semi-adherent. PSGL-1 is known to be an "adhesive" molecule; therefore, the "anti-adhesive" property reported in this thesis is contrary to previous reports. Several other proteins, such as podocalyxin and CD43 have been shown to have both adhesive and anti-adhesive properties [Larrucea *et al.*, 2008; Ostberg *et al.*, 1998].

It is hypothesized that overexpression of PSGL-1 in tumor cells will result in cells with an increased tendency to metastasize. The anti-adhesive property of PSGL-1 may be related to the

detachment of tumor cells from primary tumor sites. In this study, ECM-cell adhesion was inhibited by overexpression of PSGL-1; however, the overexpression of PSGL-1 and its affects on cell-cell adhesion was not examined. If the degree of cell-cell adhesion is also inhibited by overexpression of PSGL-1, the detachment of tumor cells from the primary tumor will be promoted. Conversely, at metastasis sites, overexpression of PSGL-1 may play a role in the attachment of endothelial cells, via binding to P- or E-selectin.

The relationship between PSGL-1 and tumor metastasis has been reported, but not extensively. Dimitroff *et al.* (2005) reported that PSGL-1 was expressed in the prostate cancer cell line, MDA PCa 2b, and that metastatic bone tissues of prostate cancer, but not normal prostate tissue or benign prostate tumor, expressed PSGL-1. Knockdown of PSGL-1 in a mouse lymphoma cell line intravenously transplanted in SPF mice was reported to decrease organ colonization of lymphoma cells, thereby delaying mortality [Raes *et al.*, 2007].

In this study, it was shown that overexpression of PSGL-1 inhibited the access of Abs to HLA I, MHC I, and/ or integrins. This suggests that overexpression of PSGL-1 may contribute to a mechanism by which tumor cells evade the immune system. However, there is no published report regarding this mechanism so far.

Unfortunately, a relationship between PSGL-1 expression and tumor malignancy could not be established. Future studies will have to concentrate on determining the mechanisms of metastasis, and hopefully, it will provide new strategies for tumor therapies targeting PSGL-1.

ACKNOWLEDGMENTS

I would like to express my sincere gratitude and appreciation to Prof. Takuya Mizuno for being a truly ideal supervisor and for patiently guiding me every step of the way. I am highly indebted to him for his stimulating suggestions and encouragement that helped me in all the time of research and writing of this thesis.

I would like to thank Prof. Masaru Okuda whose meticulous comments were an enormous help to me. I am grateful to Prof. Yasuyuki Endo (Laboratory of Veterinary Internal Medicine, Kagoshima University), Assoc. Prof. Hiroko Hiraoka (Laboratory of Veterinary Internal Medicine, Yamaguchi University), Assis. Prof. Masahito Kubo (Laboratory of Veterinary Pathology, Yamaguchi University), Prof. Toshiharu Hayashi (Laboratory of Veterinary Pathology, Yamaguchi University), Ph.D. Masayuki Shimojima (Department of Virology I, National Institute of Infectious Disease), Ph.D. Yorihiro Nishimura (Department of Virology II, National Institute of Infectious Disease), Prof. Hajime Tsujimoto (Laboratory of Veterinary Internal Medicine, The University of Tokyo), Ph.D. Jumpei Yamazaki (Fels Institute for Cancer Research and Molocular Biology, Temple University), Assis. Prof. Yasuhiko Okamura (Laboratory of Veterinary Surgery, Iwate University), Assoc. Prof. Kenji Tani (Laboratory of Veterinary Surgery, Yamaguchi University), Prof. Hiroyuki Iwata (Laboratory of Veterinary Hygiene, Yamaguchi University), Assoc. Prof. Kazuo Nishigaki (Laboratory of Veterinary Molecular Immunology and Infectious Disease, Yamaguchi University) and Assoc. Prof. Takashi Ohama (Laboratory of Veterinary pharmacology, Yamaguchi University) for all their help and kindness.

I wish to thank Ryoichi Suzuki and all the lab. members for assisting me with my experiments.

Finally, I would like to give my thanks to my family and friends for the supports in everything I do.

REFERENCES

Ardman B, Sikorski MA, Staunton DE. 1992. CD43 interferes with T-lymphocyte adhesion. Proc Natl Acad Sci U S A. 89:5001-5005.

Burnett RC, Vernau W, Modiano JF, Olver CS, Moore PF, Avery AC. 2003. Diagnosis of canine lymphoid neoplasia using clonal rearrangements of antigen receptor genes. Vet Pathol. 40:32-41.

Bussel JB, Giulino L, Lee S, Patel VL, Sandborg C, Stiehm ER. 2007. Update on therapeutic monoclonal antibodies. Curr Probl Pediatr Adolesc Health Care. 37:118-135.

Cummings RD. 1999. Structure and function of the selectin ligand PSGL-1. Braz J Med Biol Res. 32:519-528.

da Costa Martins P, Garcia-Vallejo JJ, van Thienen JV, Fernandez-Borja M, van Gils JM, Beckers C, Horrevoets AJ, Hordijk PL, Zwaginga JJ. 2007. P-selectin glycoprotein ligand-1 is expressed on endothelial cells and mediates monocyte adhesion to activated endothelium. Arterioscler Thromb Vasc Biol. 27:1023-1029.

Dimitroff CJ, Descheny L, Trujillo N, Kim R, Nguyen V, Huang W, Pienta KJ, Kutok JL, Rubin MA. 2005. Identification of leukocyte E-selectin ligands, P-selectin glycoprotein ligand-1 and E-selectin ligand-1, on human metastatic prostate tumor cells. Cancer Res. 65:5750-5760.

DuBridge RB, Tang P, Hsia HC, Leong PM, Miller JH, Calos MP. 1987. Analysis of mutation in human cells by using an Epstein-Barr virus shuttle system. Mol Cell Biol. 7:379-387.

Dobson JM, Blackwood LB, McInnes EF, Bostock DE, Nicholls P, Hoather TM, Tom BD. 2001. Prognostic variables in canine multicentric lymphosarcoma. J Small Anim Pract. 42:377-384.

Emoto Y. 2008. Cellular aggregation facilitates anoikis in MDCK cells. J Physiol Sci. 58:371-380.

Engelstaedter V, Fluegel B, Kunze S, Mayr D, Friese K, Jeschke U, Bergauer F. Expression of the carbohydrate tumour marker Sialyl Lewis A, Sialyl Lewis X, Lewis Y and Thomsen-Friedenreich antigen in normal squamous epithelium of the uterine cervix, cervical dysplasia and cervical cancer. Histol Histopathol. 27:507-514.

Folkman J, Moscona A. 1978. Role of cell shape in growth control. Nature. 273:345-349.

Gendler SJ. 2001. MUC1, the renaissance molecule. J Mammary Gland Biol Neoplasia. 6:339-353.

Ismael G, Hegg R, Muehlbauer S, Heinzmann D, Lum B, Kim SB, Pienkowski T, Lichinitser M, Semiglazov V, Melichar B, Jackisch C. 2012. Subcutaneous versus intravenous administration of (neo)adjuvant trastuzumab in patients with HER2-positive, clinical stage I-III breast cancer (HannaH study): a phase 3, open-label, multicentre, randomized trial. Lancet Oncol. 13:869-878.

Ito D, Endicott MM, Jubala CM, Helm KM, Burnett RC, Husbands BD, Borgatti A, Henson MS, Burgess KE, Bell JS, Kisseberth WC, *et al.* 2011. A tumor-related lymphoid progenitor population supports hierarchical tumor organization in canine B-cell lymphoma. J Vet Intern Med. 25:890-896.

Ito M, Hiramatsu H, Kobayashi K, Suzue K, Kawahata M, Hioki K, Ueyama Y, Koyanagi Y, Sugamura K, Tsuji K, Heike T, Nakahata T. 2002. NOD/SCID/gamma(c)(null) mouse: an excellent recipient mouse model for engraftment of human cells. Blood. 100:3175-3182.

Kaneko N, Yamamoto Y, Wada Y, Shimokawa Miyama T, Hiraoka H, Itamoto K, Mizuno T, Nakaichi M, Takahashi T, Watari T, Okuda M. 2009. Application of polymerase chain reaction to analysis of antigen receptor rearrangements to support endoscopic diagnosis of canine alimentary lymphoma. J Vet Med Sci. 71:555-559.

Keating GM. 2011. Spotlight on rituximab in chronic lymphocytic leukemia, low-grade or follicular lymphoma, and diffuse large B-cell lymphoma. BioDrugs. 25:55-61.

Khodarev NN, Pitroda SP, Beckett MA, MacDermed DM, Huang L, Kufe DW, Weichselbaum RR. 2009. MUC1-induced transcriptional programs associated with tumorigenesis predict outcome in breast and lung cancer. Cancer Res. 69:2833-2837.

Kinoshita M, Nakamura T, Ihara M, Haraguchi T, Hiraoka Y, Tashiro K, Noda M. 2001. Identification of human endomucin-1 and -2 as membrane-bound O-sialoglycoproteins with anti-adhesive activity. FEBS Lett. 499:121-126.

Kisseberth WC, Nadella MV, Breen M, Thomas R, Duke SE, Murahari S, Kosarek CE, Vernau W, Avery AC, Burkhard MJ, Rosol TJ. 2007. A novel canine lymphoma cell line: a translational and comparative model for lymphoma research. Leuk Res. 31:1709-1720.

Komatsu M, Tatum L, Altman NH, Carothers Carraway CA, Carraway KL. 2000. Potentiation of metastasis by cell surface sialomucin complex (rat MUC4), a multifunctional anti-adhesive glycoprotein. Int J Cancer. 87:480-486.

Komatsu M, Yee L, Carraway KL. 1999. Overexpression of sialomucin complex, a rat homologue of MUC4, inhibits tumor killing by lymphokine-activated killer cells. Cancer Res. 59:2229-2236.

Komatsu M, Carraway CA, Fregien NL, Carraway KL. 1997. Reversible disruption of cell-matrix and cell-cell interactions by overexpression of sialomucin complex. J Biol Chem. 272:33245-33254.

Lapointe J, Li C, Higgins JP, van de Rijn M, Bair E, Montgomery K, Ferrari M, Egevad L, Rayford W, Bergerheim U, Ekman P, DeMarzo AM, Tibshirani R, Botstein D, Brown PO, Brooks JD, Pollack JR. 2004. Gene expression profiling identifies clinically relevant subtypes of prostate cancer. Proc Natl Acad Sci U S A. 101:811-816.

Larrucea S, Butta N, Arias-Salgado EG, Alonso-Martin S, Ayuso MS, Parrilla R. 2008. Expression of podocalyxin enhances the adherence, migration, and intercellular communication of cells. Exp Cell Res. 314:2004-2015.

Laszik Z, Jansen PJ, Cummings RD, Tedder TF, McEver RP, Moore KL. 1996. P-selectin glycoprotein ligand-1 is broadly expressed in cells of myeloid, lymphoid, and dendritic lineage and in some nonhematopoietic cells. Blood. 88:3010-3021.

Lawrenson ID, Wimmer-Kleikamp SH, Lock P, Schoenwaelder SM, Down M, Boyd AW, Alewood PF, Lackmann M. 2002. Ephrin-A5 induces rounding, blebbing and de-adhesion of EphA3-expressing 293T and melanoma cells by CrkII and Rho-mediated signalling. J Cell Sci. 115:1059-1072.

Li F, Erickson HP, James JA, Moore KL, Cummings RD, McEver RP. 1996. Visualization of P-selectin glycoprotein ligand-1 as a highly extended molecule and mapping of protein epitopes for monoclonal antibodies. J Biol Chem. 271:6342-6348.

Marconato L, Gelain ME, Comazzi S. 2012. The dog as a possible animal model for human non-Hodgkin lymphoma: a review. Hematol Oncol. published on line 2012 Jun 6.

Matsumoto M, Miyasaka M, Hirata T. 2009. P-selectin glycoprotein ligand-1 negatively regulates T-cell immune responses. J Immunol. 183:7204-7211.

Mizuno T, Suzuki R, Umeki S, Okuda M. 2009. Crossreactivity of antibodies to canine CD25 and Foxp3 and identification of canine CD4+CD25 +Foxp3+ cells in canine peripheral blood. J Vet Med Sci. 71:1561-1568.

Momoi Y, Okai Y, Watari T, Goitsuka R, Tsujimoto H, Hasegawa A. 1997. Establishment and characterization of a canine T-lymphoblastoid cell line derived from malignant lymphoma. Vet Immunol Immunopathol. 59:11-20.

Moore AS, Leveille CR, Reimann KA, Shu H, Arias IM. 1995. The expression of P-glycoprotein in canine lymphoma and its association with multidrug resistance. Cancer Invest. 13:475-479.

Morita S, Kojima T, Kitamura T. 2000. Plat-E: an efficient and stable system for transient packaging of retroviruses. Gene Ther. 7:1063-1066.

Nadella MV, Kisseberth WC, Nadella KS, Thudi NK, Thamm, DH, McNiel EA, Yilmaz A, Boris-Lawrie K, Rosol TJ. 2008. NOD/SCID mouse model of canine T-cell lymphoma with humoral hypercalcaemia of malignancy: cytokine gene expression profiling and in vivo bioluminescent imaging. Vet Comp Oncol. 6:39-54.

Nakaichi M, Taura Y, Kanki M, Mamba K, Momoi Y, Tsujimoto H, Nakama S. 1996. Establishment and characterization of a new canine B-cell leukemia cell line. J Vet Med Sci. 58:469-471.

Nishimura Y, Shimojima M, Tano Y, Miyamura T, Wakita T, Shimizu H. 2009. Human P-selectin glycoprotein ligand-1 is a functional receptor for enterovirus 71. Nat Med. 15:794-797.

Norgard KE, Moore KL, Diaz S, Stults NL, Ushiyama S, McEver RP, Cummings RD, Varki A. 1993. Characterization of a specific ligand for P-selectin on myeloid cells. A minor glycoprotein with sialylated O-linked oligosaccharides. J Biol Chem. 268:12764-12774.

Okada S, Harada H, Ito T, Saito T, Suzu S. 2008. Early development of human hematopoietic and acquired immune systems in new born NOD/Scid/Jak3null mice intrahepatic engrafted with cord blood-derived CD34 + cells. Int J Hematol. 88:476-482.

Okawa T, Kurio Y, Morimoto M, Hayashi T, Nakagawa T, Sasaki N, Okuda M, Mizuno T. 2011. Calreticulin expression in neoplastic versus normal dog mammary glands: a cDNA subtraction-based study. Res Vet Sci. 92:80-91.

Ostberg JR, Barth RK, Frelinger JG. 1998. The Roman god Janus: a paradigm for the function of CD43. Immunol Today. 19:546-550.

Ostberg JR, Dragone LL, Driskell T, Moynihan JA, Phipps R, Barth RK, Frelinger JG. 1996. Disregulated expression of CD43 (leukosialin, sialophorin) in the B cell lineage leads to immunodeficiency. J Immunol. 157:4876-4884.

Pouyani T, Seed B. 1995. PSGL-1 recognition of P-selectin is controlled by a tyrosine sulfation consensus at the PSGL-1 amino terminus. Cell. 83:333-343.

Raes G, Ghassabeh GH, Brys L, Mpofu N, Verschueren H, Vanhecke D, De Baetselier P. 2007. The metastatic T-cell hybridoma antigen/P-selectin glycoprotein ligand 1 is required for hematogenous metastasis of lymphomas. Int J Cancer. 121:2646-2652.

Rivera-Nieves J, Burcin TL, Olson TS, Morris MA, McDuffie M, Cominelli F, Ley K. 2006. Critical role of endothelial P-selectin glycoprotein ligand 1 in chronic murine ileitis. J Exp Med. 203:907-917.

Sako D, Comess KM, Barone KM, Camphausen RT, Cumming DA, Shaw GD. 1995. A sulfated peptide segment at the amino terminus of PSGL-1 is critical for P-selectin binding. Cell. 83:323-331.

Sako D, Chang XJ, Barone KM, Vachino G, White HM, Shaw G, Veldman GM, Bean KM, Ahern TJ, Furie B, *et al.* 1993. Expression cloning of a functional glycoprotein ligand for P-selectin. Cell. 75:1179-1186.

Sawada R, Sun SM, Wu X, Hong F, Ragupathi G, Livingston PO, Scholz WW. 2011. Human monoclonal antibodies to sialyl-Lewis (CA19.9) with potent CDC, ADCC, and antitumor activity. Clin Cancer Res. 17:1024-1032.

Seiser EL, Thomas R, Richards KL, Kathryn Kelley M, Moore P, Suter SE, Breen M. 2011. Reading between the lines: molecular characterization of five widely used canine lymphoid tumour cell lines. Vet Comp Oncol. published on line 2011 Nov 23.

Shimojima M, Miyazawa T, Sakurai Y, Nishimura Y, Tohya Y, Matsuura Y, Akashi H. 2003. Usage of myeloma and panning in retrovirus-mediated expression cloning. Anal Biochem. 315:138-140.

Sinkora J, Samankova P, Kummer V, Leva L., Maskova J, Rehakova Z, Faldyna M. 2007. Commercially available rabbit anti-human polyclonal antisera as a useful tool for immune system studies in veterinary species. Vet Immunol Immunopathol. 119:156-162.

Suter SE, Small GW, Seiser EL, Thomas R, Breen M, Richards KL. 2011. FLT3 mutations in canine acute lymphocytic leukemia. BMC Cancer. 11:38.

Umeki S, Suzuki R, Shimojima M, Ema Y, Yanase T, Iwata H, Okuda M, Mizuno T. 2011. Characterization of monoclonal antibodies against canine P-selectin glycoprotein ligand-1 (PSGL-1). Vet Immunol Immunopathol. 142:119-125.

Vail DM, Young KM. 2007. Canine lymphoma and lymphoid leukemias. pp. 699-733. In: Small Animal Clinical Oncology, 4th ed (Withrow SJ, Vail DM, editors.), Saunders, Philadelphia.

Van Brocklyn JR, Tu Z, Edsall LC, Schmidt RR, Spiegel S. 1999. Sphingosine 1-phosphate-induced cell rounding and neurite retraction are mediated by the G protein-coupled receptor H218. J Biol Chem. 274:4626-4632.

van de Wiel-van Kemenade E, Ligtenberg MJ, de Boer AJ, Buijs F, Vos HL, Melief CJ, Hilkens J, Figdor CG. 1993. Episialin (MUC1) inhibits cytotoxic lymphocyte-target cell interaction. J Immunol. 151:767-776.

Wesseling J, van der Valk SW, Vos HL, Sonnenberg A, Hilkens J. 1995. Episialin (MUC1) overexpression inhibits integrin-mediated cell adhesion to extracellular matrix components. J Cell Biol. 129:255-265.

Wilkins PP, Moore KL, McEver RP, Cummings RD. 1995. Tyrosine sulfation of P-selectin glycoprotein ligand-1 is required for high affinity binding to P-selectin. J Biol Chem. 270:22677-22680.

Wreesmann VB, Sieczka EM, Socci ND, Hezel M, Belbin TJ, Childs G, Patel SG, Patel KN, Tallini G, Prystowsky M, Shaha AR, Kraus D, Shah JP, *et al.*. 2004. Genome-wide profiling of papillary thyroid cancer identifies MUC1 as an independent prognostic marker. Cancer Res. 64:3780-3789.

Yang J, Hirata T, Croce K, Merrill-Skoloff G, Tchernychev B, Williams E, Flaumenhaft R, Furie BC, Furie B. 1999. Targeted gene disruption demonstrates that P-selectin glycoprotein ligand 1 (PSGL-1) is required for P-selectin-mediated but not E-selectin-mediated neutrophil rolling and migration. J Exp Med. 190:1769-1782.

Yang J, Galipeau J, Kozak CA, Furie BC,Furie B. 1996. Mouse P-selectin glycoprotein ligand-1: molecular cloning, chromosomal localization, and expression of a functional P-selectin receptor. Blood. 87:4176-4186.

Yi Y, Kamata-Sakurai M, Denda-Nagai K, Itoh T, Okada K, Ishii-Schrade K, Iguchi A, Sugiura D, Irimura T. 2010. Mucin 21/epiglycanin modulates cell adhesion. J Biol Chem. 285:21233-21240.

Zwingenberger AL, Vernau W, Shi C, Yan W, Chen X, Gordon IK, Kent MS. 2012. Development and characterization of 5 canine B-cell lymphoma cell lines. Leuk Res. 36:601-606.

Tables

Table I-1. Antibodies used in this study

		Clone	Isotype	Source
Primary antibodies	CD3	CA17.2A12	mouse IgG1	AbD Serotec
	CD4	CA13.1E4	mouse IgG1	P.F. Moore (U.C. Davis)
	CD8α	CA9.JD3	mouse IgG2a	P.F. Moore (U.C. Davis)
	CD11a	CA11.4D3	mouse IgG1	P.F. Moore (U.C. Davis)
	CD11b	CA16.3E10	mouse IgG1	P.F. Moore (U.C. Davis)
	CD11c	CA11.6A1	mouse IgG1	P.F. Moore (U.C. Davis)
	CD14	CAM36A	mouse IgG1	VMRD
	CD18	CA1.4E9	mouse IgG1	P.F. Moore (U.C. Davis)
	CD21	CA2.1D6	mouse IgG1	P.F. Moore (U.C. Davis)
	CD34 Biotin*	2E9	mouse IgG1	BioLegend
	CD45	CA12.10C12	mouse IgG1	P.F. Moore (U.C. Davis)
	CD45RA	CA4.1D3	mouse IgG1	P.F. Moore (U.C. Davis)
	Thy-1	CA1.4G8	mouse IgG1	P.F. Moore (U.C. Davis)
	MHCII	CA2.1C12	mouse IgG1	P.F. Moore (U.C. Davis)
	TCRαβ	CA15.8G7	mouse IgG1	P.F. Moore (U.C. Davis)
	TCRγδ	CA20.8H1	mouse IgG2a	P.F. Moore (U.C. Davis)
	IgM FITC		goat IgG	BETHYL Laboratories
	IgG FITC		sheep IgG	BETHYL Laboratories
Isotype control antibodies	mouse IgG1			Santa Cruz Biotechnology
	mouse IgG2a			Santa Cruz Biotechnology
	mouse IgG1 Biotin*			BioLegend
	goat IgG FITC			Jackson ImmunoResearch
	sheep IgG FITC			Jackson ImmunoResearch
Secondary antibody	anti-mouse IgG-FITC			Southern Biotech

* Biotin conjugated antibodies, detected by streptavidin PE (Source: eBioscience)

Abbrebiations: FITC=fluorescein isothiocyanate; PE=phycoerythrin

Table I-2. Patient and initial tumor characteristics of the samples used for establishment of cell lines

Cell line	Dog	Breed	Sex	Age (Years)	Grade	PARR		Flow cytometry	
						TCRγ	IgH	CD3	CD21
Ema	Case 1	English Springer Spaniel	F	6	High	+	−	ND	
CLC	Case 2	French Bulldog	F	8	High	−	−	+	−
CLK	Case 3	Grate Pyrenees	F	8	High	+	−	+	−
Nody-1	Case 4	Shiba	M	8	High	ND		ND	
UL-1	Case 5	Labrador Retriever mix	M	6	High	+	+	−	−

ND, not determined

Table I-3. Phenotypic characteristics of canine lymphoma cell lines

	Flow cytometry																		PARR	
Cell line	CD3	CD4	CD8α	CD11a	CD11b	CD11c	CD14	CD18	CD21	CD34	CD45	CD45RA	CD90	TCRαβ	TCRγδ	MHCII	IgM	IgG	TCRγ	IgH
Ema	+	−	−	−	−	−	−	−	−	−	+	+	+	−	+	−	−	−	+	−
CLC	−	−	−	−	−	−	−	+	−	−	+	+	−	−	−	+	−	−	−	−
CLK	−	−	+	+	−	+	−	+	−	−	+	+	+	−	−	−	−	−	+	−
Nody-1	+	−	−	−	−	−	−	+	−	−	+	+	−	−	−	+	−	−	+	−
UL-1	−	−	+	−	−	−	−	+	−	−	+	+	−	−	−	−	−	−	+	−

Table I-4. *In vivo* characteristics of canine lymphoma cell lines in NOD/SCID mice

Cell line	No. of dead mice before Day 21	No. of mice with ascites	No. of mice with tumor in peritoneal cavity[a]	No. of mice with miroscopic infiltration with each cell line into organ								
				Liver	Kidney	Spleen	Pancreas	Stomach	Small intestine	Large intestine	Mesentery	Regional lymph node[b]
Ema	0	3 (0.2-1 ml)	3	0	0	0	3	3	2	2	3	1[c]
CLC	3 (day 12 & 13)	4 (3.7-11 ml)	4	3	0	0	4	3	3	2	3	3[d]
CLK	0	0	0	0	0	0	0	0	0	0	0	1[e]
Nody-1	1 (day 19)	3 (0.3-3.7 ml)	3	3	4	3	4	3	3	4	3	3[f]
UL-1	0	3 (0.5-3 ml)	4	1	0	0	4	0	0	0	4	0

a, No. animals in which visible tumor developed; b, except mesenteric; c, mediastinal (1 mouse); d, iliac (3 mice), mediastinal (1 mouse) and inguinal (1 mouse); e, mediastinal (1 mouse); f, iliac (3 mice) and sacral (1 mouse)

Table II-1. The primers used in this study

Primer name	Nucleotide sequence (5' to 3')	Direction	Purpose
YTM178	CCACCGCCCTCAAAGTAGACG	F	to amplify the genomic insert in the pMxs vector
YTM206	CCTCACATTGCCAAAAGACG	R	
YTM263	CCATGCCTCTGCAAGTCC	F	to amplify the full length of cPSGL-1
YTM264	TTAAGGGAGGAAGCTCTGC	R	
YTM310	GTCGATGTCATGATCTTTATAATCAGGGAGGAAGCTCTG	R	add FLAG tag
YTM311	TCACTAGTCATCGTCATCCTTGTAGTCGATGTCATG	R	
YTM178	CCACCGCCCTCAAAGTAGACG	F	bind to 5' site upstream of MCS in the pMxs vector
YTM179	ACACCGGCCTTATTCCAAG	R	bind to 3' site downstream of MCS in the pMxs vector
YTM516	CTCCTCATCCACTTGGAGGCTGTCGCCAGA	R	construction of pMx-IG-cPSGL-DM1
YTM518	GCCCCCTCTGTGAGCCTCCTGCCCCGGGC	R	construction of pMx-IG-cPSGL-DM2
YTM520	GCCCTTCACGGTGGCTGGAGCCTCCGTGGT	R	construction of pMx-IG-cPSGL-DM3
YTM522	GATGGCCAGCAGGCATGGATCTGTGGACGG	R	construction of pMx-IG-cPSGL-DM4
YTM515	TCTGGCGACAGCCTCCAAGTGGATGAGGAG	F	construction of pMx-IG-cPSGL-DM1
YTM517	GCCCGGGGCAGGAGGCTCACAGAGGGGGCT	F	construction of pMx-IG-cPSGL-DM2
YTM519	ACCACGGAGGCTCCAGCCACCGTGAAGGGC	F	construction of pMx-IG-cPSGL-DM3
YTM521	CCGTCCACAGATCCATGCCTGCTGGCCATC	F	construction of pMx-IG-cPSGL-DM4
YTM574	CTATGGAGTAGTCAAATACGTCC	R	construction of pMx-IG-cPSGL-Y52F-FLAG
YTM576	CTATGGAGAAGTCATATACGTCC	R	construction of pMx-IG-cPSGL-Y54F-FLAG
YTM578	CTATGGAGAAGTCAAATACGTCC	R	construction of pMx-IG-cPSGL-Y52,54F-FLAG
YTM573	GGACGTATTTGACTACTCCATAG	F	construction of pMx-IG-cPSGL-Y52F-FLAG
YTM575	GGACGTATATGACTTCTCCATAG	F	construction of pMx-IG-cPSGL-Y54F-FLAG
YTM577	GGACGTATTTGACTTCTCCATAG	F	construction of pMx-IG-cPSGL-Y52,54F-FLAG

MCS, multicloning site; F, forward; R, reverse

Table II-2. Summary of antibody reactivity and predicted epitopes

mAb	Subclass	P3U1/cPSGL-1								Ema		Predicted epitopes				
		WT	Deletion mutants				Tyrosine mutants			Enzyme Treatment						
			△19-41	△42-144	△145-274	△275-345	Y52F	Y54F	Y52FY54F	OSGE	sialidase	A	B	C	D	E
6-1	IgG2a, κ	○	○	×	○	○	○	○	○	×	△					■
30-2	IgG2a, κ	◎	○	×	◎	◎	◎	◎	◎	×	◎	■				
53-1	IgG1, κ	◎	○	×	◎	◎	◎	◎	◎	×	◎	■				
64-1	IgG2a, κ	○	○	×	○	○	○	○	○	×	○				■	
85-1	IgG2a, κ	◎	○	×	◎	◎	◎	◎	◎	×	◎	■				
88-1	IgG2a, κ	◎	◎	×	◎	◎	×	◎	×	×	◎		■			
90-1	IgG2a, κ	◎	◎	×	◎	◎	×	◎	×	×	◎		■			
97-1	IgG2a, κ	◎	◎	×	◎	◎	×	◎	×	×	◎		■			
150-5	IgG2a, κ	○	○	×	○	○	○	○	○	×	○				■	
151-7	IgG2a, κ	◎	◎	×	◎	◎	×	×	×	×	◎			■		
167-1	IgG2a, κ	◎	◎	×	◎	◎	×	×	×	×	◎			■		
176-15	IgG2b, κ	○	○	×	○	○	○	○	○	×	○				■	
177-1	IgG2a, κ	○	○	×	○	○	○	○	○	×	×					■

◎ : strongly positive, ○ : positive, △ : slightly positive, × : negative

Grey shading indicates that reactivity was decreased as compared to wild type (WT).
Black shading indicates predicted epitopes.
OSGE, O-sialoglycoprotein endopeptidase

Table III-1. The primers used in this study

Primer name	Nucleotide sequence (5' to 3')	Direction	Purpose
YTM407	CCATGCCTCTGCAACTCC	F	to amplify the full length of hPSGL-1
YTM408	CTAAGGGAGGAAGCTGTGC	R	
YTM178	CCACCGCCCTCAAAGTAGACG	F	bind to 5' site upstream of MCS in the pMxs vector
YTM179	ACACCGGCCTTATTCCAAG	R	bind to 3' site dow nstream of MCS in the pMxs vector
YTM469	ATATTCGGTGGCCTGCAAGCTGTTGCCAGG	R	construction of pMx-IG-hPSGL-DM1
YTM473	ACCTCTTTTGGTAGTTGAATCCGTGGACAG	R	construction of pMx-IG-hPSGL-DM3
YTM477	GATGGCCAGCAGGCAAGGTTCCATGGACAG	R	construction of pMx-IG-hPSGL-DM5
YTM535	TGCCTCCATGGCTGTTCTCCGGTCCCGGGC	R	construction of pMx-IG-hPSGL-DM8
YTM537	TGAATCCGTGGACAGTCTCCGGTCCCGGGC	R	construction of pMx-IG-hPSGL-DM9
YTM539	GGCCGTCAGTCGAGTTGAATCCGTGGACAG	R	construction of pMx-IG-hPSGL-DM10
YTM468	CCTGGCAACAGCTTGCAGGCCACCGAATAT	F	construction of pMx-IG-hPSGL-DM1
YTM472	CTGTCCACGGATTCAACTACCAAAAGAGGT	F	construction of pMx-IG-hPSGL-DM3
YTM476	CTGTCCATGGAACCTTGCCTGCTGGCCATC	F	construction of pMx-IG-hPSGL-DM5
YTM534	GCCCGGGACCGGAGAACAGCCATGGAGGCA	F	construction of pMx-IG-hPSGL-DM8
YTM536	GCCCGGGACCGGAGACTGTCCACGGATTCA	F	construction of pMx-IG-hPSGL-DM9
YTM538	CTGTCCACGGATTCAACTCGACTGACGGCC	F	construction of pMx-IG-hPSGL-DM10
YTM618	GACGTGTTCCAGAACTTACGG	F	to amplify the full length of mouse CD86
YTM619	TTTCCTCAGGCTCTCACTGC	R	
YTM620	TTCTACGCGTGGAGACGCAAGCTTATTTC	F	to amplify the CD86 fragment
YTM627	GTTAACGGTTTGGAGGAAATCTTCAT	R	
YTM622	AAACGCGTAGCATTTCTGGAGGCTCCGT	R	to amplify the 5' part of hPSGL-1
YTM628	AACTACCAAAAGAGGTCTG	F	to amplify the 3' part of hPSGL-1
YTM910	GCGGCCGC-GCTATGGGGAGCCGGAC	F	to amplify the full length of human CD49e
YTM911	tacgta-TCAGGCATCAGAGGTGGCTG	R	

MCS, multicloning site; F, forw ard; R, reverse

Figures

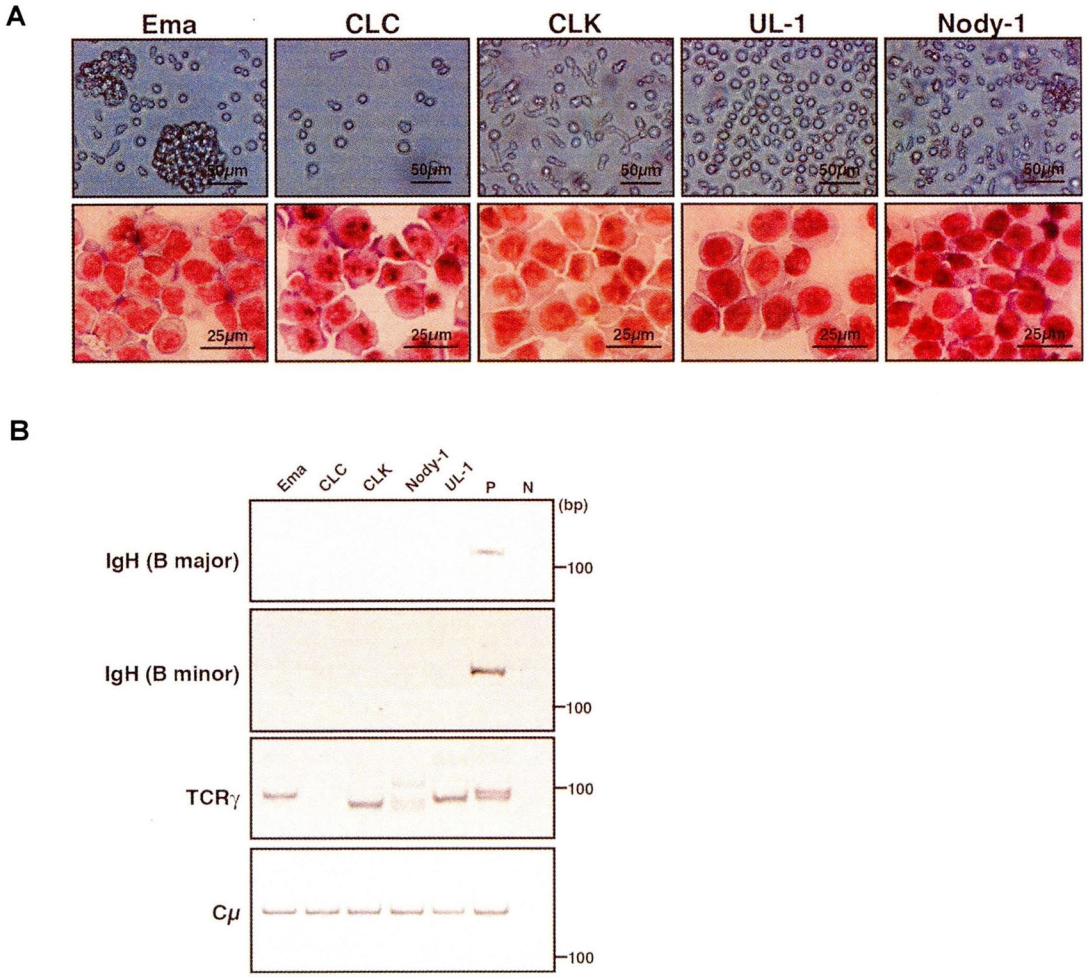

Fig. I-1. Morphological characteristics and polymerase chain reaction for antigen receptor rearrangement (PARR) in canine lymphoma cell lines. A: Phase contrast microscopy (upper panels) and Giemsa staining (lower panels) of five canine lymphoma cell lines are shown. (magnification, ×400). B: PARR analysis was performed using genomic DNA from each canine lymphoma cell line. Amplification of the Cμ region was used as a PCR control. P, positive control; N, negative control.

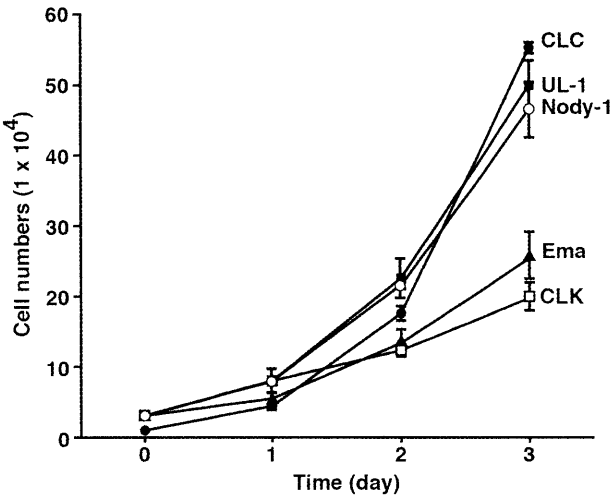

Fig. I-2. *In vitro* cell growth analysis of canine lymphoma cell lines. 1×10^4 (CLC) or 3×10^4 (other cell lines) cells were plated in triplicate and counted every 24 hr by trypan blue dye exclusion. One of three representative experiments is shown.

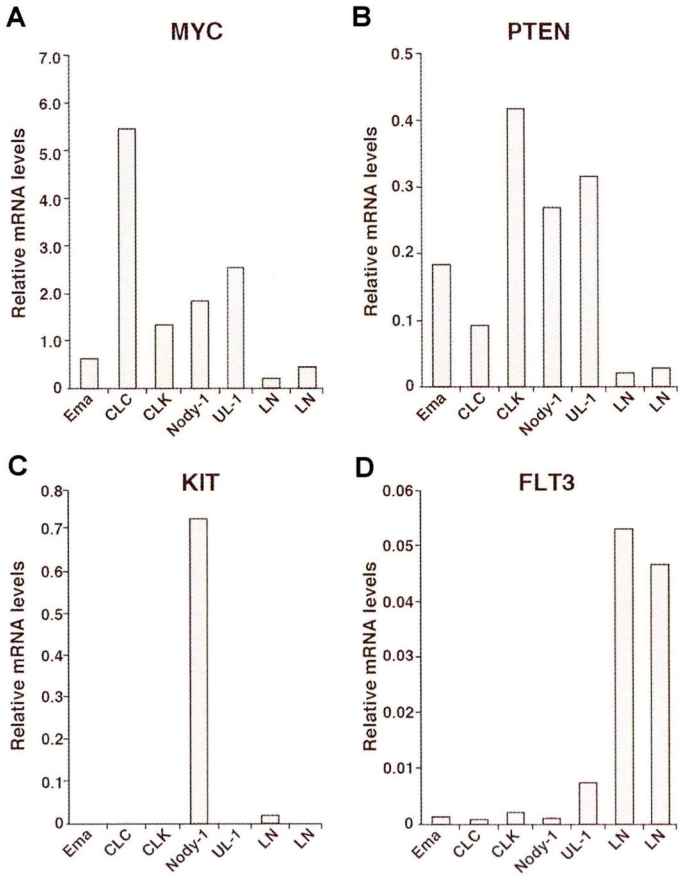

Fig. I-3. Quantitative real-time PCR analysis of gene expression in canine lymphoma cell lines. mRNA levels for *MYC* (A), *PTEN* (B), *KIT* (C) and *FLT3* (D) in canine lymphoma cell lines were compared with normal lymph node cells (LN) from two healthy dogs. Gene expression was normalized to *RPL32*.

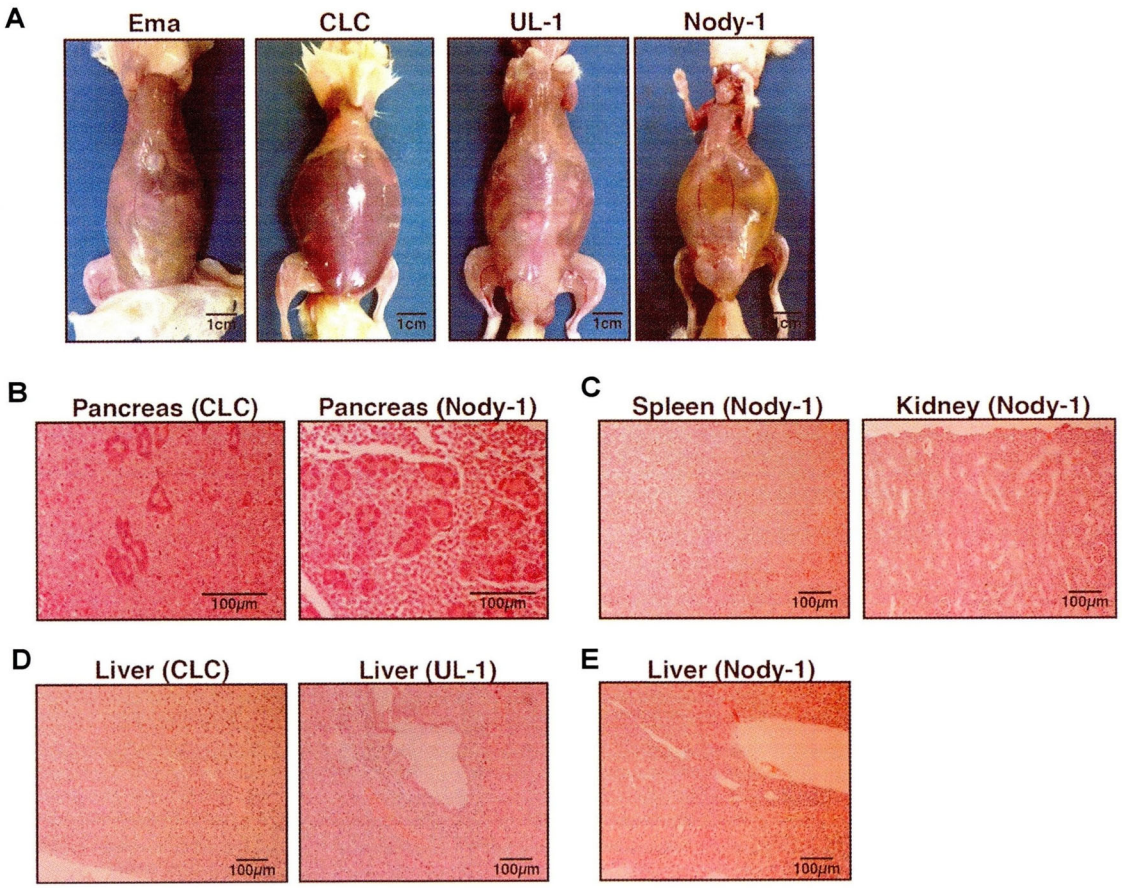

Fig. I-4. Intraperitoneal xenotransplantation of canine lymphoma cell lines in NOD/SCID mice. A: Photographs of ascites-bearing mice intraperitoneally inoculated with Ema, CLC, UL-1, or Nody-1 cell lines. B–D: Morphologic characteristics of cell lines from xenograft tumors in NOD/SCID mice (hematoxylin and eosin (H&E) staining). B: Infiltration of CLC and Nody-1 cell lines in the pancreas is shown (magnification, ×200). C: Infiltration of the Nody-1 cell line in the spleen and kidney (magnification, ×100). D: Infiltration of CLC and UL-1 cell lines in the liver. A tumor border is shown (magnification, ×100). E: Infiltration of Nody-1 cells in the liver. Tumor cells infiltrated around the hepatic triad (magnification, ×100).

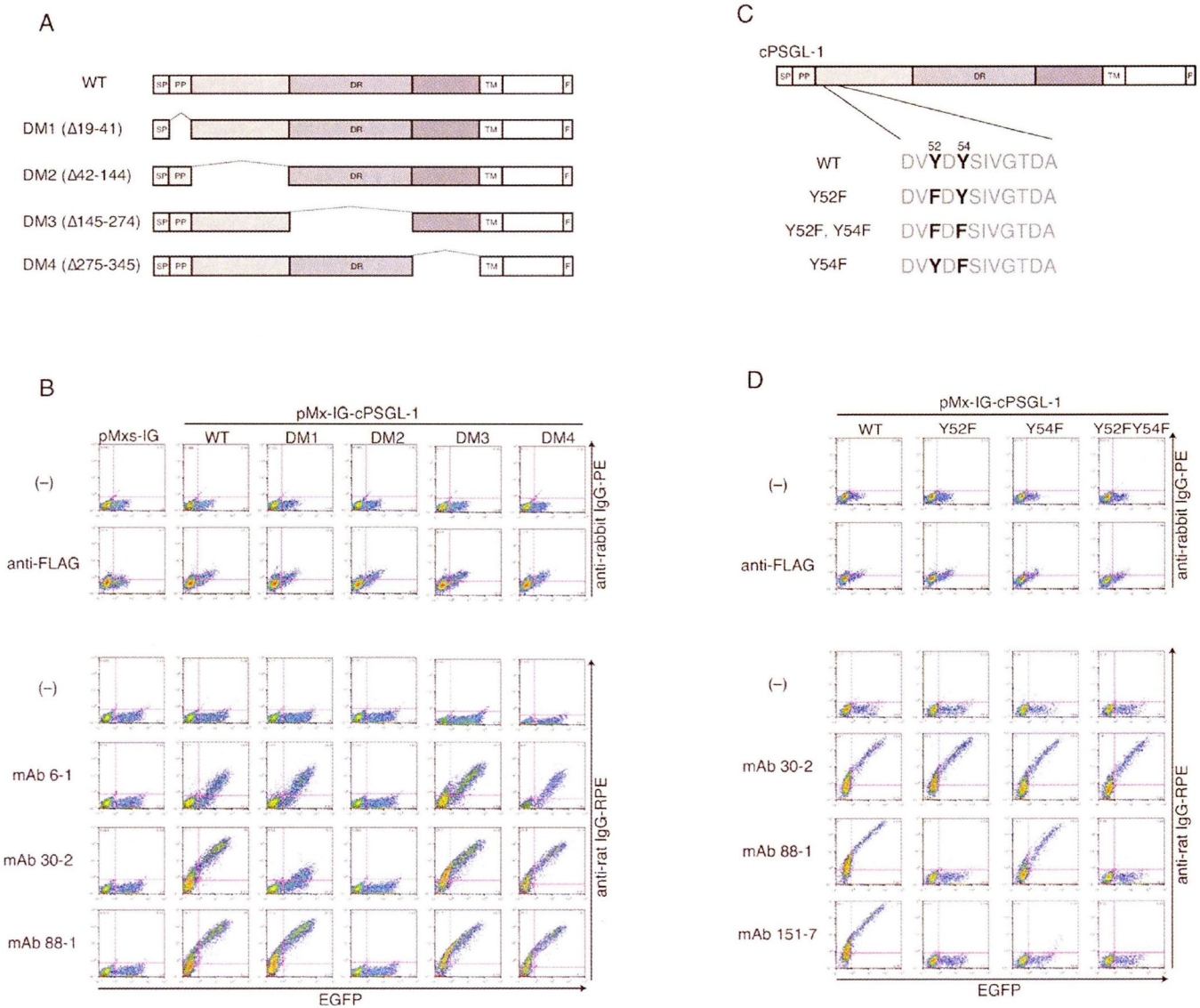
A
WT
DM1 (Δ19-41)
DM2 (Δ42-144)
DM3 (Δ145-274)
DM4 (Δ275-345)
SP
PP
DR
TM
F
C
cPSGL-1
52 54
WT DVYDYSIVGTDA
Y52F DVFDYSIVGTDA
Y52F, Y54F DVFDFSIVGTDA
Y54F DVYDFSIVGTDA
B
pMx-IG-cPSGL-1
pMxs-IG
WT
DM1
DM2
DM3
DM4
(–)
anti-FLAG
anti-rabbit IgG-PE
mAb 6-1
mAb 30-2
mAb 88-1
anti-rat IgG-RPE
EGFP
D
pMx-IG-cPSGL-1
WT
Y52F
Y54F
Y52FY54F
(–)
anti-FLAG
anti-rabbit IgG-PE
mAb 30-2
mAb 88-1
mAb 151-7
anti-rat IgG-RPE
EGFP

Fig. II-1. Reactivity of each mAb to deletion mutants (A, B) or tyrosine mutants (C, D) of cPSGL-1. A: Schematic representation of the deletion mutants of cPSGL-1. DM1, DM2, DM3, and DM4 have deletions of amino acids 19–41, 42–144, 145–274, or 274–345, respectively. SP, signal peptide domain; PP, propeptide domain; DR, decameric repeat domain; TM, transmembrane domain; F, FLAG tag. B: Flow cytometric analysis of P3U1 cells transduced with pMx-IG (EGFP only) or with pMx-IG encoding a series of cPSGL-1 deletion mutants and stained with an anti-FLAG Ab (upper two panels) or the indicated mAb (bottom panels). First and second Abs are indicated on the left and right of the panels, respectively. The monoclonal Abs 64-1, 150-5, 176-15 and 177-1 showed a similar staining pattern to mAb 6-1. Monoclonal Abs 53-1 and 85-1 showed a similar staining pattern to mAb 30-2. Monoclonal Abs 90-1, 97-1, 151-7 and 167-1 showed a similar staining pattern to mAb 88-1. One of three comparable experiments is shown. C: Schematic representation of the point mutations introduced into wild-type (WT) cPSGL-1. Tyrosine (Y) 52, tyrosines 52 and 54, or tyrosine 54 were replaced with phenylalanine (F). D: P3U1 cells transduced with WT cPSGL-1 or a series of point mutated clones were stained with an anti-FLAG Ab (upper two panels) or the indicated mAb (bottom panels) and analyzed by flow cytometry. First and secondary Abs are described on the left and right of the panels, respectively. One of three comparable experiments is shown.

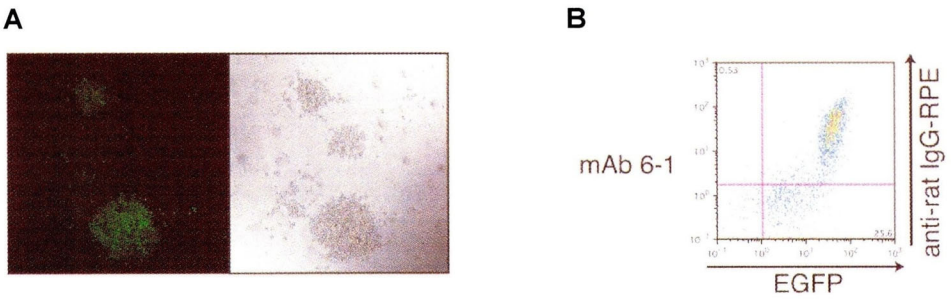

Fig. II-2. Isolation of colonies of P3U1 cells expressing an Ema cDNA library by a panning method. A: P3U1 cells transduced with an Ema cDNA library in which expressed proteins are simultaneously expressed with EGFP were trapped onto a dish coated with an anti-rat IgG Ab followed by the mAb 6-1. The photographs show representative colonies formed on the dishes. Left, Two EGFP-expressing colonies under a fluorescent microscope. Right, The same field under a light microscope. (200× magnification) B: One of the isolated colonies was stained with mAb 6-1 followed by anti-rat IgG-RPE Ab, and analyzed by flow cytometry.

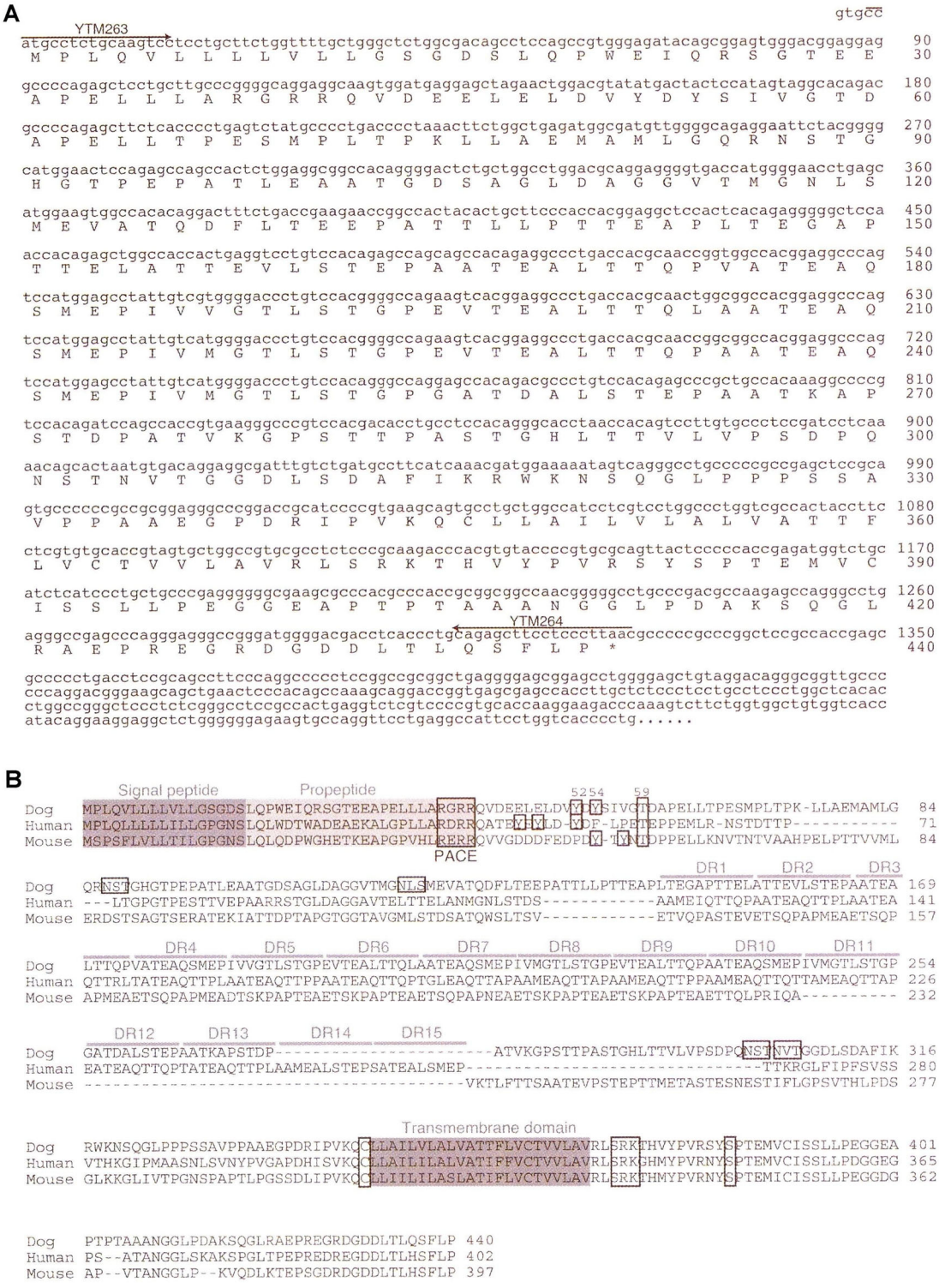
A
YTM263
YTM264
B
Signal peptide
Propeptide
PACE
DR1
DR2
DR3
DR4
DR5
DR6
DR7
DR8
DR9
DR10
DR11
DR12
DR13
DR14
DR15
Transmembrane domain
Dog
Human
Mouse

Fig. II-3. Nucleotide and predicted amino acid sequence of cPSGL-1. A: The predicted amino acid sequence of cPSGL-1 is shown below the nucleotide sequence. The asterisk represents the stop codon. The numbers on the right side refer to the cPSGL-1 cDNA nucleotide position or the amino acid sequence position. The arrows indicate the primers used for amplification of full length cPSGL-1. The nucleotide sequence data reported in this paper were submitted to the DNA Data Bank of Japan (DDBJ)/European Molecular Biology Laboratory (EMBL)/GenBank ID: AB614446). B: Comparison of the predicted amino acid sequences of PSGL-1 from different species. The amino acid sequence of cPSGL-1 was aligned with that of its human and murine counterpart using "ApE" software. The numbers on the right refer to the amino acid positions. The amino acid sequences of human and mouse PSGL-1 were obtained from the NCBI database (ID: NM_003006.3 and NM_009151.3 respectively). The dashes indicate gaps introduced for maximal alignment. The signal peptide, propeptide and transmembrane domains are shaded and labeled. The bars over the amino acid sequence show the 15 decameric repeat domains (DR). The PACE domain is boxed and labeled. Several tyrosine (Y) residues and the conserved threonine (T) residue close to the PACE domain are boxed. Four putative N-glycosylation sites (one NLS, one NVT and two NST) in the extracellular domain and the cysteine residue next to the transmembrane domain are also boxed. The extracellular domain of cPSGL-1 contains more than 50 serine and threonine residues that are potential sites for serine/threonine-linked O-glycosylation, and has 4 potential sites for N-glycosylation. Boxes in the cytoplasmic domain indicate amino acids that are believed to be important for binding to moesin.

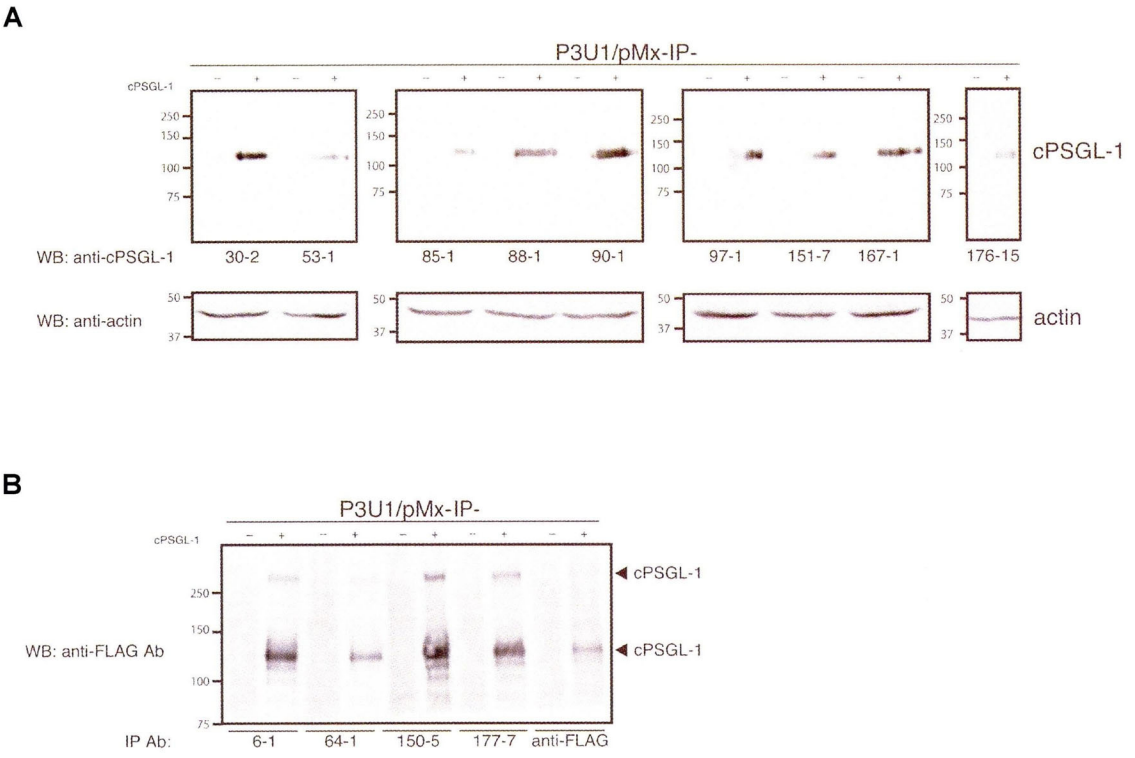

Fig. II-4. Analysis of mAb reactivity with cPSGL-1 overexpressed in P3U1 cells by Western blotting. A: Total protein was extracted from P3U1 cells transduced with pMx-IP (indicated as cPSGL-1 − on the top of the photos) or pMx-IP-cPSGL-1 (indicated as cPSGL-1 +, on the top of the photos), electrophoresed and blotted with the mAbs indicated below the upper panel. The same blot was stripped and re-probed with an anti-actin Ab used as a loading control. The data are representative of three comparable experiments. B: After extraction of cellular protein, cPSGL-1 was immunoprecipitated with the mAbs indicated at the bottom of the panel or with the anti-FLAG Ab. Immunoprecipitated protein was electrophoresed and blotted with the anti-FLAG Ab. One of two comparable experiments is shown.

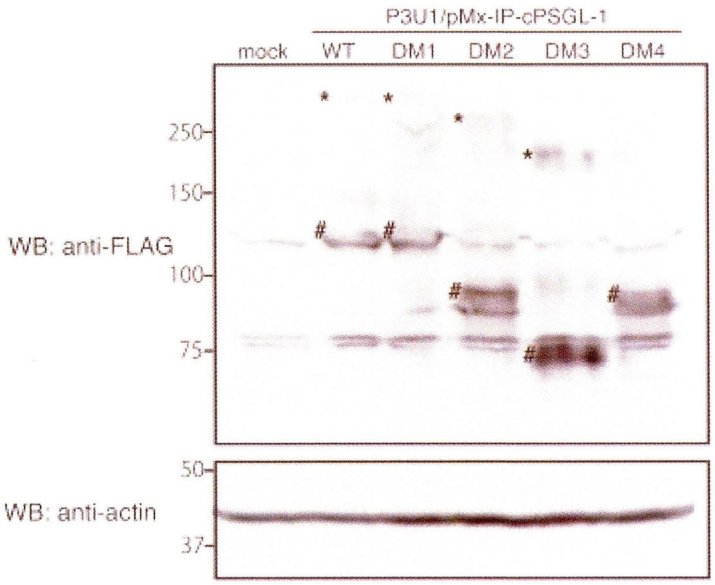

Fig. II-5. Expression of deletion mutant of cPSGL-1 in P3U1 cells. Total protein was extracted from P3U1 cells transduced with pMx-IP (mock), pMx-IP-cPSGL-1 (WT), or with pMx-IP-cPSGL-1-DM1, -DM2, -DM3 or -DM4. After electrophoresis and blotting, cPSGL-1 was detected with an anti-FLAG Ab. The same blot was stripped and reprobed with an anti-actin Ab used as a loading control. * and # represent dimeric and monomeric forms of cPSGL-1, respectively. Wilde- type cPSGL-1 migrated both as a dimer, with a molecular mass of >240 kDa, and as a monomer that migrated with a molecular mass of approximately 120 kDa. cPSGL-1-DM1 (lacking residues 19-41) migrated at a similar molecular weight as wild-type PSGL-1. cPSGL-1-DM2 (lacking residues 42-144) migrated as several 80- to 90-kDa bands, consistent with deletion of 103 amino acids from cPSGL-1. cPSGL-1-DM3 (lacking 130 amino acids; residues 145-274), migrated as two forms with molecular masses of 75 kDa (monomeric form) and 160 kDa (dimeric form). cPSGL-1-DM4 (lacking 103 amino acids; residues 275-345) migrated at a similar molecular weight as cPSGL-1-DM2, which also lacked 103 amino acids.

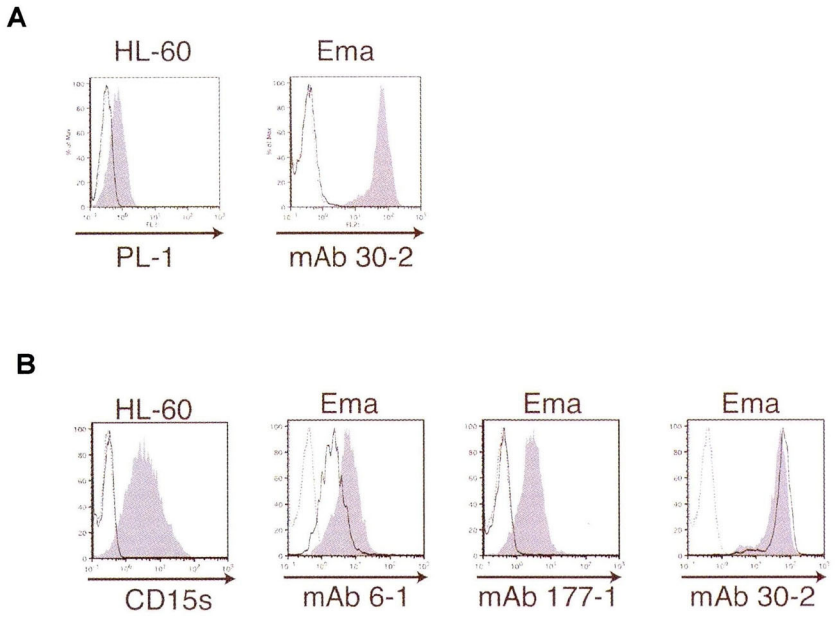

Fig. II-6. The effect of enzyme treatment on the reactivity of each mAb with Ema cells. A: Ema cells were treated with O-Sialoglycoprotein endopeptidase (OSGE) and then stained with the mAb 30-2. The HL-60 cell line was used as a positive control to show the effect of OSGE on the reactivity of the PL-1 Ab with human PSGL-1. B: Ema cells were treated with neuraminidase and then stained with the indicated mAbs. The HL-60 cell line was used as positive control to show the effect of neuraminidase on the reactivity of the CD15s Ab to sialyl Lewis X. For (A) and (B) the shaded region and the lines in the histograms indicate reactivity without or with enzyme, respectively. The dotted lines indicate staining with isotype control.

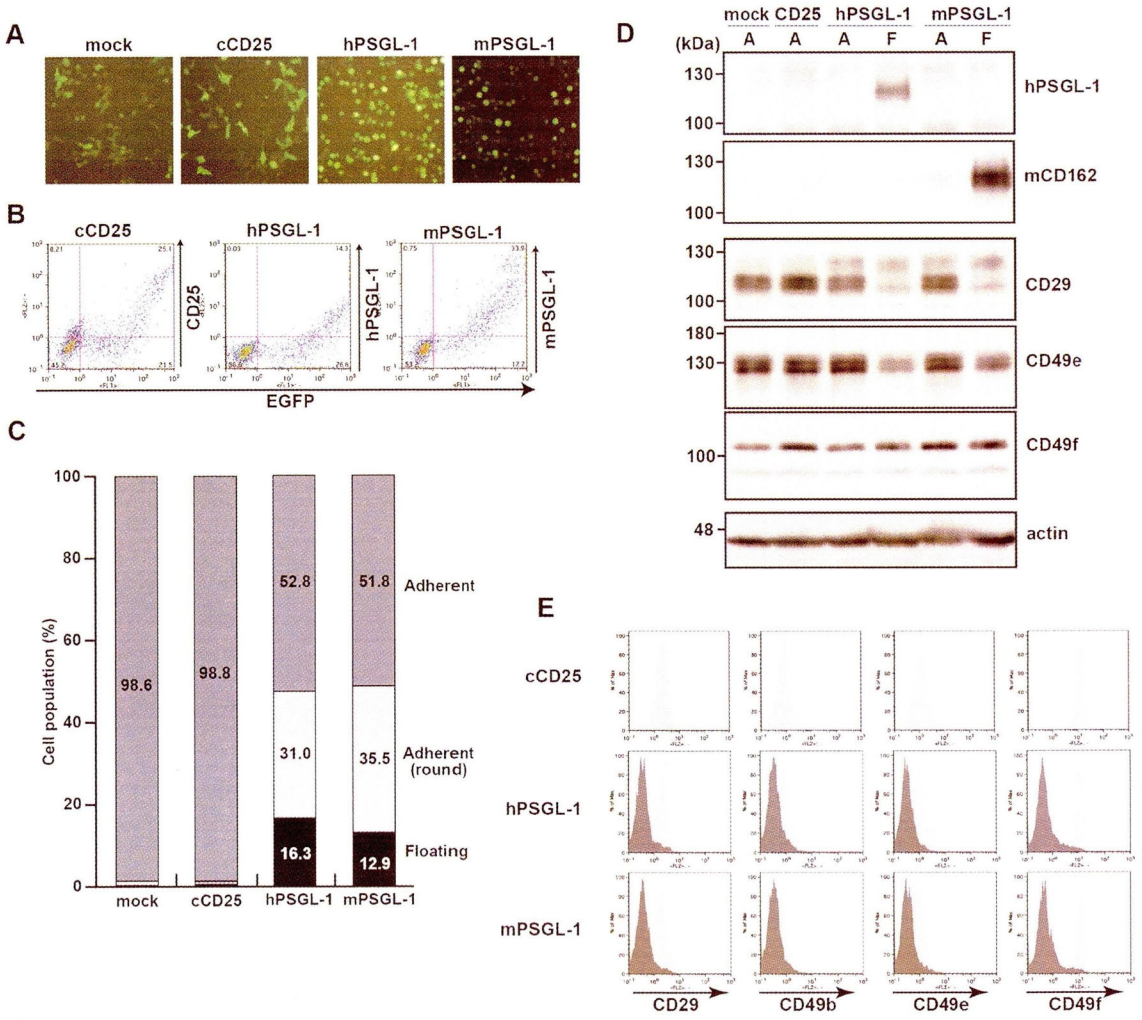

Fig. III-1. Adherent cells were detached after PSGL-1 overexpression. A: HEK293T cells were transfected with pMXs-IG, pMx-IG-cCD25, pMx-IG-hPSGL-1#1 or pMx-IG-mPsgl-1. The cells were observed by phase contrast and fluorescent microscopy 48 h after transfection. Each Photo was overlayed. These results are representative results of two experiments. Magnification, 200 ×. B: Forty-eight hours after transfection, the cells were collected and analyzed by flow cytometry using the anti-CD25, anti-human PSGL-1 or anti-mouse PSGL-1 antibody. The result is representative of two experiments that showed a similar trend. C: Forty-eight hours after transfection, adherent cells, adherent cells but with a round shape (adherent (round)), and floating cells were counted as described in MATERIALS AND METHODS. D: Forty-eight hours after transfection, adherent cells (including adherent with round shape; A) or floating cells (F) were collected and analyzed by Western blotting using the anti-human PSGL-1, anti-mouse PSGL-1 (mCD162) and anti-integrin antibodies (CD29, CD49e and CD49f). E: Adherent cells (light gray shades) and floating cells (dark gray shades) were individually stained with the anti-integrin antibodies (CD29, CD49b, CD49e and CD49f), and were analyzed using flow cytometry at 48 h after transfection.

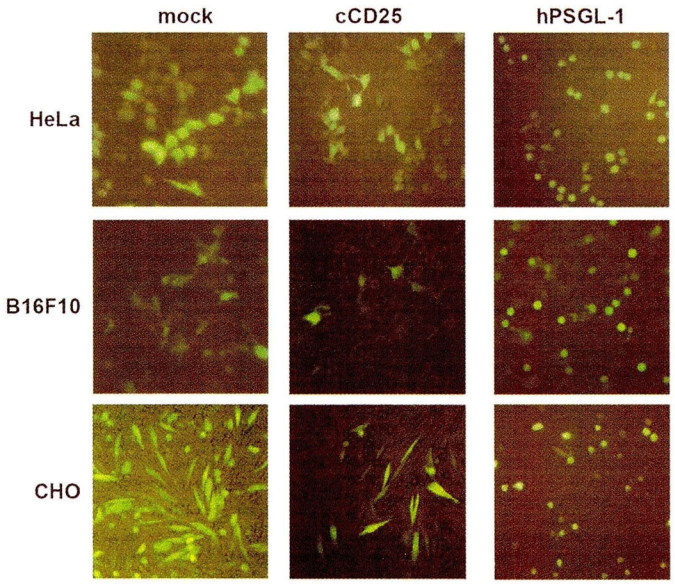

Fig. III-2. Several adherent cell lines showed rounded cells, or detached cells, after PSGL-1 transfection. Each cell line was transfected with either pMxs-IG, pMx-IG-cCD25 or pMx-IG-hPSGL-1#1, and observed by fluorescent microscopy 48 h after transfection. This result is representative of two experiments. Magnification, 200 ×.

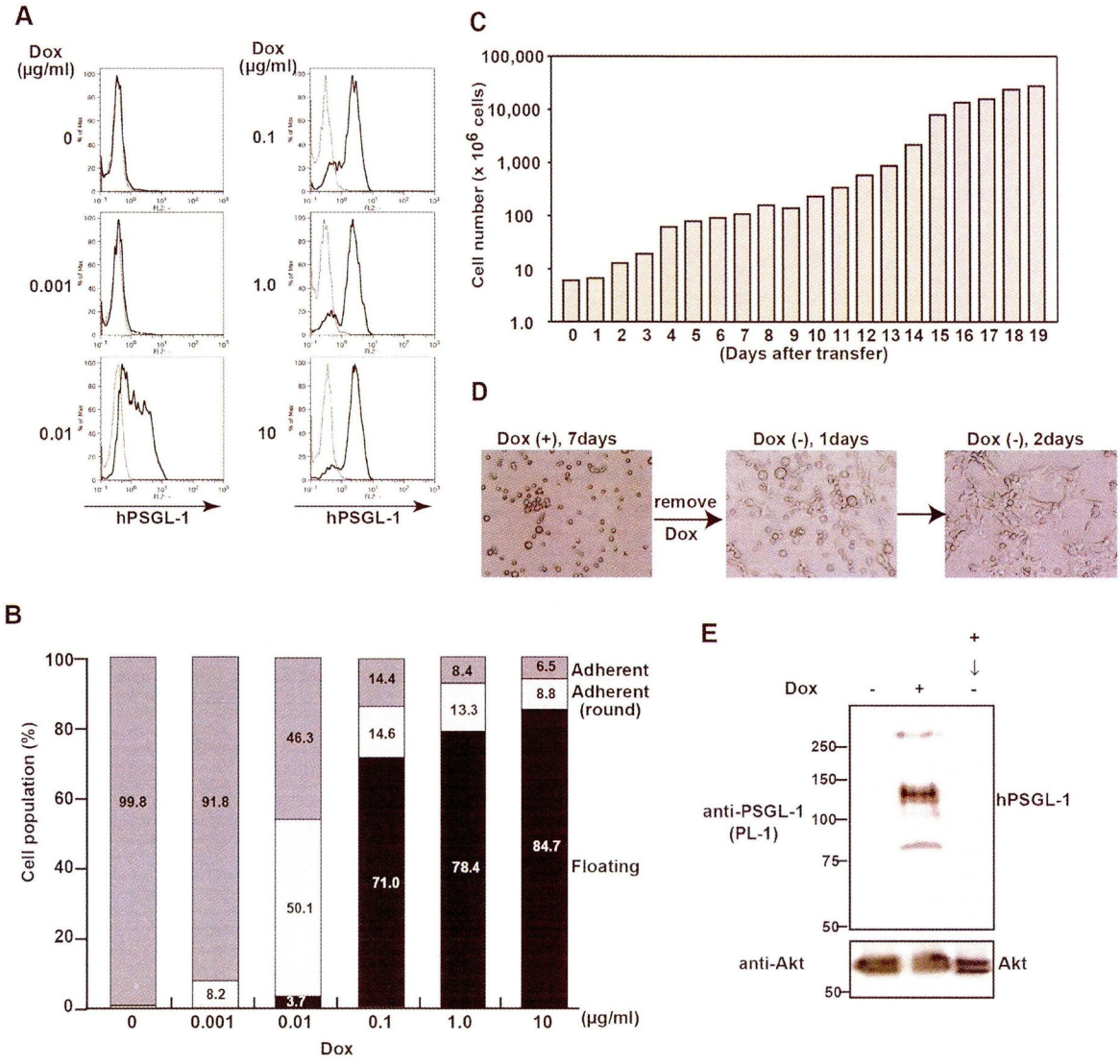

Fig. III-3. PSGL-1 was induced by doxycycline (Dox) in a dose-dependent manner in HEK293/Tet-ON/hPSGL-1 cells. HEK293/Tet-ON/hPSGL-1 cells were cultured in the presence of 0.001 to 10 μg/ml of doxycycline (A and B) or 1 μg/ml of doxycycline (C, D and E) for indicated time. A: Fourty-eight hours after incubation, the collected cells were stained with the anti-human PSGL-1 antibody (black line) or isotype antibody (gray line), and were analyzed using flow cytometry. B: Fourty-eight hours after incubation, the cells of different morphology were counted as described in MATERIALS AND METHODS. Each result is representative of two experiments that showed a similar trend. C: The cell number was counted every day. Every 3 days, the cells were diluted to a concentration of 6.0×10^4 cells/ml using fresh D10, containing doxycycline. D: At the indicated time point after start of the culture, some of the cells were collected, washed with fresh media and transferred to a new well to start a doxycycline minus subculture. At the indicated time points, cells were photographed using phase-contrast microscopy. Each result is a representative result of two experiments,

which showed a similar trend. E: The cells were collected before (-), 8 days after Dox treatment (+), or 8 days after Dox treatment followed by 4 days after of Dox removal (+→-) and analyzed by Western blotting using the anti-human PSGL-1 antibody (PL-1). The blot was re-probed with an anti-Akt antibody, which was used as a loading control. Each result is a representative result of two experiments, which showed a similar trend.

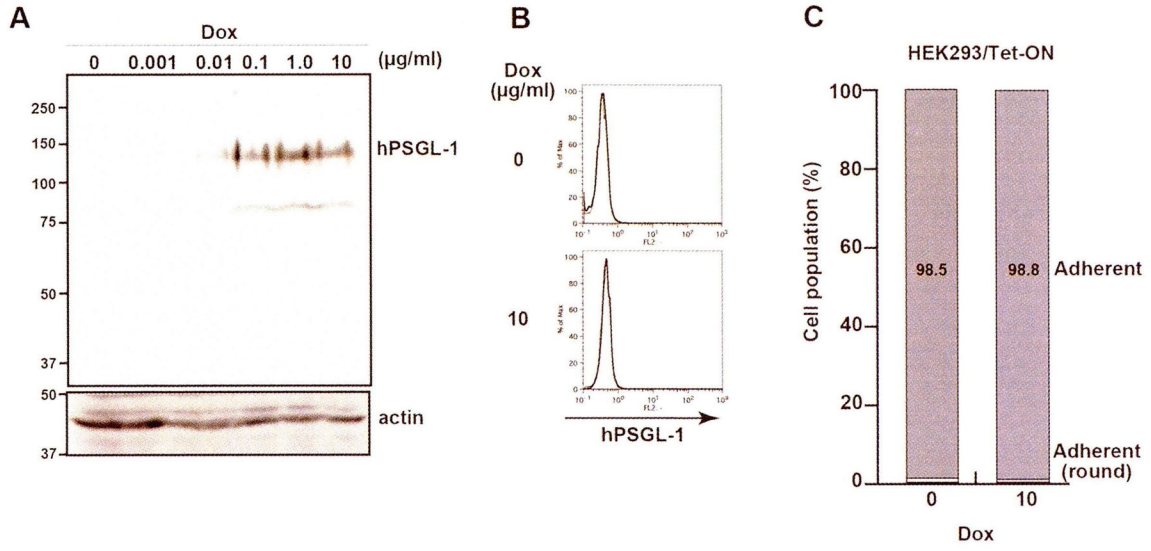

Fig. III-4. Doxycycline treatment induced PSGL-1 expression at dose dependent manner in HEK293/Tet-ON/hPSGL-1 cells (A), but not in HEK293/Tet-ON cells (B and C). A: HEK293/Tet-ON/hPSGL-1 cells were cultured in the presence of 0-10 μg/ml of doxycycline for 18 hrs. B and C: HEK293/Tet-ON cells were cultured in the presence of 10 μg/ml of doxycycline for 18 hrs. The cells were collected, stained with anti-human PSGL-1 antibody (PL-1) (black line) or isotype antibody (grey line) and analyzed by flow cytometry (B). The percentage of adherent, adherent round, and floating cells was counted as described in Materials and Methods (C). Each result is a representative result of two experiments, which showed a similar trend.

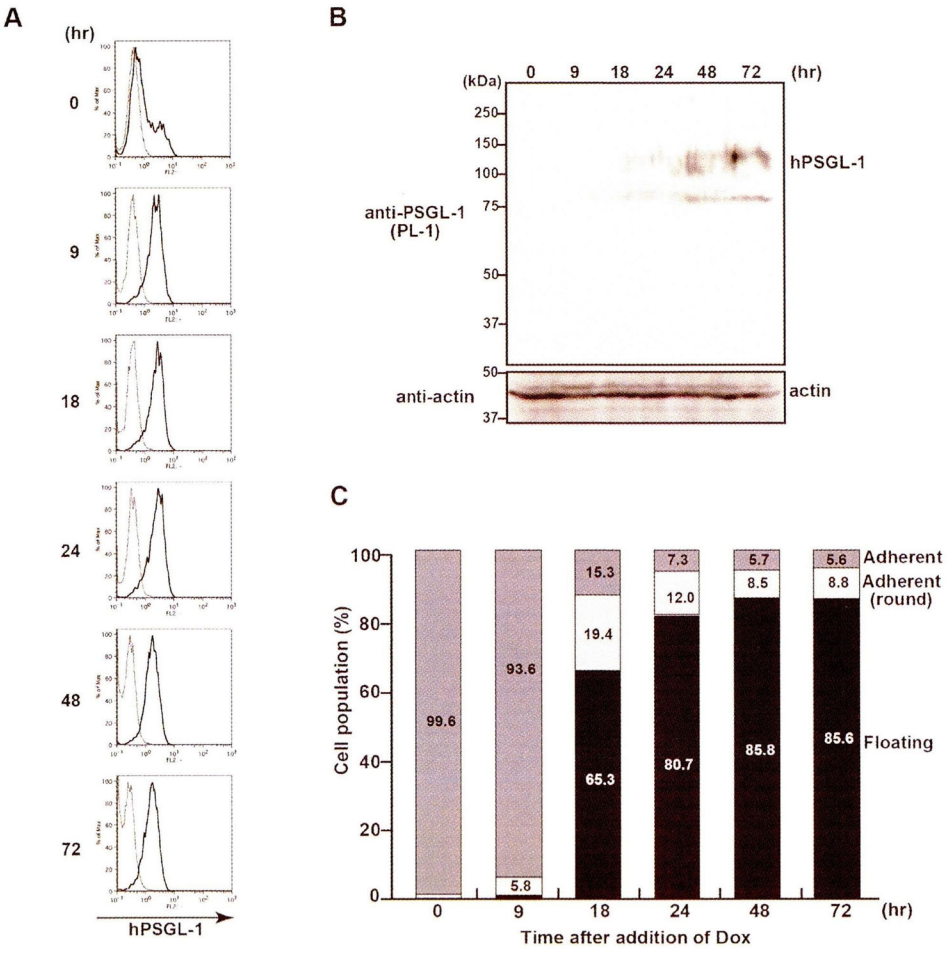

Fig. III-5. PSGL-1 overexpression-induced cell floating was observed 18 h after PSGL-1 induction by addition of doxycycline (Dox). HEK293/Tet-ON/hPSGL-1 cells were cultured in the presence of 1 μg/ml of doxycycline for the indicated times and were then analyzed as follows: A: The cells were collected and stained with the anti-human PSGL-1 antibody (black line) or isotype antibody (gray line), and were analyzed using flow cytometry. B: Western blotting of cell lysates with the anti-human PSGL-1 antibody (clone PL-1) was performed. The same membrane was re-probed with an anti-actin antibody. Molecular weight markers are shown at left. C: The percentage of adherent, adherent round, and floating cells was counted as described in Materials and Methods. Each result is a representative result of two experiments, which showed a similar trend.

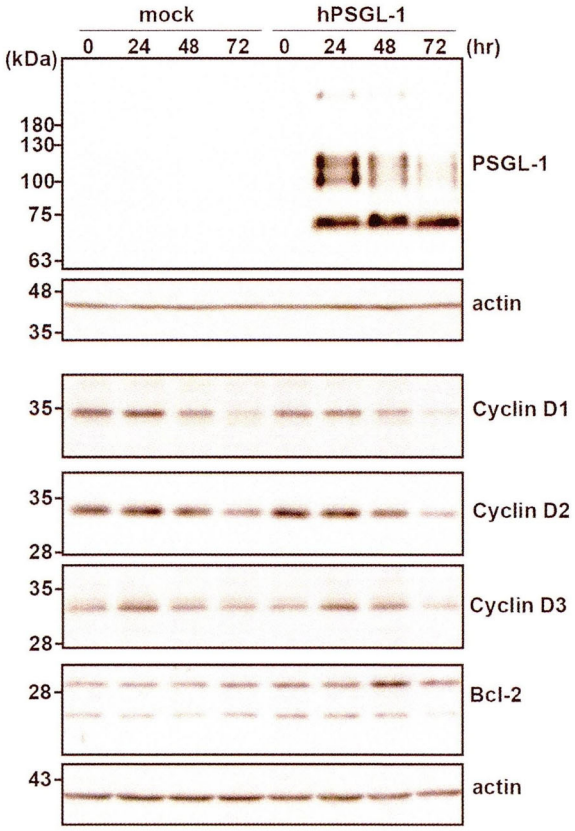

Fig. III-6. The time-dependent expression levels of Cyclin D1, D2, D3 and Bcl-2 were analyzed by Western blotting with each cognate antibody. HEK293/Tet-ON cells (mock) and HEK293/Tet-ON/hPSGL-1 cells (hPSGL-1) were cultured in the presence of 1 μg/ml of doxycycline for the indicated times. The blot was re-probed with an anti-actin antibody.

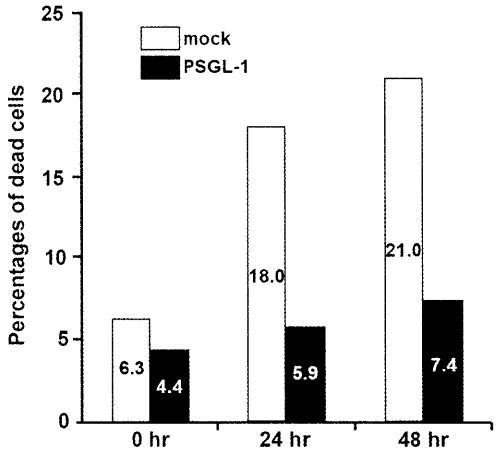

Fig. III-7. PSGL-1 overexpression inhibited anoikis in MDCK cells. MDCK/pMxs-IP cells or floating MDCK.pMx-IP-hPSGL-1 cells were cultured on the polyhydroxyethylmethacrylate (poly-HEMA) coated 96-well plate and were stained with propidium iodide (PI) and Hoechest 33342 at 0, 24, 48 h after culture. The graph shows the percentage of PI-positive dead cells.

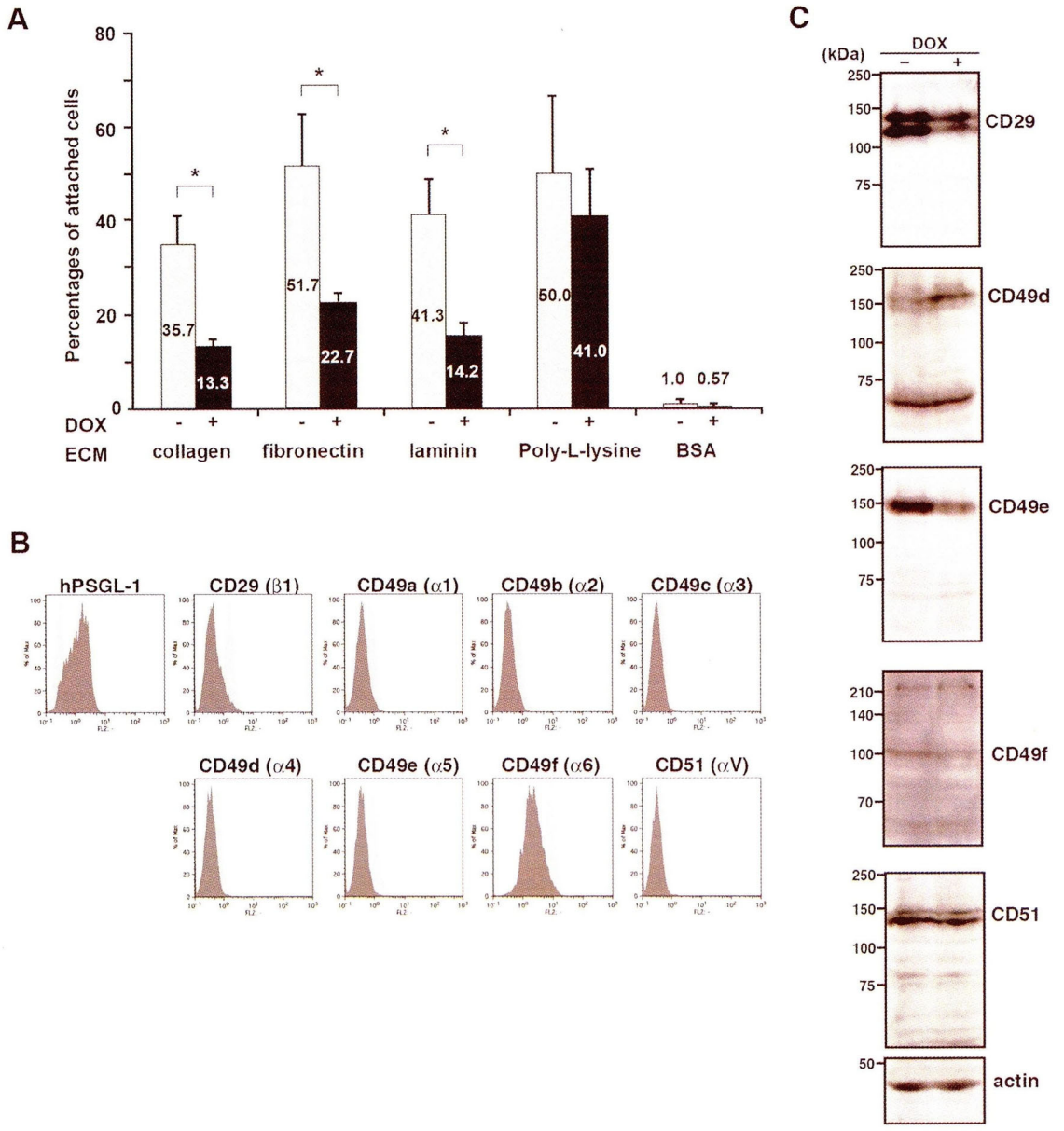

Fig. III-8. PSGL-1-expressing floating cells have decreased attachment to the ECM due to ablated cell surface expression of integrins. A: Doxycycline-treated floating cells (black bars) or doxycycline-untreated attached cells (gray bars) were transferred to ECM-coated or positive (Poly-L-lysine-coated) or negative (BSA-coated) control wells. After incubation for 1 h, attached cells were counted and their number was calculated as a percentage of inoculated cells. The results are expressed as means ± S.D. of three independent experiments. *, $p<0.05$. B and C: HEK293/Tet-ON/hPSGL-1 cells were incubated with or without doxycycline (1 μg/ml) for 48 h. The cells incubated with (dark gray shades) or without (light gray shades) doxycycline were individually stained with the indicated anti-integrin antibodies, and were analyzed using flow cytometry (B). Collected cells were analyzed by Western blotting using anti-human integrin antibodies (C).

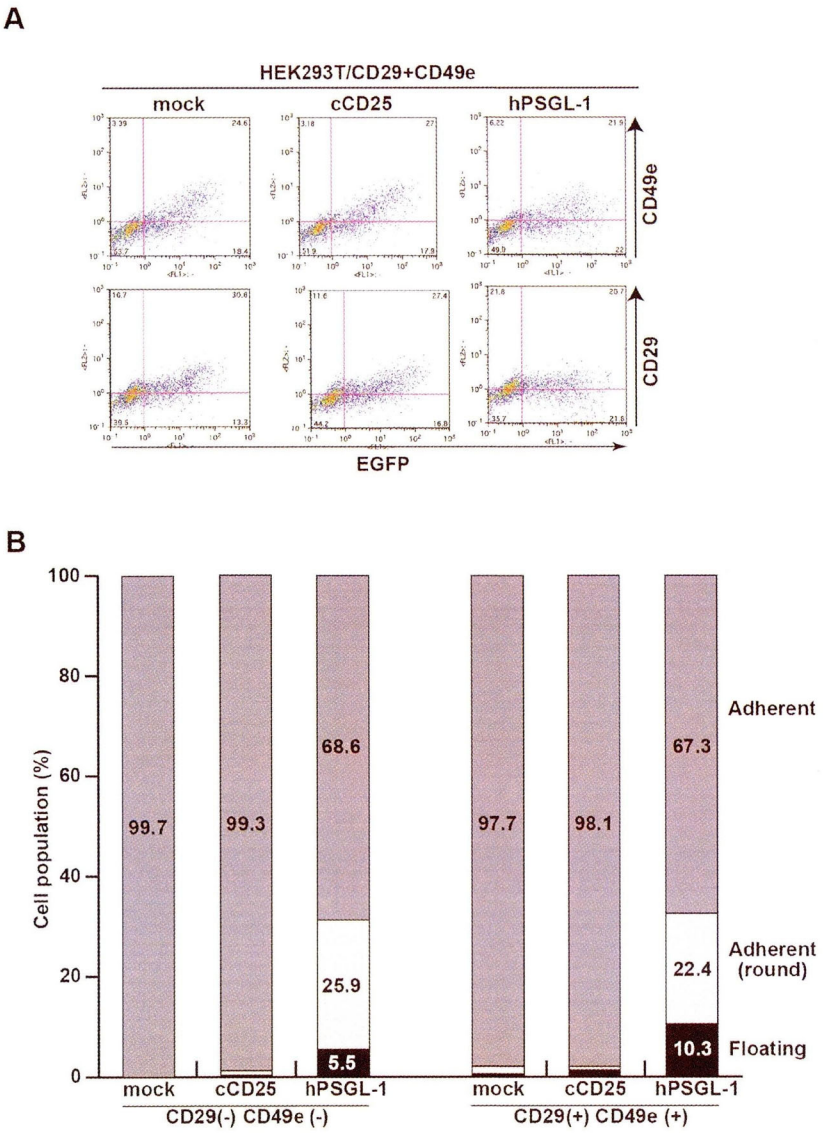

Fig. III-9. Overexpression of CD29 and CD49e in HEK293T cells did not prevent cell detachment induced by PSGL-1 overexpression. A and B: HEK293T cells were transfected with pMx-IB-ITGB1 (CD29), pMx-IP-ITGA5#4 (CD49e), and either of pMxs-IG (mock), pMxs-IG-cCD25 (cCD25) or pMx-IG-hPSGL-1#1 (hPSGL-1). Fourty-eight hours after transfection, the cells of different morphology were counted as described in MATERIALS AND METHODS (B), and remaining of cells were collected and stained with the anti-integrin antibodies (CD49e and CD29) (A).

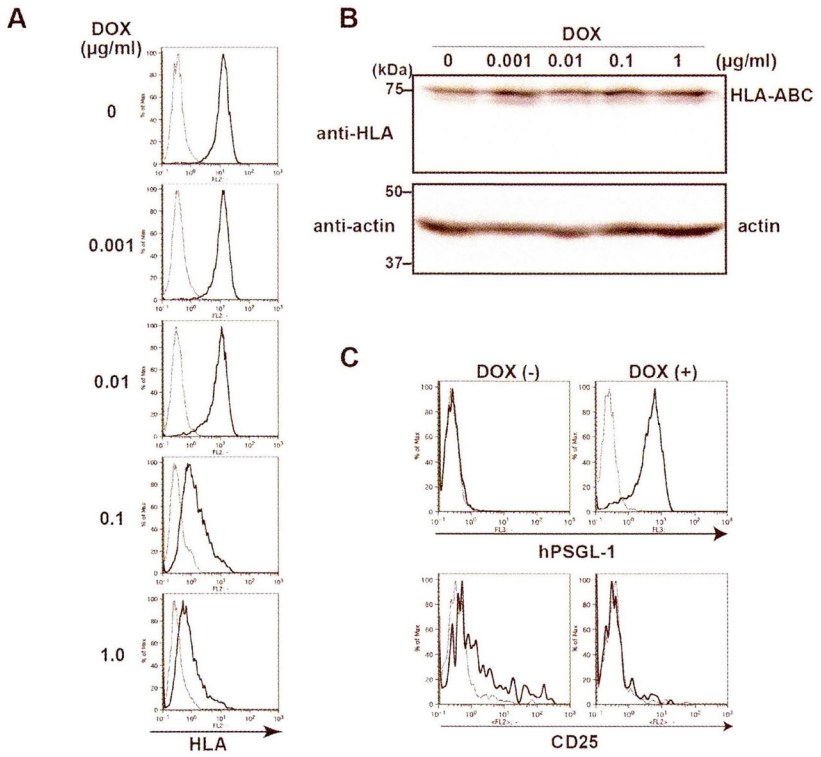

Fig. III-10. Overexpression of PSGL-1 inhibited detection of cell surface HLA and CD25 by their cognate antibodies. A and B: HEK293/Tet-ON/hPSGL-1 cells were treated with doxycycline at the indicated concentration for 24 h. After incubation, the cells were stained with anti-human HLA-ABC antibody (black line) or appropriate isotype antibody (gray line), and were subjected to flow cytometric analysis (A). Protein extracts of the cells were Western blotted using an anti-human HLA-ABC antibody. The blot was re-probed with an anti-actin antibody, which was used as a loading control (B). C: HEK293/Tet-ON/hPSGL-1 cells were transfected with pMx-IG-cCD25#1 and incubated for 48 h. After incubation, 1 μg/ml of doxycycline was added to the culture to induce the expression of PSGL-1. Forty-eight hours after induction, the cells were collected and stained with the anti-PSGL-1 antibody (PL-1) or anti-CD25 antibody, followed by flow cytometric analysis. Each result is representative of two experiments that showed a similar trend.

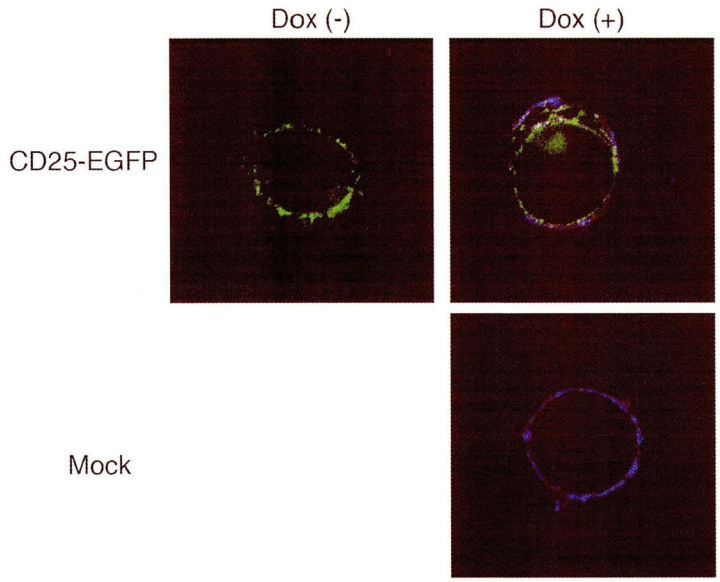

Fig. III-11. PSGL-1 and CD25 were similarly distributed in the floating cells. HEK293/Tet-ON/hPSGL-1 cells were transfected with pEGFP-N1-cCD25 and cultured for 24 hours, followed by addition of doxycycline and additional 24 hours culture. Resultant cells were collected and stained with anti-human PSGL-1 antibody (blue) and analyzed by confocal microscopy. CD25 was shown in green due to EGFP expression.

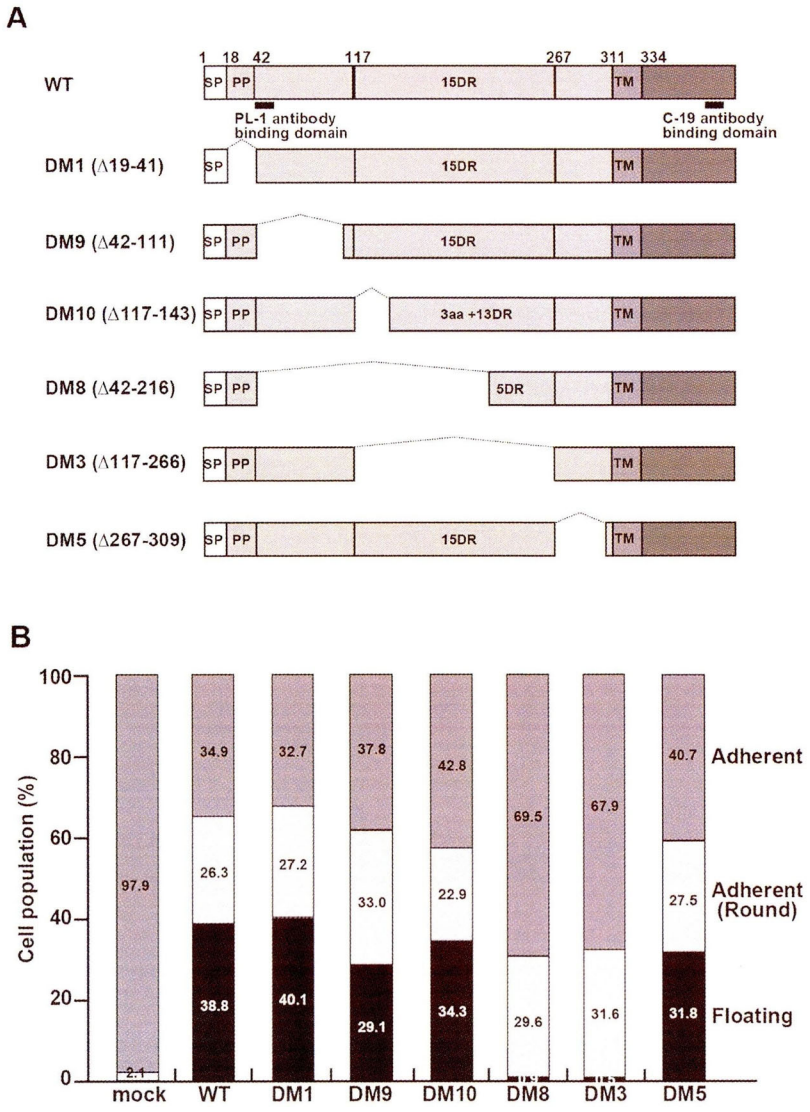

Fig. III-12. Specific PSGL-1 deletion mutant clones abrogated PSGL-1-induced cell detachment. A: Schematic representation of the deletion mutants of hPSGL-1 constructed. DM1, DM9, DM10, DM8, DM3, and DM5 have deletions of amino acids 19-41, 42-111, 117-143, 42-216, 117-266 and 267-309, respectively. SP, signal peptide domain; PP, propeptide domain; DR, decameric repeat domain; TM, transmembrane domain. B: Forty-eight hours after transfection, adherent cells, adherent cells but with a round shape (adherent (round)), and floating cells were counted as described in MATERIALS AND METHODS. The result is representative of three experiments that all showed a similar trend.

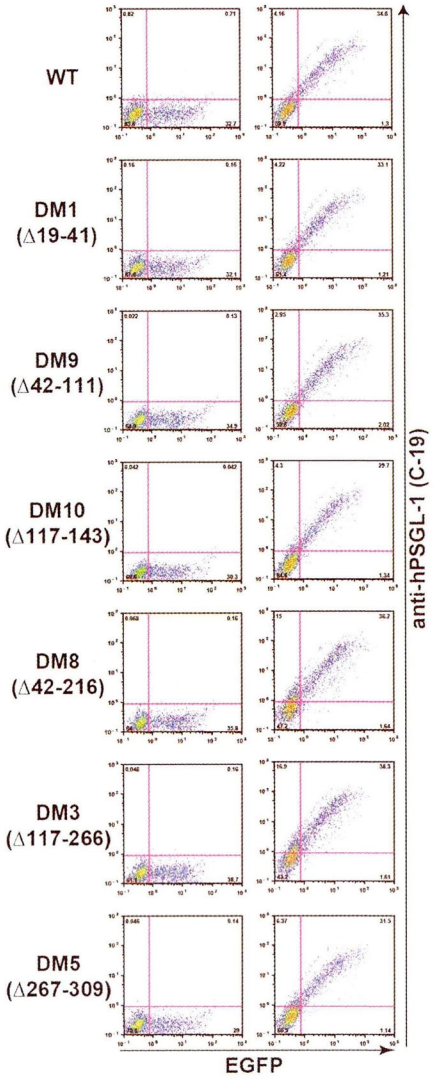

Fig. III-13. A similar amount of specific PSGL-1 deletion mutant clones were expressed in HEK293T cells. Each mutant was transfected into HEK293T cells. Forty-eight hours after transfection, the cells were collected and analyzed by flow cytometry using the anti-human PSGL-1 antibody, C-19. The result is representative of two experiments that showed a similar trend.

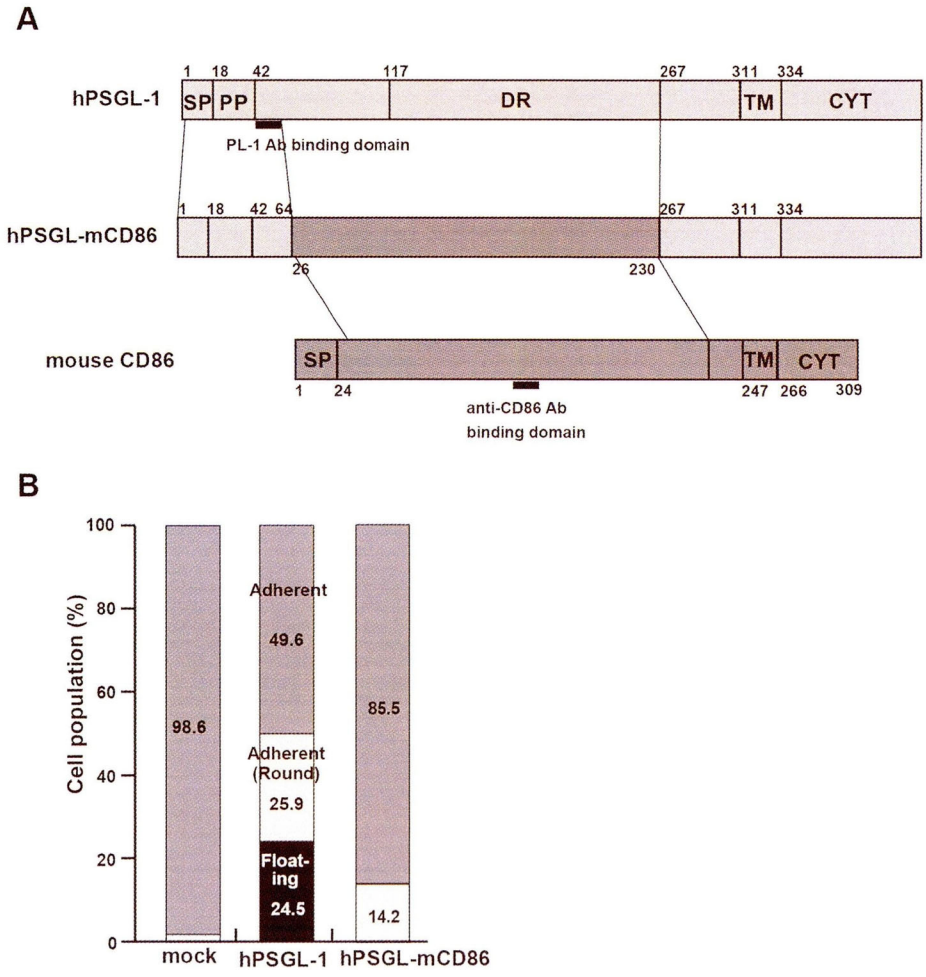

Fig. III-14. A chimeric protein of hPSGL-1 and mouse CD86 induced cell rounding of HEK293T cells. A: Schematic representation of the hPSGL-1/mouse CD86 chimera. SP, signal peptide domain; PP, propeptide domain; DR, decameric repeat domain; TM, transmembrane domain; CYT, cytoplasmic domain.nB: pMXs-IG (mock), pMx-IG-hPSGL-1#1, or pMx-IG-hPSGL-mCD86 was transfected into HEK293T cells. Forty-eight hours after transfection, the cells with different morphologies were counted.

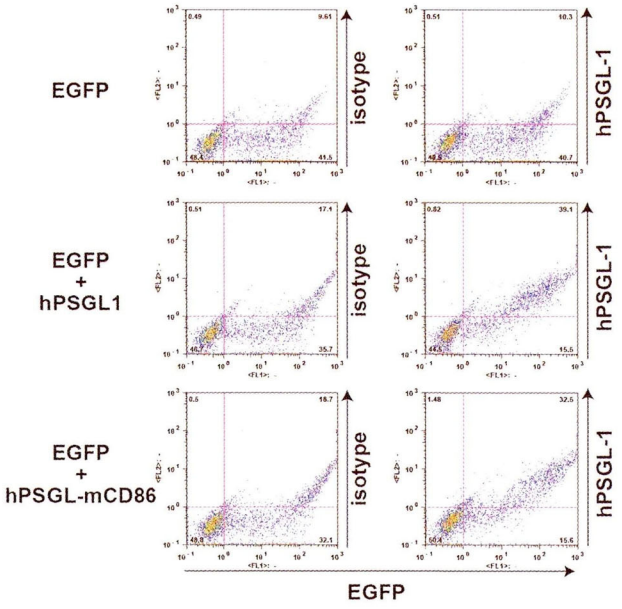

Fig. III-15. A similar amount of chimeric protein of hPSGL-1 and mouse CD86 was expressed in HEK293T cells. Each mutant was transfected into HEK293T cells. Forty-eight hours after transfection, the cells were collected and analyzed by flow cytometry using the anti-human PSGL-1 antibody, C-19. The result is representative of two experiments that showed a similar trend.

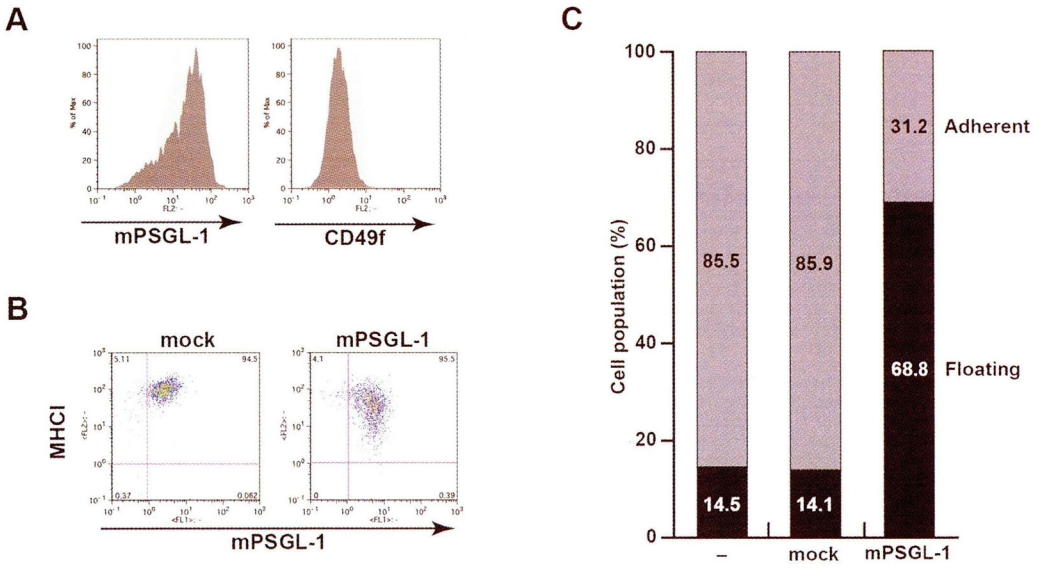

Fig.III-16. Overexpression of PSGL-1 inhibited detection of cell surface CD49f and MHCI by their cognate antibodies in P3U1 cells. P3U1 cells stably expressing mPSGL-1 was established by retroviral techniques. A: P3U1/mPSGL-1 cells (dark gray shades) and P3U1/pMxs-IP cells (light gray shades) were stained with anti-mPSGL-1 or anti-CD49f antibodies, followed by flow cytometric analysis. B: P3U1/mPSGL-1 cells (right) and P3U1/pMxs-IP cells (left) were stained with anti-mPSGL-1 and anti-MHCI antibodies, followed by flow cytometric analysis. C: Twenty-four hours after seeding, adherent and floating cells in P3U1 cells (-), P3U1/pMxs-IP cells (mock) and P3U1/mPSGL-1 (mPSGL-1) were counted as described in MATERIALS AND METHODS.

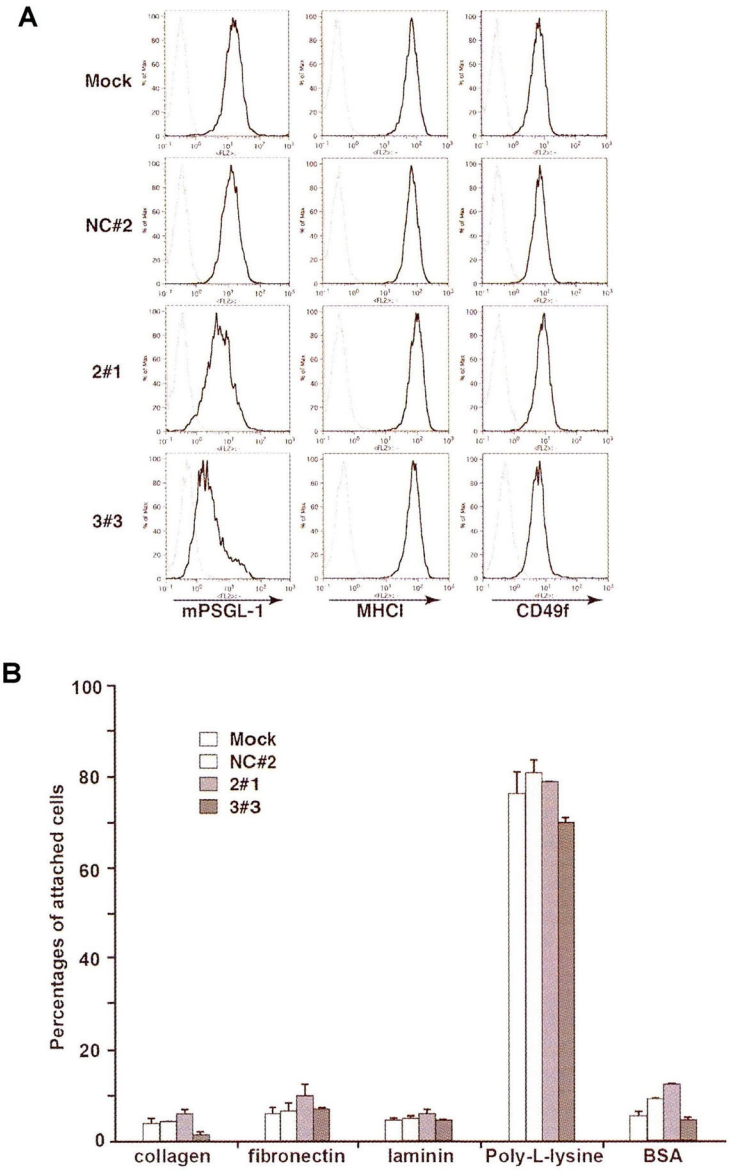

Fig. III-17. PSGL-1 knockdown in P3U1 cells did not altered the reactivities of antibody to the cell surface molecules and the binding property to ECMs. A: P3U1 (Mock), P3U1/sh-NC#2 (NC#2) as negative control, P3U1/sh-mSleplg-2#1 (2#1) and P3U1/sh-mSleplg (3#3) cells were stained with anti-mPSGL-1, anti-MHCI or anti-CD49f antibodies (each black line) or appropriate isotype antibody (each gray line). B: Mock, NC#2, 2#1 or 3#3 - transduced P3U1 cells were transferred to ECM-coated or positive (Poly-L-lysine-coated) or negative (BSA-coated) control wells. After incubation for 1 h, attached cells were counted and shown as a percentage of inoculated cells. The results are expressed as means ± S.D.